UNIVERSIDADE ESTADUAL DO OESTE DO PARANÁ
CENTRO DE CIÊNCIAS BIOLÓGICAS E DA SAÚDE
PROGRAMA DE PÓS-GRADUAÇÃO STRICTO SENSU EM CONSERVAÇÃO E MANEJO DE RECURSOS NATURAIS – NÍVEL MESTRADO

MAILOR WELLINTON WEDIG AMARAL

DIATOMÁCEAS EPILÍTICAS DE RIACHOS SUBTROPICAIS COM ALTAS CONCENTRAÇÕES DE ALUMÍNIO E FERRO, SUL DO BRASIL

CASCAVEL-PR
Abril/2022

MAILOR WELLINTON WEDIG AMARAL

DIATOMÁCEAS EPILÍTICAS DE RIACHOS SUBTROPICAIS COM ALTAS CONCENTRAÇÕES DE ALUMÍNIO E FERRO, SUL DO BRASIL

Dissertação apresentado ao Programa de Pós-graduação Stricto Sensu em Conservação e Manejo de Recursos Naturais – Nível Mestrado, do Centro de Ciências Biológicas e da Saúde, da Universidade estadual do Oeste do Paraná, como requisito parcial para a obtenção do título de Mestre em Conservação e Manejo de Recursos Naturais

Área de Concentração: Ciências Ambientais

Orientadora: Norma Catarina Bueno

Coorientadora: Thelma Alvim Veiga Ludwig

CASCAVEL-PR

Abril/2022

Ficha de identificação da obra elaborada através do Formulário de Geração Automática do Sistema de Bibliotecas da Unioeste.

Amaral, Mailor Wellinton Wedig
Diatomáceas epilíticas de riachos subtropicais com altas concentrações de alumínio e ferro, Sul do Brasil / Mailor Wellinton Wedig Amaral; orientadora Norma Catarina Bueno; coorientadora Thelma Alvim Veiga Ludwig. -- Cascavel, 2021.
94 p.

Dissertação (Mestrado Acadêmico Campus de Cascavel) -- Universidade Estadual do Oeste do Paraná, Centro de Ciências Biológicas e da Saúde, Programa de Pós-Graduação em Conservação e Manejo de Recursos Naturais, 2021.

1. Taxonomia. 2. Diatomáceas. 3. Perifíton. 4. Teratologias. I. Bueno, Norma Catarina, orient. II. Ludwig, Thelma Alvim Veiga, coorient. III. Título.

unioeste
Universidade Estadual do Oeste do Paraná
CENTRO DE CIÊNCIAS BIOLÓGICAS E DA SAÚDE
Campus de Cascavel - PR
Rua Universitária, 2069 – CEP 85819-110
FONE 45 3220-3275

PPRN Unioeste
Programa de pós Graduação
em Conservação e Manejo de Recursos Naturais
https://www5.unioeste.br/portalunioeste/pos/pprn
cascavel.pos.cmrn@unioeste.br

Programa de Pós-Graduação em Conservação e Manejo de Recursos Naturais

ATA DA DEFESA PÚBLICA DA DISSERTAÇÃO DE MESTRADO DE MAILOR WELLINTON WEDIG AMARAL, ALUNO(A) DO PROGRAMA DE PÓS-GRADUAÇÃO EM CONSERVAÇÃO E MANEJO DE RECURSOS NATURAIS DA UNIVERSIDADE ESTADUAL DO OESTE DO PARANÁ - UNIOESTE, E DE ACORDO COM A RESOLUÇÃO DO PROGRAMA E O REGIMENTO GERAL DA UNIOESTE.

Aos 17 dias do mês de setembro de 2021 às 14h00min, por videoconferência, de forma remota, realizou-se a sessão pública da Defesa de Dissertação do candidato **MAILOR WELLINTON WEDIG AMARAL,** aluno do Programa de Pós-Graduação em Conservação e Manejo de Recursos Naturais - nível de Mestrado, na área de concentração em Ciências Ambientais. A comissão examinadora da Defesa Pública foi aprovada pelo Colegiado do Programa de Pós-Graduação em Conservação e Manejo de Recursos Naturais. Integraram a referida Comissão as Professoras Doutoras: Norma Catarina Bueno, Angela Maria da Silva-Lehmkuhl e Elaine Cristina Rodrigues Bartozek. Os trabalhos foram presididos pela Norma Catarina Bueno. Tendo satisfeito todos os requisitos exigidos pela legislação em vigor, o aluno foi admitido à Defesa de DISSERTAÇÃO DE MESTRADO, intitulada: **" Epilithic diatoms from subtropical streams with high concentrations of aluminum and iron, Southern Brazil ".** A Senhora Presidente declarou abertos os trabalhos, e em seguida, convidou o candidato a discorrer, em linhas gerais, sobre o conteúdo da Dissertação. Feita a explanação, o candidato foi arguido sucessivamente, pelas professoras doutoras: Angela Maria da Silva-Lehmkuhl, Elaine Cristina Rodrigues Bartozek. Findas as arguições, o(a) Senhor(a) Presidente suspendeu os trabalhos da sessão pública, a fim de que, em sessão secreta, a Comissão expressasse o seu julgamento sobre a Dissertação. Efetuado o julgamento, o(a) candidato(a) foi aprovado. A seguir, a Senhora Presidente reabriu os trabalhos da sessão pública e deu conhecimento do resultado. E, para constar, o Coordenador do Programa de Pós-Graduação em Conservação e Manejo de Recursos Naturais, da Universidade Estadual do Oeste do Paraná – UNIOESTE - Campus de Cascavel, lavra a presente ata, e assina juntamente com os membros da Comissão Examinadora e o candidato.

Em tempos:____

____

____

____

NCBueno

Orientador(a) - Norma Catarina Bueno
Universidade Estadual do Oeste do Paraná - Campus de Cascavel (UNIOESTE)

Angela Maria da Silva Lehmkuhl
Universidade Federal do Amazonas (UFAM)

Universidade Estadual do Oeste do Paraná
CENTRO DE CIÊNCIAS BIOLÓGICAS E DA SAÚDE
Campus de Cascavel - PR
Rua Universitária, 2069 – CEP 85819-110
FONE 45 3220-3275

PPRN Unioeste
Programa de pós Graduação em Conservação e Manejo de Recursos Naturais
https://www5.unioeste.br/portalunioeste/pos/pprn
cascavel.pos.cmrn@unioeste.br

Elaine C. R. Bartozek

Elaine Cristina Rodrigues Bartozek
Universidade Federal da Integração Latino-Americana (Unila)

Mailor W Wedig A.

Mailor Wellinton Wedig Amaral
Aluno(a)

Coordenador(a) do Programa de Pós-Graduação em Conservação e Manejo de Recursos Naturais

Aos meus pais,

com amor

“As coisas mais importantes não estão escritas num livro,
é preciso aprendê-las vivenciando-as sozinho.”

Sakura Haruno em Naruto Shippuden

AGRADECIMENTOS

Agradeço primeiramente a mim mesmo. O mestrado é, acima de tudo, um período de autoconhecimento. Nossos medos, angústias e inseguranças são, muitas vezes, colocados em segundo plano em prol do bom desenvolvimento da nossa dissertação. O crescimento pessoal e profissional atingido ao final dessa etapa também é resultado de nosso esforço e dedicação.

Aos meus pais, pelo amor incondicional e por todo o suporte e incentivo ao longo da minha vida. Sua humildade e honestidade são motivo de muita admiração. Vocês me impulsionam na busca de ser uma pessoa melhor. E ao meu irmão Marroni, pelo companheirismo durante todos esses anos. Estendo o agradecimento também aos meus avós, Mario (em memória) e Walmi, pessoas extremamente batalhadoras e merecedoras de suas conquistas. Obrigado por todo o amor e carinho.

Ao meu companheiro (agora marido) Yuri, pela paciência e compreensão. Você foi e continua sendo meu alicerce, sempre apoiando minhas decisões e encorajando meus sonhos. Palavras são insuficientes para expressar o quanto agradeço por ter te conhecido.

À minha orientadora professora Dra. Norma Catarina Bueno por me receber abertamente no laboratório no segundo ano da graduação. Desde então, nossa parceria tem gerado bons resultados, algo que é fruto de sua incansável dedicação ao trabalho e aos orientados. Obrigado pelo incentivo desde o primeiro dia e por compreender minhas limitações. Nunca serei grato o suficiente.

À minha coorientadora professora Dra. Thelma Alvim Veiga Ludwig pela oportunidade única de conhecer o laboratório e pela ajuda nas identificações. Nossas conversas foram de imensa valia e me fizeram perceber que a taxonomia das diatomáceas é um belíssimo mundo a ser explorado. Obrigado por acreditar no meu potencial.

Ao coordenador, aos professores, e aos funcionários que fazem parte do Programa de Pós-graduação em Conservação e Manejo de Recursos Naturais (PPRN), pela oportunidade de realizar o mestrado e pelo engajamento na formação de profissionais. Agradeço ainda aos professores do curso de Ciências Biológicas da Unioeste/Cascavel, cujos ensinamentos foram cruciais para minha formação como biólogo, refletindo positivamente no meu progresso durante o mestrado.

À Gabriela Medeiros (Gabi), colega de laboratório e amiga para a vida. Nossa troca de conhecimentos, sejam científicos ou pessoais, contribuíram muito para ser quem sou hoje. Espero que nossa amizade seja igual ao nosso gosto por um bom cafézinho: interminável.

Agradeço também à Thaís Tagliati da Silva e à Maria Clara Pillati que, em companhia com a Gabi, tornaram as coletas de campo mais divertidas (lembram dos tombos, das mexericas, das aranhas, dos almoços de pés descalços?). Guardarei para sempre essas boas lembranças.

Às demais amizades que fiz durante minha trajetória no laboratório de Ficologia: Camila Aquino, Francys Montesso, Maria Júlia Lopes, Yara Medeiros e Yasmin Vilboski. Obrigado pelos inúmeros momentos de aprendizado e descontração.

Agradeço também aos queridos amigos que fiz no mestrado, Amanda de Souza Machado, Lázaro Henrique S. de M. Conceição, Larissa Inês Squinzani e Matheus Cezar Zanetti, pelos encontros, embora tenham sido poucos devido a pandemia, e pelos momentos de desabafo. Essa etapa se tornou mais leve graças a vocês. Coloco em destaque a grande amizade com a Amanda: mulher, negra e cientista. Você é motivo de muita inspiração!

À Rafaela Varassin Pegoraro, Ariane Andressa Lazzarin, Dominique Elizandra Mota e Renata Nicoski pelos laços construídos na graduação, mas que perduraram durante o mestrado. Com toda a certeza, vocês estarão para sempre em meu coração. Em especial à Rafa, que mesmo agora, tendo uma rotina totalmente diferente da minha, continua sendo minha melhor amizade desde o primeiro dia de aula da graduação.

Do Rio Grande do Sul ao Rio Grande do Norte, agradeço aos meus amigos Gabriel Baggio, Indira Coan Zanatta e Aline Senger Rover. Obrigado por continuarem fazendo parte da minha vida e sobretudo por me ensinarem a rir diante de todas as situações.

Aos amigos Felipe Hoffmann e Margaret Seghetto Nardelli (Marga) pelo conhecimento compartilhado durante minha iniciação científica com as diatomáceas. E Marga... precisamos viajar para um congresso novamente!

À Ivone Granatta, técnica do laboratório de ficologia da Unioeste, por ser uma pessoa extremamente prestativa e querida.

Ao professor Dr. Vladimir Pavan Margarido por conceder o uso do fotomicroscópio, ao Centro de Microscopia Eletrônica (CME) da UFPR por conceder o uso do microscópio de varredura, ao laboratório Acquasollus de Campo Mourão – PR pelas análises da água, e ao laboratório de análises agronômicas do PGEAGRI da Unioeste por conceder o uso dos materiais e pelo auxílio nas análises de metais no sedimento.

Às bancas de qualificação e de dissertação, Dra. Elaine Cristina Rodrigues Bartozek, Dra. Margaret Seghetto Nardelli e Dra. Angela Maria da Silva-Lehmkuhl pelas enormes contribuições para melhoria dos dois artigos que compõem este trabalho.

Agradeço à Alexandra Elbakyan por criar o site Sci-Hub, estreitando as barreiras entre o conhecimento científico e a sociedade.

A todos os professores e cientistas que batalham por um país melhor, tão necessários em momentos de negacionismo da ciência e divulgação de fake news.

Sou profundamente grato a inúmeros ativistas LGBTQIA+ por terem lutado e garantido muitos direitos, os quais hoje eu posso usufruir.

A Fundação Araucária (FA) e a Coordenação de Aperfeiçoamento de Pessoal de Nível Superior (CAPES) pela concessão da bolsa de mestrado, essencial para o desenvolvimento desta pesquisa.

Por fim, mas não menos importante, agradeço a Deus por me guiar e acompanhar durante minhas decisões, embora minhas convicções e minha visão sobre Ele possam ser peculiares.

Obrigado a todos que, mesmo não estando citados aqui, contribuíram de alguma maneira para a elaboração deste trabalho.

SUMÁRIO

RESUMO 13

ABSTRACT 14

ARTIGO I 15

- **Introduction** 15
- **Material and Methods** 16
- **Results** 17
- **Discussion** 22
- **References** 24

ARTIGO II 27

- **Introduction** 28
- **Material and Methods** 29
- **Results** 31
- **Discussion** 71
- **Conclusion** 74
- **References** 75

LISTA DE ILUSTRAÇÕES

ARTIGO I

Figures 1–26. *Nupela semifasciata* sp. nov., light microscopy images showing size diminution series and the variability of the valve outline 16

Figures 27–30. *Nupela semifasciata* sp. nov., SEM external whole valve views 18

Figures 31–39. *Nupela semifasciata* sp. nov., SEM external views 19

Figures 41–47. *Nupela semifasciata* sp. nov., SEM internal views................................. 20

Figures 48–50. *Nupela semifasciata* sp. nov., SEM external views showing areolae occluded by hymenes 21

ARTIGO II

Figure 1. Location of the eight sampling sites (S1–S8) in the Cascavel River microbasin, Paraná State, Southern Brazil 29

Figure 2. Epilithic diatoms from Cascavel River microbasin in LM 45

Figure 3. Epilithic diatoms from Cascavel River microbasin in LM 58

Figure 4. Epilithic diatoms from Cascavel River microbasin in LM 59

Figure 5. Epilithic diatoms from Cascavel River microbasin in LM 60

Figure 6. Epilithic diatoms from Cascavel River microbasin in LM 61

Figure 7. Epilithic diatoms from Cascavel River microbasin in LM 62

Figure 8. Epilithic diatoms from Cascavel River microbasin in LM 63

Figure 9. Epilithic diatoms from Cascavel River microbasin in LM 64

Figure 10. Epilithic diatoms from Cascavel River microbasin in LM 65

Figure 11. Epilithic diatoms from Cascavel River microbasin in LM 66

Figure 12. Epilithic diatoms from Cascavel River microbasin in SEM 67

Figure 13. Epilithic diatoms from Cascavel River microbasin in SEM 68

Figure 14. Epilithic diatoms from Cascavel River microbasin in SEM 69

Figure 15. Epilithic diatoms from Cascavel River microbasin in SEM 70

Figure 16. Epilithic diatoms from Cascavel River microbasin in SEM 71

LISTA DE TABELAS

ARTIGO I

Table 1. Range of physical, chemical, and biological variables of the water in which *Nupela semifasciata* was found 17

Table 2. Morphological information of *Nupela semifasciata* sp. nov. compared to similar taxa 23

ARTIGO II

Table 1. Epilithic diatom species identified from Cascavel River microbasin.................. 32

Table 2. Teratological diatoms found in Cascavel river microbasin, with occurrences in sampling sites, and related metals... 46

Appendix A - Table 1. Predominant land use, and physical characteristics of sampling sites 89

Appendix B – Table 1. Location of sampling sites (S), and sample register number at Universidade Estadual do Oeste do Paraná Herbarium (UNOPA) 90

Appendix C – Table 1. Limnological variables (mean ± standard deviation) analyzed from water samples collected in the eight sampling sites from Cascavel River microbasin....... 91

Appendix D - Table 1. Mean concentrations of metals in sediment samples collected from the eight sampling sites in the Cascavel River microbasin 94

Amaral, Mailor Wellinton Wedig. **Diatomáceas epilíticas de riachos subtropicais com altas concentrações de Ferro e Alumínio, Sul do Brasil**. 94 pp. Dissertação de mestrado do Programa de Pós-Graduação em Conservação e Manejo de Recursos Naturais – Universidade Estadual do Oeste do Paraná, Cascavel, 2022.

RESUMO

As diatomáceas epilíticas são microrganismos fotossintéticos crescendo aderidos ao substrato rochoso. Estudos taxonômicos abordando floras de diatomáceas são cruciais para descrever novas espécies, assim como reconhecer estresses ambientais e avaliar o status ecológico dos sistemas aquáticos. Este trabalho teve o objetivo de conduzir um levantamento taxonômico das diatomáceas epilíticas de uma microbacia hidrográfica no sul do Brasil com concentrações naturalmente altas de ferro e alumínio. A amostragem das rochas, água e sedimentos foi realizada entre 2016 e 2019. As amostras de diatomáceas foram oxidadas e analisadas em microscopia eletrônica de luz e varredura. O primeiro artivo trata da descrição de uma nova espécie do gênero *Nupela*, encontrada em córregos com pH neutro-ácido, baixa condutividade e baixas a altas concentrações de nutrientes. No segundo artigo identificamos 221 espécies de diatomáceas em nível infragenérico, enfatizando suas formas teratológicas e caracterizando as condições limnológicas e concentrações de metais onde foram encontradas. *Fragilaria spectra*, *Fragilaria tenera* var. *nanana* e *Humidophila arcuatoides* foram registradas primeiramente no estado do Paraná e *Pinnularia laucensis* representa um novo registro para o Brasil. Valvas teratológicas foram encontradas em 34 táxons, contendo contorno modificado, alterações no padrão de estrias e área central duplicada. Os metais e variáveis ambientais na microbacia do Rio Cascavel provavelmente contribuíram para as teratologias nas diatomáceas. Nosso trabalho contribui para o conhecimento taxonômico das diatomáceas epilíticas na região, bem como para ampliar o registro de táxons teratológicos na literatura.

Palavras-chave: Bacillariophyta, ambientes lóticos, metais, morfologia, espécie nova, perifíton, taxonomia, teratologia

Amaral, Mailor Wellinton Wedig. **Epilithic diatoms from subtropical streams with high concentrations of aluminum and iron, Southern Brazil**. 94 pp. Master's dissertation from the Graduate Program in Conservation and Management of Natural Resources, Western Paraná State University, Cascavel, 2022.

ABSTRACT

Epilithic diatoms are photosynthetic microorganisms growing attached to rocky substrate. Taxonomic studies approaching diatom floras are crucial for describing new species, as well as recognizing environmental stresses and assessing the ecological status of aquatic systems. This work aimed to conduct a taxonomic survey of epilithic diatoms from a hydrographic microbasin in southern Brazil with naturally high iron and aluminum concentrations. Sampling of rocks, water and sediments were carried out from 2016 to 2019. Diatom samples were oxidized and analyzed using light and scanning electron microscopy. The first article deals with the description of a new species of the genus *Nupela*, which was found in streams with acidic–neutral pH, low conductivity and low to high nutrient concentrations. In the second article we identified 221 diatom species at infrageneric level, focusing on their teratological forms and characterizing the limnological conditions and metal concentrations where they were found. *Fragilaria spectra*, *Fragilaria tenera* var. *nanana* and *Humidophila arcuatoides* were firstly recorded in the state of Paraná, and *Pinnularia laucensis* represent a new record for Brazil. We found teratological valves in 34 taxa, containing modified outline, changes in the striae pattern, and doubled central area. The metals and environmental variables in the Cascavel River microbasin probably contributed to the diatom teratologies. Our work contributes to the taxonomic knowledge of epilithic diatoms in the region, as well as extending the record of teratological taxa in the literature.

Keywords: Bacillariophyta, lotic environments, metals, morphology, new taxa, periphyton, taxonomy, teratology

Fottea, Olomouc, 21(2): 152–163, 2021
DOI: 10.5507/fot.2021.002

Nupela semifasciata (Bacillariophyceae), a new species from subtropical lotic environments in Western Paraná State, Brazil

Mailor Wellinton Wedig Amaral[1*], Gabriela Medeiros[1], Vanessa Daufenbach[2], Morgana Suszek Gonçalves[2], Thelma Alvim Veiga Ludwig[3] & Norma Catarina Bueno[1]

[1] Universidade Estadual do Oeste do Paraná, Rua Universitária, 2019, Jardim Universitário, CEP 85819–110, Cascavel, Paraná, Brasil; e–mails: wedig_npi@hotmail.com (*Corresponding author), gabsmedeiros@gmail.com, normacatarina@hotmail.com
[2] Universidade Tecnológica Federal do Paraná, Mestrado Profissional em Rede Nacional em Gestão e Regulação de Recursos Hídricos (ProfÁgua) and Laboratório de Análises ambientais e agronômicas – Acqua Sollus, Campo Mourão, Paraná, Brasil; e–mails: vanessa.daufenbach@gmail.com, morgana@utfpr.edu.br
[3] Universidade Federal do Paraná. Setor de Ciências Biológicas. Centro Politécnico, Caixa Postal 19031, Jardim das Américas, CEP 81531–980, Curitiba, Paraná, Brasil; e–mail: veiga13ufpr@gmail.com

Abstract: During a survey on freshwater epilithic diatoms from subtropical lotic environments belonging to the Cascavel River microbasin, Paraná State, Brazil, we observed populations of a new *Nupela* Vyverman et Compère species. Morphological and meristic analyses were performed using light and scanning electron microscopy, resulting in the description of *Nupela semifasciata* sp. nov. This species is characterized by elliptic–lanceolate valves containing subcapitate apices in larger individuals and broadly rostrate–rounded apices in smaller ones, while the length/width ratio gradually decreases as the individuals become smaller. The central area unilaterally reaches the margin and always interrupts the row of areolae on the valve mantle. The valve mantle is externally composed of a second row of areolae near the apices. We cross–checked information with similar *Nupela* taxa, highlighting the main features that separate them. *Nupela semifasciata* was found in streams with acidic–neutral pH, low conductivity and low to high nutrient concentrations.

Key words: diatoms, morphology, new taxa, *Nupela*, periphyton, taxonomy

Introduction

One of the major obstacles in diatom taxonomy is that light microscopy is often insufficient for species level identification (Potapova et al. 2003). This process is particularly accentuated in small–sized diatoms, such as *Nupela*, in which the individuals generally measure less than 20 µm (Spaulding & Edlund 2008). Ultrastructural analysis of frustules obtained by electron microscopy provides observation of additional features that improves accurate species diagnosis (Zimmermann et al. 2014) and, thus, supports taxonomic robustness for biodiversity conservation purposes (Thomson et al. 2018).

Nupela Vyverman et Compère was proposed as a distinct genus based on samples collected in high elevation ponds with a peaty bottom in Papua New Guinea, with *N. giluwensis* as the generitype. The authors pointed out morphological similarities with *Brachysira* Kützing and *Diadesmis* Kützing, such as striae composed of a few areolae transversally elongated, a ridge or a hyaline area at the junction of the valve face and mantle, and simple or inconspicuous proximal raphe fissures (Vyverman & Compère 1991). However, recent phylogenetic investigations suggested that *Nupela* and *Brachysira* form a non–monophyletic group, with *Nupela* not being assigned to the family Brachysiraceae (Kulikovskiy et al. 2020). In addition, Siver et al. (2007) expanded the circumscription of this genus to comprise cells with small size, terminal raphe ends externally curved to the secondary side, straight proximal raphe ends, Voigt faults indicating the secondary side of the valve, and a single row of elongated areolae throughout the valve mantle. The last feature appears to be well–established within the genus (Vyverman & Compère 1991; Siver et al. 2007; Falasco et al. 2015), along with the typical external openings of areolae covered by hymen that are larger than internal ones (Siver et al. 2007; Spaulding & Edlund 2008). Regarding the raphe, *Nupela* possesses isovalvar forms with two fully developed raphe slits, such as in *N. giluwensis* (Vyverman & Compère

1991) and *N. amabilis* (Tremarin et al. 2015); however, the vast majority of species are heterovalvar with one valve containing shortened raphe slits, as in *N. pardinhoensis* (Bes et al. 2012), rudimentary slits, as in *N. scissura* (Siver et al. 2007) and *N. rumrichorum* (Lange–Bertalot & Moser 1994), or absent raphe slits as in *N. praecipuoides* (Tremarin et al. 2015) and *N. major* (Yu et al. 2017).

Since it was established, several species have been transferred from other genera to *Nupela*, mainly *Achnanthes* Bory, due to its monoraphid condition, and *Navicula* Bory, due to the areolae openings shape, which are externally elongated and internally rounded (see Lange–Bertalot & Moser 1994; Potapova 2013; Tremarin et al. 2015). The number of new *Nupela* taxa is still increasing, consisting of 85 species taxonomically accepted for science, according to Algaebase (Guiry & Guiry 2020).

The genus generally occurs in oligotrophic waters with acidic to circumneutral pH (e.g., Monnier et al. 2003; Potapova et al. 2003; Wojtal 2009; Kulikovskiy et al. 2010), being particularly well represented in the Neotropics (Metzeltin & Lange–Bertalot 1998; Wojtal 2009). At present, seven taxa were described as new species for science based on Brazilian samples. One of them, *N. pardinhoensis* Bes, Torgan et Ector was found in slow moving waters with high dissolved oxygen, low biochemical oxygen demand, and high total phosphate concentration in the State of Rio Grande do Sul (Bes et al. 2012) and the other six, *N. amabilis* Tremarin et Ludwig, *N. difficilis* Straube, Tremarin et Ludwig, *N. kocioleckii* Straube, Tremarin et Ludwig, *N. metzeltinii* Tremarin et Ludwig, *N. praecipuoides* Tremarin et Ludwig and *N. torganiae* Tremarin et Ludwig, were generally found in rivers with high water speed, low conductivity, and neutral pH in Paraná State (Tremarin et al. 2015).

The aim of this study was to describe and illustrate a new species of *Nupela* using light and scanning electron microscopy observations, and compare it with similar taxa, thus, expanding the knowledge on the genus.

Material and Methods

Study area. The Cascavel River (24°32'and 25°17'S; 53°05' and 53°50'W) is 17.5 km long and represents the principal source of water supply for Cascavel City, with the main tributaries within the urban perimeter (Fundetec 1995). The river is located in Western Paraná, a subtropical region characterized by hot and humid summers, with an average annual temperature of 22 °C (Alvares et al. 2013).

For the study, we selected eight sampling sites (S) along the Cascavel River microbasin, as follows: S1 – urban perimeter, inside the conservation area of Paulo Gorski Ecological Park, with presence of *Hydrochoerus hydrochaeris* Linnaeus populations. Stream with visible silting up process. S2 – urban area, close to a highway, containing ciliary vegetation. S3 – urban area, close to a highway, lacking ciliary vegetation and visible silting up process. S4 – urban area, close to a garbage collection property, containing sparce ciliary vegetation and receiving water from storm drains. Presence of a bridge over the stream for pedestrian traffic. S5 – rural area, close to temporary croplands and a highway, containing ciliary vegetation. Presence of a bridge over the stream for pedestrian traffic. S6 – conservation area within a rural property, with goat farming, *Pinus* sp. plantation and temporary croplands. S7 – urban area, close to a deactivated fridge, containing ciliary vegetation. Stream with visible silting up process. S8 – rural area with temporary croplands, close to a basalt mining company using mineral deposits. Presence of a bridge over the stream for vehicle traffic.

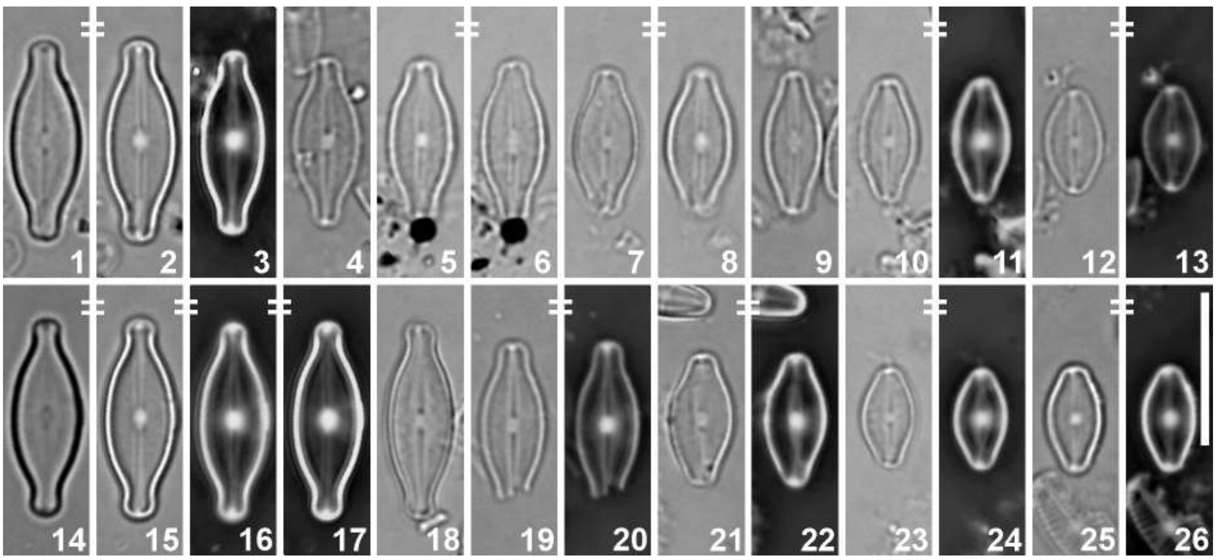

Figs 1–26. *Nupela semifasciata* sp. nov., light microscopy images showing size diminution series and the variability of the valve outline: (1, 2) are the holotype, (3, 11, 13, 16, 17, 20, 22, 24, 26) were taken in phase contrast. The = symbol represents different valves of the same frustule. Scale bar represents 10 µm.

Table 1. Range of physical, chemical, and biological variables of the water in which *Nupela semifasciata* was found. Legend: (Temp) water temperature, (Cond) electrical conductivity, (DO) dissolved oxygen, (Turb) turbidity, (COD) chemical oxygen demand, (BOD) biochemical oxygen demand, (TKN) Kjeldahl nitrogen, (NO_3) nitrate, ($N–NH_3$) ammoniacal nitrogen, (TP) total phosphorus, (PO_4^-) orthophosphate, (TS) total solids, (DS) dissolved solids, (SS) suspended solids, (CLa) chlorophyll–a, (TC) total coliforms, (*E. coli*) *Escherichia coli*.

Variables	Range (min – max)
Temp (°C)	16.67–23.70
Cond ($mS.cm^{-1}$)	0.001–0.091
DO ($mg.l^{-1}$)	6.53–14.27
pH	5.40–7.42
Turb (NTU)	0.06–41.90
COD ($mg.l^{-1}$)	5.10–24.32
BOD ($mg.l^{-1}$)	1.19–9.90
TKN ($mg.l^{-1}$)	0.00–0.92
NO_3 ($mg.l^{-1}$)	0.32–14.00
$N–NH_3$ ($mg.l^{-1}$)	0.003–0.448
TP ($mg.l^{-1}$)	0.005–0.060
PO_4^- ($mg.l^{-1}$)	0.002–0.030
TS ($mg.l^{-1}$)	4.00–81.00
DS ($mg.l^{-1}$)	3.30–66.70
SS ($mg.l^{-1}$)	0.20–40.00
CLa ($\mu g.l^{-1}$)	0.000–16.382
TC (NMP 100 ml^{-1})	1–606000
E. coli (NMP 100 ml^{-1})	1–606000

Field and laboratory procedures. Samplings were performed seasonally from 2016 to 2018, comprising eight samplings. We collected periphytic substrates (stones) in triplicates at each sampling site, totaling 204 qualitative samples. Water samples for physical, chemical, and biological analysis were collected one per sampling site.

The physical and chemical variables, such as water temperature, conductivity, dissolved oxygen, pH, and turbidity were measured in situ with a HORIBA U–5000 multiparameter probe. Additionally, water samples were collected using polyethylene bottles immersed in the surface of the water column, being adequately cooled, and kept in the dark, from which the environmental variables function of chemical oxidation and organic material, concentrations of total Kjeldahl nitrogen, nitrate, ammoniacal nitrogen, total phosphorus, orthophosphate, and total, dissolved, and suspended solids were measured. The biological variables chlorophyll–a, total coliforms, and *Escherichia coli* were also analyzed. All analyses were realized following the Standard Methods (APHA 2012). The flow ($m^3.s^{-1}$) and depth (m) were measured using a ruler, metric tape, and polystyrene floating object, in a transect previously delimited for each stream. The flow was calculated by multiplying the length of the transect and the average speed resulting from the object's displacement.

Diatoms were scraped off the stones and fixed in Transeau solution 1:1 according to Bicudo & Menezes (2017). Subsamples of 10 ml were oxidized following the Simonsen (1974) technique, modified by Moreira–Filho & Valente–Moreira (1981). Permanent slides were mounted from the cleaned diatom material using Naphrax® for light microscopy (LM) observations, using an Olympus BX60 microscope with a DP 71 capture camera attached, at 1000×. Cleaned samples were also placed in aluminum stubs, sputter–coated with gold in Balzers Union SCD 030, and examined with JEOL JSM 6360LV scanning electron microscope, operated at 15 kV and 9–10 mm of working distance. Species description follows the terminology of specialized literature.

Results

Nupela semifasciata **Amaral, T.Ludwig et Bueno sp. nov. (Figs 1–50)**

Description

Light microscopy (Figs 1–26): frustules heterovalvar regarding the raphe development, sometimes asymmetrical about apical and transapical planes (Figs 1–26). Length/width ratio gradually decreases as the valves become smaller, while the valve outline is modified. Valves elliptic–lanceolate containing subcapitate apices in larger individuals (Figs 1–3, 14–18) and rostrate in middle ones (Figs 4–11, 19–22), slightly drawn–out, becoming broadly rostrate–rounded in smaller individuals (Figs 12, 13, 23–26). Axial area narrowly lanceolate, slightly broadening toward the central area. Central area transversely expanded, asymmetric, unilaterally reaching the valve margin, discernible only in phase contrast images (Figs 3, 11, 13, 16, 17, 20, 22, 24, 26). One valve with long raphe slits and the other valve with slightly shorter raphe slits (compare Figs 1 to 2, 5 to 6, 7 to 8, 14 to 15).

Measurements (n= 89, occurring in 46 diatom samples): 6.7–16.4 µm long; 3.2–4.8 µm wide; 1.7–3.7 ratio length/width.

Scanning electron microscopy (Figs 27–39, 48–50 external views, Figs 41–47 internal views): axial area appears narrowly lanceolate (Figs 28–30, 41) or broadly lanceolate (Fig 27), sometimes with external siliceous thickenings surrounding the raphe and delicate depressions along the apical axis (Figs 27, 28, 31, 33, 49, 50). Central area broadly asymmetric, limited by irregular shortened marginal striae, ranging from rectangular (Fig 31) to rounded (Figs 28–30, 32) or rhombic (Figs 27, 33) shape, unilaterally reaching the secondary margin of the valve. The fascia is variable in shape, large or reduced, and always extends onto the valve mantle (Figs 27, 29, 31–33). Sometimes, a single areola appears in the fascia (Figs 31, 41). Valve mantle ornamented with one row of transversely elongated areolae along the valve (Fig 28) and at the end of

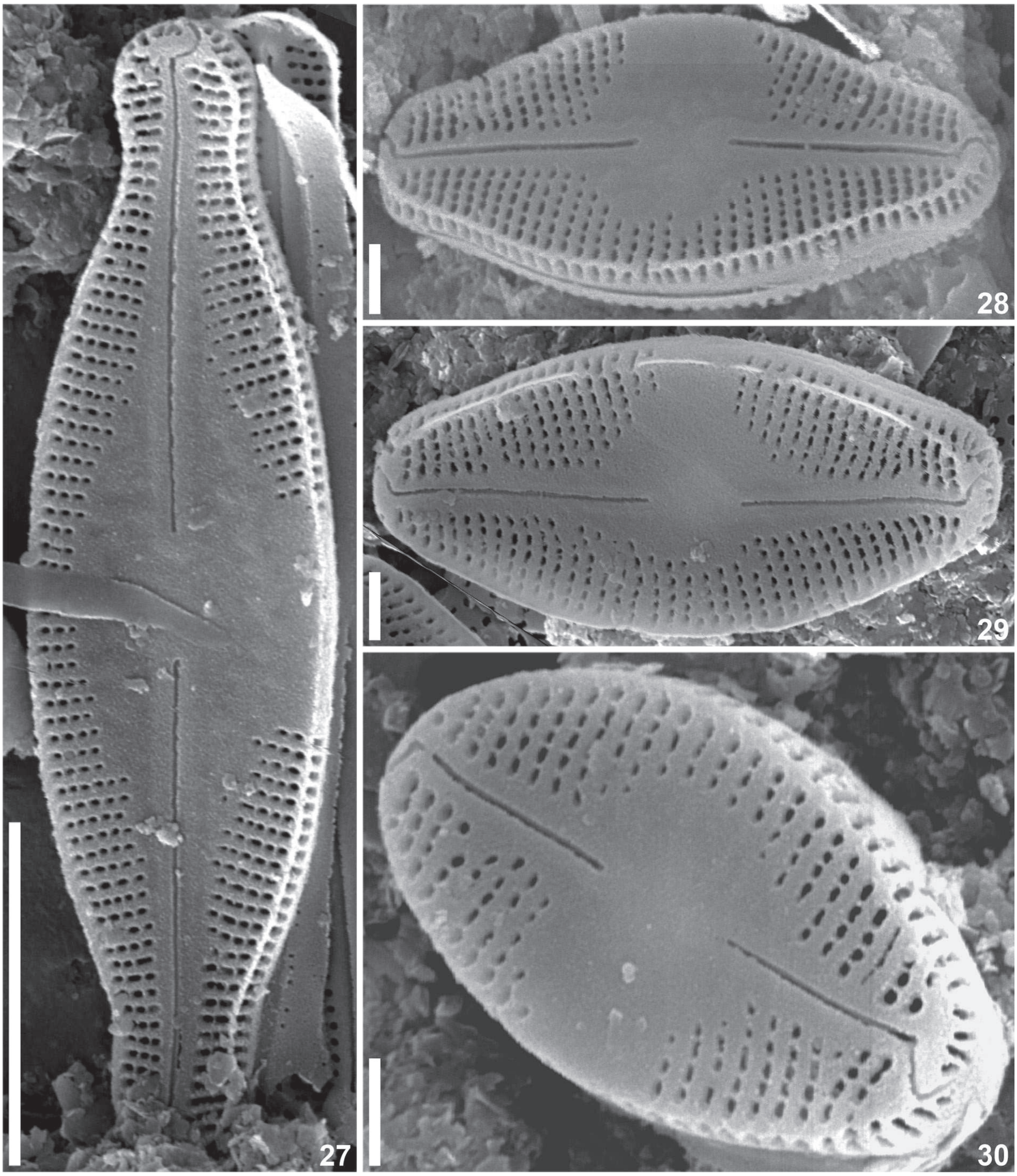

Figs 27–30. *Nupela semifasciata* sp. nov., SEM external whole valve views: (27) entire valve with shorter raphe slits showing the siliceous thickenings surrounding the raphe, delicate depressions along the apical axis, and the rhombic–shaped central area. Also note the ridge along the valve face–mantle junction and the interrupted mantle. (28, 29) entire valves with long raphe slits showing the mantle composed of one row of transversely elongated areolae along the whole valve, becoming two rows near the apices (28), and interrupted by the unilateral fascia (29). Note the asymmetrically rounded central area. (30) entire valve of a smaller individual with shorter raphe slits. Detail of the asymmetrically rounded central area and the hook–shaped terminal raphe fissure extending onto the valve mantle, interrupting the row of elongated areolae. Note the Voigt fault (27–30) on the secondary side of the valve, marked as a change in the striae pattern from radiate to convergent. Scale bars represent 5 µm (27), 1 µm (28–30).

the apex (Figs 30, 36), however, externally becoming two rows of elliptic areolae near the apices (white arrows in figs 34–39). Internally, the mantle appears to be ornamented with only one row of areolae (Figs 41, 47). The mantle is interrupted by the central area on the secondary margin (Figs 27, 29) and by the terminal raphe fissures at the apices (Figs 30, 34–36, 38, 39). In some cases, a ridge is evident on the valve face–mantle junction (Figs 27–29). Raphe filiform, almost straight (Fig 28, 41, 49) or slightly sinuous (Figs 27,

 Fottea, Olomouc, 21(2): 152–163, 2021
DOI: 10.5507/fot.2021.002

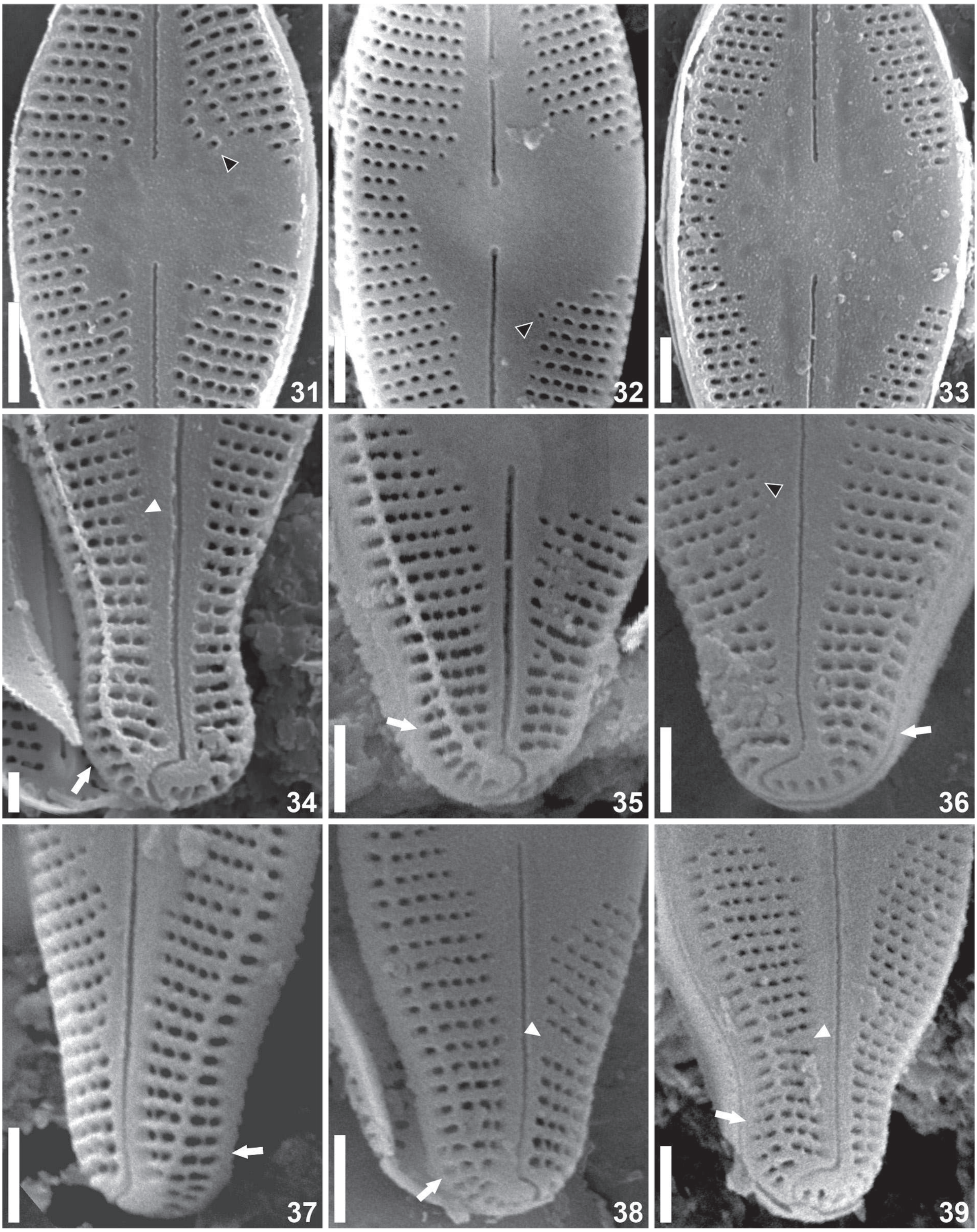

Figs 31–39. *Nupela semifasciata* sp. nov., SEM external views: (31–33) asymmetrically shaped central area, rectangular (31), rounded (32), or rhombic (33). Note the single areola in the middle of the fascia (31). Raphe with long slits (32) or slightly shorter (31, 33). Proximal raphe endings simple (31, 33) or pore–like (32), straight (31) or slightly curved to the secondary side of the valve (32, 33). Note the siliceous thickenings surrounding the raphe and delicate depressions along the apical axis (31, 33). (34–39) valve apices. Second row of areolae on the valve mantle (white arrows in 34–39). White arrowheads indicate Voigt fault as a missing areola (34) or as a marked change in striae pattern (39). Black arrows indicate an isolated areola at the end of striae (31, 32, 36). Scale bars represent 1 µm.

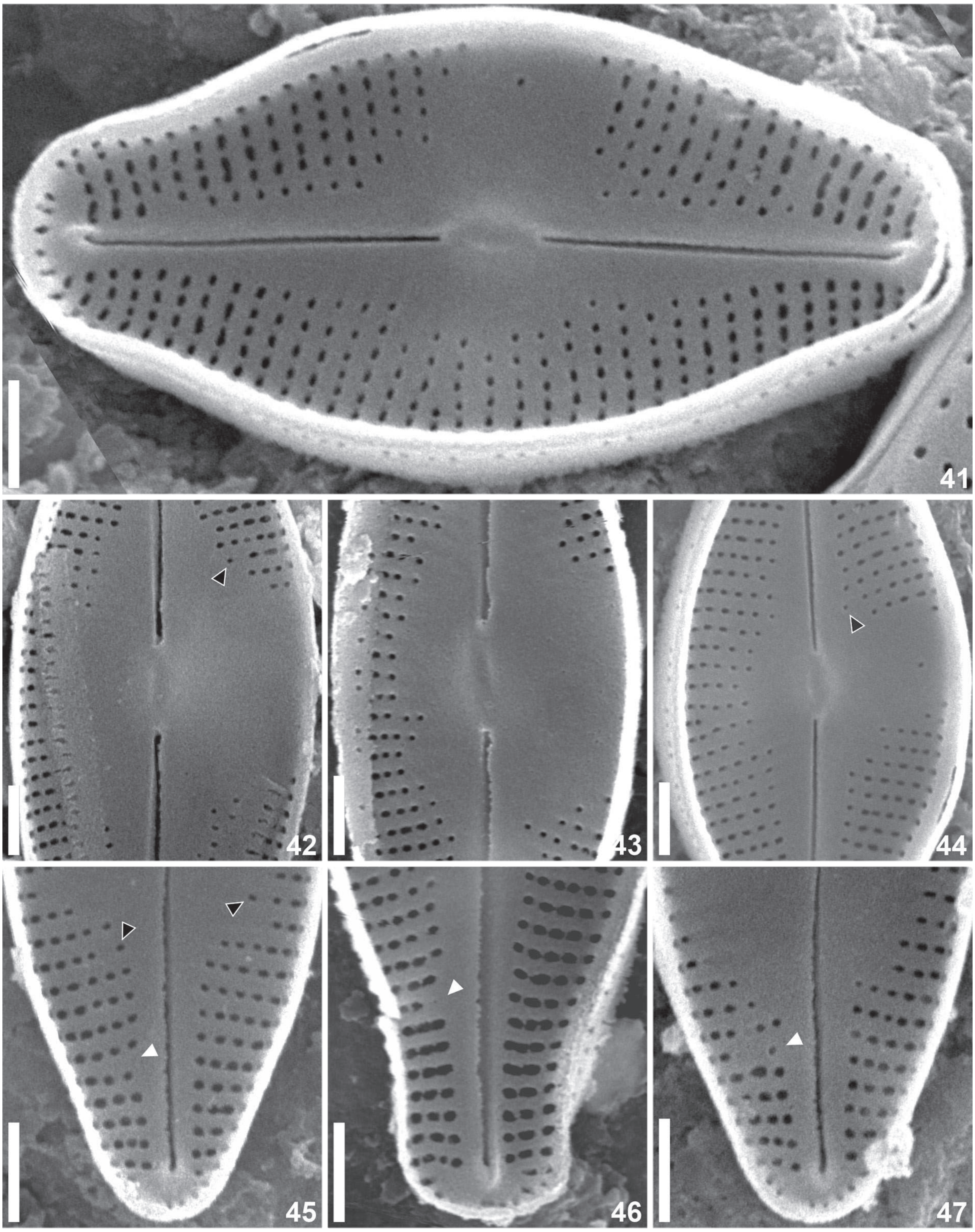

Figs 41–47. *Nupela semifasciata* sp. nov., SEM internal views: (41) whole valve. Axial area narrowly lanceolate, raphe almost straight, and small inner areolae openings. Note the single areola in the middle of the fascia. (42–44) central area. Proximal raphe endings straight (42, 43) or bent (44), simple (44) or pore–like (42, 43). Note the mantle interrupted by the unilaterally expanded fascia. (45–47) valve apices. Terminal raphe ends finishing in small helictoglossa, straight (46) or slightly curved (45, 47). Note the Voigt fault as a marked change in striae pattern (white arrowhead in 45, 47) or like a missing areola (white arrowhead in 46). Also note isolated areola in (42, 44, 45) (black arrowheads). Scale bars represent 1 µm.

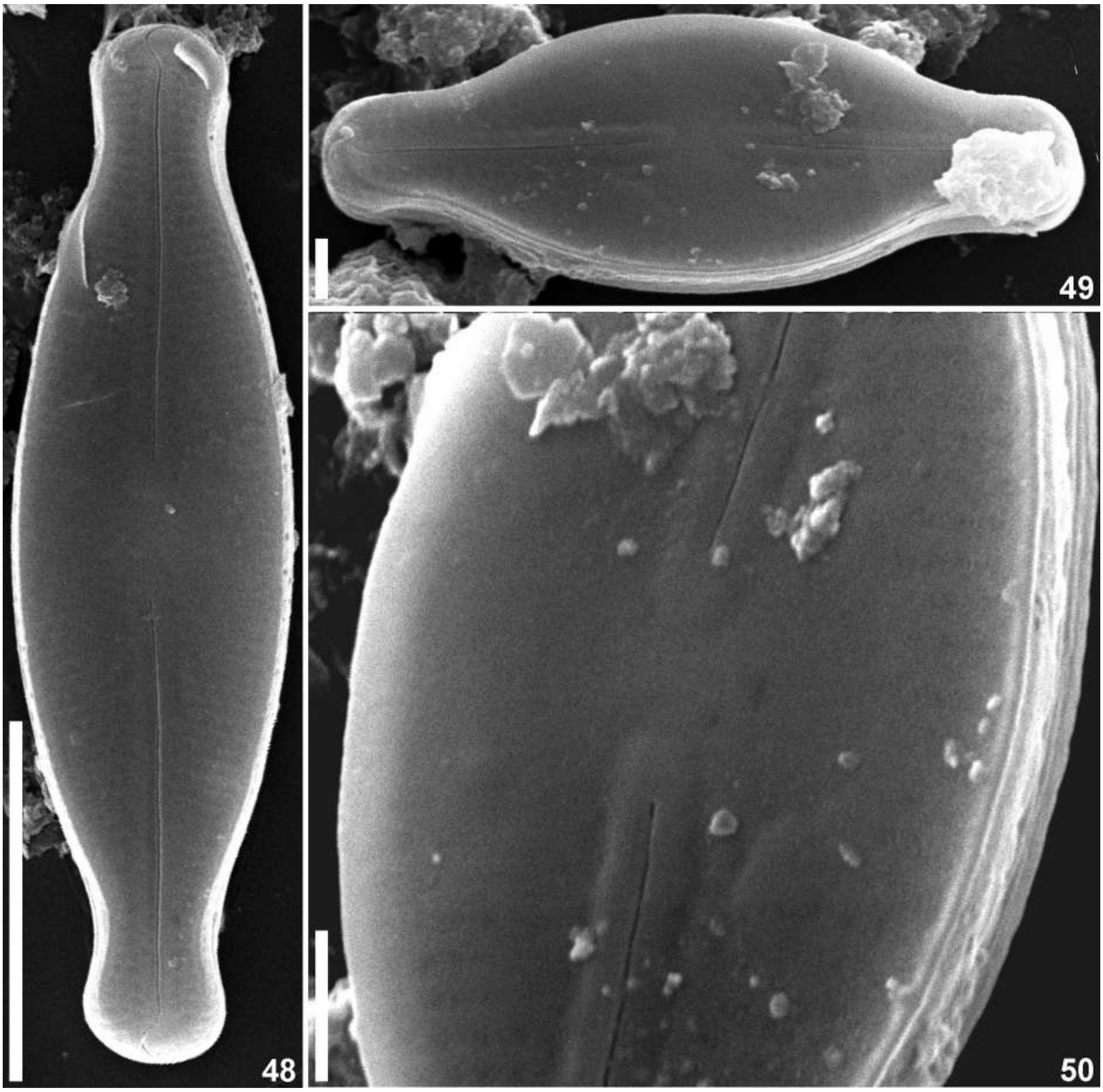

Figs 48–50. *Nupela semifasciata* sp. nov., SEM external views showing areolae occluded by hymenes: (48–49) whole valve views. Raphe filiform, almost straight (49) or slightly sinuous (48), with simple proximal ends, slightly curved to one side, and terminal ends hook–shaped, reaching the mantle. (50) detail of central region of valve. Raphe with simple proximal raphe ends, curved to the same side, and surrounded by siliceous thickenings. Scale bars represent 5 µm (48), 1 µm (49, 50).

29, 30, 48). Proximal raphe ends are simple (Figs 31, 33, 44, 48, 49) or pore–like (Figs 32, 42, 43), straight (Figs 31, 42, 43) or somewhat bent to the primary side of the valve (Figs 32, 33, 44, 48, 49). Terminal raphe ends are externally hook–shaped, curved to the secondary side of the valve, reaching the valve mantle (Figs 34–39, 48, 49) and internally finishing in small helictoglossa, straight (Fig 46) or slightly curved (Figs 45, 47). Voigt fault occurs as a markedly changing striae pattern (white arrowheads in figs 38, 39, 45, 47) or seems like an areola is missing (white arrowhead in figs 34, 46). Striae radiate throughout the valve, becoming slightly (Figs 36–39, 45–47) to strongly (Figs 30, 34, 35) convergent near the apices, 40–48/10 µm. Striae are composed by a variable number of areolae (commonly 4–6), arranged in continuous lines of areolae, although an isolate areola can be present at the end of some striae (black arrowheads in Figs 31, 32, 36, 42, 44, 45). Areolae small, rounded to transversally elongated in elliptic or rectangular shape (Figs 27–39), internally smaller in diameter relative to outer openings (Fig 41–47), 39–59/10 µm, commonly ca. 50. Outer openings of areolae are occluded by hymenes (Figs 48–50).

Holotype: slide no. 5364, sample site 4, designated here in figs 1 and 2, deposited in Norma C. Bueno collection at the Herbarium of Western Paraná State University (UNOPA), Cascavel municipality, Brazil.

Type locality: Brazil, State of Paraná, Cascavel municipality, Cascavel River, 24°32' and 25°17'S; 53°05' and

53°50'W, epilithic samples, collected by G. Medeiros et al. on 03/08/2018.

Etymology: the specific epithet refers to the wide central area unilaterally reaching the margin, always interrupting the single row of mantle areolae.

Ecology: *Nupela semifasciata* was found in 46 of 204 epilithic samples analyzed, from which the average values of ecological parameters were calculated, considering the eight samplings performed. The new species occurred in streams with low flow (average of 0.24 $m^3.s^{-1}$), low depth (average of 0.06 m), low conductivity (average of 0.05 $mS.cm^{-1}$), low to high nutrient concentrations (e.g., NO_3: 2.00–14.00 $mg.l^{-1}$), and low pH (average of 6.28) (Table 1). Other diatom taxa co–occurred in the samples, such as *Achnanthidium minutissimum* (Kützing) Czarnecki, *Humidophila contenta* (Grunow) Lowe, Kociolek, Johansen, Van de Vijver, Lange–Bertalot et Kopalová, *Sellaphora saugerresii* (Desmazières) Wetzel et Mann, *Sellaphora nigri* (De Notaris) Wetzel et Ector and some other unidentified species of *Eunotia* Ehrenberg and *Nupela* Vyverman et Compère.

DISCUSSION

Nupela semifasciata is characterized by elliptic–lanceolate valves containing subcapitate apices in larger individuals and broadly rostrate–rounded apices in smaller ones, while the length/width ratio gradually decreases as the individuals become smaller. The central area unilaterally reaches the margin and always interrupts the row of areolae on the valve mantle. The valve mantle is externally composed of a second row of areolae near the apices.

The new species shares morphological and morphometric similarities with some currently known species of the genus, but some features can be used to differentiate them (see Table 2). *N. deformis* Lange–Bertalot has deeper depressions along the apical axis, clearly visible in LM images, one valve with rudimentary raphe, and higher striae density (ca. 60 vs 40–48/10 µm) (LANGE–BERTALOT & MOSER 1994). *N. lesothensis* (Schoeman) Lange–Bertalot contains a considerably higher number of areolae in 10 µm (50–68 in SCHOEMAN 1973; 50–74 in SALA et al. 2014; 50–70 in KULIKOVSKIY et al. 2020 vs 39–59 in our study) and one valve with rudimentary raphe slits (SCHOEMAN 1973; SALA et al. 2014). Additionally, the central area does not always reach the valve margin (see SALA et al. 2014). The main features that differentiate *N. paludigena* (Scherer) Lange–Bertalot are the wider and often capitate apices, smaller central area, and proximal raphe ends, externally teardrop–shaped and internally t–shaped (LANGE–BERTALOT & MOSER 1994; SIVER et al. 2007). *N. tenuicephala* (Hustedt) Lange–Bertalot slightly resembles *N. semifasciata*, however, it has dorsiventral valves with strongly capitate apices, the internal proximal raphe ends are hook–shaped, and the striae are generally higher in number (50–60 vs 40–48/10 µm), composed of wider areolae (LANGE–BERTALOT 1993). Lastly, *N. neotropica* Lange–Bertalot and *N. subpallavicinii* Metzeltin et Lange–Bertalot share the fascia that unilaterally reaches the valve margin, but in both taxa, the internal proximal raphe endings are hook–shaped (LANGE–BERTALOT & MOSER 1994; SALA et al. 2014, respectively). In addition, *N. subpallavicinii* has a radiate striae pattern along the whole valve (METZELTIN & LANGE–BERTALOT 1998), and *N. neotropica* has wider areolae (LANGE–BERTALOT & MOSER 1994).

Nupela wellneri (Lange–Bertalot) Lange–Bertalot, the most similar taxon, was first described in Germany as *Navicula wellneri* by LANGE–BERTALOT & KRAMMER (1987) and was later transferred to *Nupela* based on samples collected in the Andean region by RUMRICH et al. (2000). *Nupela semifasciata* and *Nupela wellneri* possess lanceolate valve outlines, one valve containing long raphe slits and the other valve containing shorter raphe slits, as well as a broad central area, expanded more pronouncedly to one side of the valve. However, in comparison to the protologue, the individuals found in our samples have broader variation in size (length: 6.7–16.4 vs 12–14 µm; width: 3.2–4.8 vs 4–4.8 µm), striae (40–48/10 µm vs ca. 45/10 µm) and areolae densities (39–59/10 µm vs ca. 50/10 µm). Previous studies registered *N. wellneri* with a larger range in size (8.5–15 µm long and 3–4.5 µm wide in POTAPOVA et al. 2003; 11.8–16.6 µm long and 3.7–4.4 µm wide in TREMARIN et al. 2015), striae (38–42/10 µm in POTAPOVA et al. 2003; ca. 42/10 µm in TREMARIN et al. 2015), and areolae (40–50/10 µm in TREMARIN et al. 2015). However, this species was not described and illustrated showing gradual length/width diminution associated with valve outline modification, as we observed in *N. semifasciata*. While in *N. semifasciata* the axial area varies from narrow to wide and the central area always extends onto the valve margin, LANGE–BERTALOT & KRAMMER (1987) originally described *N. wellneri* with broadly expanded axial and central areas, limited by very short striae. POTAPOVA et al. (2003), POTAPOVA (2010), and TREMARIN et al. (2015) illustrated individuals of *N. wellneri* similar to the protologue, but exemplars with a narrower axial area (Figs 76, 77; internal view; 137, 139, respectively) and the central area reaching the margin (Figs 78, 79 in POTAPOVA et al. 2003 and internal view in POTAPOVA 2010) are included, suggesting the close relationship of these specimens with *N. semifasciata*.

Considering the central area, its symmetry, shape, size, and extent are important morphological features within *Nupela* (see SIVER et al. 2007; WOJTAL 2009; BAHLS 2011; YU et al. 2017; GENKAL & YARUSHINA 2018; RYBAK et al. 2020). The central area unilaterally reaching the margin, consistently observed in *N.*

Table 2. Morphological information of *Nupela semifasciata* sp. nov. compared to similar taxa.

Species	***N. semifasciata***	***N. deformis***	***N. lesothensis***	***N. neotropica***	***N. paludigena***	***N. subpallavicinii***	***N. tenuicephala***	***N. wellneri***
Reference	Our study	Lange–Bertalot & Moser (1994)	Schoeman (1973)[1] Sala et al. (2014)[2]	Lange–Bertalot & Moser (1994)	Siver et al. (2007)	Metzeltin & Lange–Bertalot (1998)[1] Sala et al. (2014)[2]	Hustedt (1942)[1] Lange–Bertalot (1993)[2]	Lange–Bertalot & Krammer (1987)
Length (µm)	6.7–16.4	11–18	5.3–13.5[1]	12–18	10–20	11–16[1]	11–15[1]	12–14
Width (µm)	3.2–4.8	4–5.5	2.6–3.2[1]	3–4	3–5	3.3–4.7[1]	2.5–3[1]	4–4.8
Length/width	1.7–3.7	n.d.	3–3.6[2]	n.d.	n.d.	n.d.	n.d.	n.d.
Striae in 10 µm	40–48	ca. 60	42–46[1]	50–55	38–45	40–45[1]	n.d.	45
Areolae in 10 µm	39–59	n.d.	50–68[1]	n.d.	n.d.	28–37[2]	n.d.	50
Valve outline	Elliptical–lanceolate, with subcapitate to broadly rostrate–rounded apices	Elliptical–lanceolate, with rostrate apices	Elliptical–lanceolate, with capitate to broadly rounded apices[1]	Elliptical–lanceolate, with abruptly rostrate–protracted apices	Elliptical–lanceolate to linear–lanceolate, with rostrate to capitate apices	Elliptical, with capitate apices[1]	Linear, with small and capitate apices[1]	Lanceolate, with subcapitate–rounded protracted apices
Central area	Asymmetric, broadly rhombic to rounded, unilaterally reaching the mantle	Asymmetric, lanceolate, not reaching the mantle	Asymmetric, indistinct, unilaterally reaching the mantle[1]	Asymmetric*, unilaterally reaching the mantle	Asymmetric*, elliptical to rectangular, not reaching the mantle	Asymmetric*, broadly triangular, unilaterally reaching the mantle[1]	Symmetric*, indistinctly linear, unilaterally reaching the mantle*[2]	Asymmetric, broadly lanceolate, not reaching the mantle*
Valve mantle	Single row of areolae, interrupted at center, becoming two rows near the apices	n.d.	Single row of areolae, interrupted near the apices[2]	Single row of areolae, interrupted by the central area*	Single row of areolae, not interrupted	Single row of areolae, interrupted at the apices and at the center[2]	Single row of areolae, interrupted by the central area*[2]	n.d.
Raphe development	One valve with long raphe slits and the other valve with slightly shorter raphe slits	One valve with long raphe slits and the other valve with rudimentary raphe slits	One valve with long raphe slits and the other valve with rudimentary raphe slits[1]	Both valves with long raphe slits*	Both valves with long raphe slits	At least one valve with long raphe slits*	One valve with long raphe slits and the other valve with short raphe slits" with "One valve with long raphe slits and the other valve with short raphe slits[1,2]	Both valves with long raphe slits*
External/internal proximal raphe ends	Simple or pore–like	Inconspicuous / n.d.	Slightly expanded[1,2]	Pore–like / n.d.	Teardrop–shaped / T–shaped	Pore–like[1] / Hook–shaped[2]	Pore–like[2] / Hook–shaped[2]	Pore–like / Simple*

*Personal observations based on cited literature. n.d.: no data.

semifasciata, is shared by some other *Nupela* taxa (see Lange–Bertalot 1993, 1999; Lange–Bertalot & Moser 1994; Metzeltin & Lange–Bertalot 1998; Siver & Hamilton 2005; Siver et al. 2007; Potapova 2011; Kulikovskiy et al. 2015; Tremarin et al. 2015; Bahls 2017), indicating a well–established feature that should be considered for species level identification within this genus.

The mantle ornamentation of *N. semifasciata* highlights interesting morphological details. Firstly, the mantle partially lacks the row of transversely elongated areolae due to the central area that reaches the valve margin and extends toward the mantle. In fact, *Nupela* species with a central area expanded onto the margin are observed in *N. amabilis*, *N. torganiae* (see Tremarin et al. 2015, fig 9 on page 81, and figs 124, 127 on page 89), *N. potapovae* (see Bahls 2011, fig 14 on page 170 and figs 19, 21 on page 171), *N. elongata* and *N. vasta* (see Kulikovskiy et al. 2015, fig 10 on page 267, and fig 23 on page 271), but the row of areolae on the mantle is continuous, not interrupted as in *N. semifasciata.*

Further, the mantle is composed of a single row of elongated areolae throughout the whole valve, and a second row can be visualized near the apices. Taxa sharing similar morphological aspects were recently described by Kulikovskiy et al. (2015) based on samples from Lake Baikal, in south–eastern Siberia, Russia. *Nupela gomphosphenioides* Kulikovskiy et Lange–Bertalot possesses one or two areolae at the junction with the valve mantle and the second row appearing near the apices (Fig 24 on page 257). *N. neogracillima* subsp. *baicalensis* Kulikovskiy et Lange–Bertalot contains one or two areolae at the edge of the valve face and mantle, with the second row more evident in the median region of the valve (Figs 1, 2 on page 279). Despite that, those taxa appear to have areolae only at the junction between face and valve mantles, differing from *N. semifasciata*, in which the two areolae are always positioned in the mantle. Moreover, *N. potapovae* Bahls seems to have a second row of areolae near the apices on the valve mantle (Bahls 2011, fig 16 on page 170), although the author has not pointed this out. Both of these aspects were not highlighted in the descriptions of *N. wellneri* provided by Lange–Bertalot & Krammer (1987), Potapova et al. (2003), and Tremarin et al. (2015), however, they represent important features to distinguish *Nupela* species.

Considering the striae, *N. wellneri* in Lange–Bertalot & Krammer (1987) has a radiate pattern throughout the valve, almost parallel in the apices, while Potapova et al. (2003, figs 77–79 on page 304), Potapova (2010, internal view), and Tremarin et al. (2015, fig 139 on page 90) depicted some specimens with slightly convergent striae patterns near the apices. In *N. semifasciata,* the convergent pattern near the apices was quite common due to the occurrence of well–marked Voigt fault.

The proposition of the new species is supported by observations in our populations compared to descriptions of other *Nupela* taxa provided in the literature. Particularly, *Navicula wellneri* (= *Nupela wellneri*), which shares the closest morphological features, differs by the broadly expanded axial and central area limited by shortened striae, not reaching the valve margin, and by the radiate striae pattern along the valve. This contributes to support the idea that individuals sharing these same aspects, described as *Nupela wellneri* by Potapova et al. (2003), Potapova (2011), and Tremarin et al. (2015), might be considered *Nupela semifasciata*. Furthermore, it is possible that the second row of areolae at the junction of the valve face and mantle, or even the second areolae positioned in the mantle, instead of a single row, appeared several times in *Nupela*, but further studies, especially those using molecular and phylogenetic techniques, are needed in order to clarify whether this feature represents a homoplasy. Considering that the number of *Nupela* taxa continues to increase, we suggest the central area unilaterally reaching the valve mantle, interrupting the row of areolae, and the second row of areolae on the valve mantle as morphological criteria that must be considered for species level identification within the genus *Nupela*.

Acknowledgments

The authors are thanked to Fundação Araucária and to Coordenação de Aperfeiçoamento Pessoal de Nível Superior (CAPES) for master's degree scholarship granted to M.W.W. Amaral and doctoral scholarship granted to G. Medeiros. To the staff of the Electron Microscopy Center (CME) of Universidade Federal do Paraná for technical assistance. To Acquasollus laboratory for the water chemical analyzes. To CNPq for scientific productivity grant of T.A.V. Ludwig (311876/2019–6).

References

Alvares, C.A.; Stape, J.L.; Sentelhas, P.C.; Gonçalves, J.L. de M. & Sparovek, G. (2013): Köppen's climate classification map for Brazil. – Meteorologische Zeitschrift 22: 711–728. DOI: https://doi.org/10.1127/0941–2948/2013/0507.

APHA, A.W.W.A. (2012): Standard Methods for the Examination of Water and Wastewater. – 541 pp., 22nd ed. Copyright, Washington.

Bahls, L.L. (2011): *Nupela potapovae* sp. nov. (Bacillariophyta), a lentic alpine species from North America. – Diatom Research 26: 167–174. DOI: https://doi.org/10.1080/0269249X.2011.597586.

Bahls, L.L. (2017): Diatoms from western North America 1. Some new and notable biraphid species. – 52 pp., Montana Diatom Collection, Helena.

Bes, D.; Ector, L.; Torgan, L.C. & Lobo, E.A. (2012): Composition of the epilithic diatom flora from a subtropical river, Southern Brazil. – Iheringia – Série Botânica 67: 93–125.

Bicudo, C.E. de M. & Menezes, M. (2017): Gêneros de algas de águas continentais do Brasil (chave para identificação e descrições). – 552 pp., 3rd ed. RiMa

Editora, São Carlos.

Falasco, E.; Bona, F.; Isaia, M.; Piano, E.; Wetzel, C.E.; Hoffmann, L. & Ector, L. (2015): *Nupela troglophila* sp. nov., an aerophilous diatom (Bacillariophyta) from the Bossea cave (NW Italy), with notes on its ecology. – Fottea 15: 1–9. DOI: https://doi.org/10.5507/fot.2015.001.

FUNDETEC – Fundação para o desenvolvimento científico e tecnológico. (1995): Bacia Hidrográfica do Rio Cascavel – Proposta para recuperação ambiental. – 164 pp., FUNDETEC, Cascavel.

Genkal, S.I. & Yarushina, M.I. (2018): Species of the genus *Nupela* Vyverman & Compère (Bacillariophyta) in the water bodies of the far North of Western Siberia and Russian far East. – International Journal on Algae 20: 377–386. DOI: https://doi.org/10.15407/alg28.04.449.

Guiry, M.D. & Guiry, G.M. (2020): AlgaeBase. World–wide electronic publication, National University of Ireland, Galway. Available from: http://www.algaebase.org (accessed: 6 November 2020).

Hustedt, F. (1942): Diatomeen aus der Umgebung von Abisko in Schwedisch–Lappland. – Archiv für Hydrobiologie 39(1): 87–174.

Kulikovskiy, M.; Lange–Bertalot, H.; Witkowski, A.; Dorofeyuk, N.I. & Genkal, S.I. (2010): Diatom assemblages from *Sphagnum* bogs of the world. Part I: Nur bog in northern Mongolia. – In: Lange–Bertalot, H. & Kociolek, P. (eds): Bibliotheca Diatomologica 55. – 326 pp., J. Cramer. Berlin–Sttutgart.

Kulikovskiy, M.S.; Lange–Bertalot, H. & Kuznetsova, I. V. (2015): Lake Baikal: Hotspot of Endemic Diatoms II. – In: Lange–Bertalot, H. (ed): Iconographia Diatomologica 26. Annotated Diatom Monographs – 656 pp., Koeltz Scientific Books, Oberreifenberg.

Kulikovskiy, M.S.; Maltsev, Y.I.; Glushchenko, A.M.; Gusev, E.S.; Kapsutin, D.A.; Kuznetsova, I.V.; Frolova, L. & Kociolek, J.P. (2020): Preliminary molecular phylogeny of the diatom genus *Nupela* with the description of a new species and consideration of the interrelationships of taxa in the suborder Neidiineae D.G.Mann sensu E.J. Cox. – Fottea 20: 192–204.

Lange–Bertalot, H. (1993): 85 neue Taxa und über 100 weitere neu definierte Taxa ergänzend zur Süsswasserflora von Mitteleuropa, Vol. 2/1–4. – In: Lange–Bertalot, H. (ed.): Bibliotheca Diatomologica 27. – 454 pp., J. Cramer, Berlin–Sttutgart.

Lange–Bertalot, H. (1999): Neue Kombinationen von taxa aus *Achnanthes* Bory (sensu lato). – In: Iconographia Diatomologica. Annotated Diatom Monographs 6. – pp. 276–289, Koeltz Scientific Books, Königstein, Germany.

Lange–Bertalot, H. & Krammer, K. (1987): Bacillariaceae, Epithemiaceae, Surirellaceae. Neue und wenig bekannte Taxa, neue Kombinationen und Synonyme sowie Bemarkungen und Ergänzungen zu den Naviculaceae. – In: Lange–Bertalot, H. (ed.): Bibliotheca Diatomologica 15. – 289 pp., J. Cramer, Berlin–Sttutgart.

Lange–Bertalot, H. & Moser, G. (1994): *Brachysira*, Monographie der Gattung. – In: Lange–Bertalot, H. (ed.): Bibliotheca Diatomologica 29. – 212 pp., J. Cramer, Berlin–Stuttgart.

Metzeltin, D. & Lange–Bertalot, H. (1998): Tropical Diatoms of South America I: About 700 predominantly rarely known or new taxa representative of the neotropical flora. – In: Lange–Bertalot, H. (ed): Iconographia Diatomologica 5. – 695 pp., Koeltz Scientific Books, Königstein, Germany.

Monnier, O.; Lange–Bertalot, H. & Bertrand, J. (2003): *Nupela exotica* species nova: une diatomée d'un aquarium tropical d'eau douce. Avec des remarques sur la biogéographie du genre. – Diatom Research 18: 273–291. DOI: https://doi.org/10.1080/0269249X.2003.9705592.

Moreira–Filho, H. & Valente–Moreira, I.M. (1981): Avaliação taxonômica e ecológica das diatomáceas (Bacillariophyceae) epífitas em algas pluricelulares obtidas nos litorais dos Estados do Paraná, Santa Catarina e São Paulo. – Boletim do Museu Botânico Municipal 47: 1–17.

Potapova, M. (2010): *Nupela wellneri*. Diatoms of North America. Available from: https://diatoms.org/species/nupela_wellneri (accessed: 29 June 2020)

Potapova, M. (2011): New species and combinations in the genus *Nupela* from the USA. – Diatom Research 26: 73–87. DOI: https://doi.org/10.1080/0269249X.2011.575111.

Potapova, M.G. (2013): Transfer of *Achnanthes decipiens* to the genus *Nupela*. – Diatom Research 28: 139–142.

Potapova, M.G.; Ponader, K.C.; Lowe, R.L.; Clason, T.A. & Bahls, L.L. (2003): Small–celled *Nupela* species from North America. – Diatom Research 18: 293–306. DOI: https://doi.org/10.1080/0269249X.2003.9705593.

Rumrich, U.; Lange–Bertalot, H. & Rumrich, M. (2000): Diatoms of the Andes. From Venezuela to Patagonia/Tierra del Fuego and two additional contributions. – In: Lange–Bertalot, H. (ed): – Iconographia Diatomologica 9. Annotated Diatom Monographs. Phytogeography–Diversity–Taxonomy. – 673 pp., Koeltz Scientific Books, Königstein, Germany.

Rybak, M.; Solak, C.N.; Noga, T.; Glushchenko, A.; Williams, D.M. & Kulikovskiy, M. (2020): *Nupela brevistriata* sp. nov.–a new, terrestrial diatom species from Southeast Asia. – Diatom Research 34: 251–258. DOI: https://doi.org/10.1080/0269249X.2019.1698467.

Sala, S.; Vouilloud, A.A.; Plata–Díaz, Y.; Pedraza, E. & Pimienta, A. (2014): *Nupela* species (Naviculales: Bacillariophyceae) from Colombian lowland waters including *N. acaciensis* nov. sp. and *N. catatumbensis* nov. sp. – Revista de Biología Tropical 62: 241–255. DOI: https://doi.org/10.15517/rbt.v62i1.8363.

Schoeman, F.R. (1973): A systematical and ecological study of the diatom flora of Lesotho with special reference to the water quality. – pp. 1–355, V & R Printers, Pretoria.

Simonsen, R. (1974): The diatom plankton of the Indian Ocean Expedition of RV Meteor 1964–1965. Meteor Forschungsergebnisse. – Reihe D. Biologie 19: 1–107.

Siver, P.A. & Hamilton, P.B. (2005): Observations on new and rare species of freshwater diatoms from Cape Cod, Massachusetts, USA. – Canadian Journal of Botany 83: 362–378. DOI: https://doi.org/10.1139/B05–010.

Siver, P.A.; Hamilton, P.B. & Morales, E.A. (2007): Notes on the genus *Nupela* (Bacillariophyceae) including the description of a new species, *Nupela scissura* sp. nov. and an expanded description of *Nupela paludigena*. – Phycological Research 55: 125–134. DOI: https://doi.org/10.1111/j.1440–1835.2007.00455.x.

SPAULDING, S.A. & EDLUND, M.B. (2008): *Nupela*. Diatoms of North America. Available from: https://diatoms.org/genera/Nupela (accessed: 5 May 2020)

THOMSON, S.A. et al. (2018): Taxonomy based on science is necessary for global conservation. – PLOS Biology 16: 1–12. DOI: https://doi.org/10.1371/journal.pbio.2005075.

TREMARIN, P.I.; STRAUBE, A. & LUDWIG, T.A.V. (2015): *Nupela* (Bacillariophyceae) in littoral rivers from south Brazil, and description of six new species of the genus. – Fottea 15: 77–93. DOI: https://doi.org/10.5507/fot.2015.007.

VYVERMAN, W. & COMPÈRE, P. (1991): *Nupela giluwensis* gen. & spec. nov. A new genus of naviculoid diatoms. – Diatom Research 6: 175–179. DOI: https://doi.org/http://dx.doi.org/10.1080/0269249X.1991.9705156.

WOJTAL, A.Z. (2009): *Nupela marvanii* sp. nov., and *N. lapidosa* (Krasske) Lange–Bertalot in Poland with notes on the distribution and ecology of the genus *Nupela* (Bacillariophyta). – Fottea 9: 233–242. DOI: https://doi.org/10.5507/fot.2009.024.

YU, P.; YOU, Q.; KOCIOLEK, J.P.; LOWE, R. & WANG, Q. (2017): *Nupela major* sp. nov., a new diatom species from Maolan Nature Reserve, central–south of China. – Phytotaxa 311: 245–254. DOI: https://doi.org/10.11646/phytotaxa.311.3.4.

ZIMMERMANN, J.; ABARCA, N.; ENK, N.; SKIBBE, O.; KUSBER, W.H. & JAHN, R. (2014): Taxonomic reference libraries for environmental barcoding: A best practice example from diatom research. – PLoS ONE 9. DOI: https://doi.org/10.1371/journal.pone.0108793.

Received August 27, 2020
Accepted January 18, 2021

Taxonomy of epilithic diatoms and their teratological forms under the presence of metals in the surface sediment

MAILOR WELLINTON WEDIG AMARAL[1,6*], GABRIELA MEDEIROS[2,7], VANESSA DAUFENBACH[3,4,8], MORGANA SUSZEK GONÇALVES[3,9], THELMA ALVIM VEIGA LUDWIG[5,10] & NORMA CATARINA BUENO[1,11]

[1]*Graduate Program in Conservation and Management of Natural Resources, Western Paraná State University, Universitária Street, 2019, Jardim Universitário, zip code 85819-110, Cascavel, Paraná, Brazil*

[2]*Graduate Program in Agricultural Engineering, Western Paraná State University, Universitária Street, 2019, Jardim Universitário, zip code 85819-110, Cascavel, Paraná, Brazil*

[3]*National Network Professional Master in Water Resources Management and Regulation (ProfÁgua), Federal University of Technology – Paraná. Rosalina Maria Ferreira Street, 1233, Vila Carola, zip code 87301-899, Campo Mourão, Paraná, Brazil*

[4]*Environmental and Agronomic Analysis Laboratory – Acqua Sollus. Goioerê Avenue, 219-A, Centro, zip code 87302-070, Campo Mourão, Paraná, Brazil*

[5]*Graduate Program in Botany, Federal University of Paraná. Life Sciences department. Centro Politécnico, mailbox Postal 19031, Jardim das Américas, zip code 81531-980, Curitiba, Paraná, Brazil*

[6] *E-mail: wedig_npi@hotmail.com; https://orcid.org/0000-0003-0749-4499*

[7] *E-mail: gabsmedeiros@gmail.com; https://orcid.org/0000-0002-5444-3064*

[8] *E-mail: vanessa.daufenbach@gmail.com*

[9] *E-mail: morgana@utfpr.edu.br; https://orcid.org/0000-0002-7576-2937*

[10] *E-mail: veiga13ufpr@gmail.com; https://orcid.org/0000-0003-0576-3499*

[11] *E-mail: normacatarina@hotmail.com; https://orcid.org/0000-0001-6939-9222*

[*]*Corresponding author*

Abstract

Periphytic diatom species in eight sampling sites of the Cascavel River microbasin were taxonomically analyzed. The studied streams are located in a predominantly urban microbasin, with distroferric red latosol (rich in Fe and Al), being characterized by distinct metals, predominantly acidic pH, and high conductivity. Overall, 221 diatom species were identified at infrageneric level. *Pinnularia* was the most representative genus in number of species (28 spp.), followed by *Eunotia* (25 spp.), *Gomphonema* Ehrenberg (17 spp.), *Nitzschia* Hassall (14 spp.), and *Navicula* (11 spp.). This is the first record of *Fragilaria spectra*, *Fragilaria tenera* var. *nanana* and *Humidophila arcuatoides* for the state of Paraná, and the first record of *Pinnularia laucensis* in Brazil. We found teratological valves in 34 taxa, containing modified outline, changes in the striae pattern, and doubled central area. The genus *Eunotia* showed the highest number of altered taxa (8 spp.). Mixed teratologies (deformed valve outline + unusual striae pattern) were found only in *Ulnaria ulna*,

Encyonema neomesianum, and *Gomphonema graciledictum*. The metals and environmental variables in the Cascavel River microbasin probably contributed to the diatom teratologies. Our work contributes to the taxonomic knowledge of epilithic diatoms in the region, as well as extending the record of teratological taxa in the literature.

Keywords: Bacillariophyta, lotic environments, metals, morphology, periphyton, taxonomy, teratology

Introduction

Epilithic diatoms are photosynthetic microorganisms growing attached to rocky substrate (Townsend & Gell 2005, McGowan *et al*. 2018). The siliceous cell wall ornamentations are the basis for the group's taxonomy, as they allow the description and classification of individuals (Cavalier-Smith 2015, Schoefs *et al.* 2020). Taxonomic studies approaching diatom floras are crucial for recognizing environmental stresses and assessing the ecological status of aquatic systems (Morin *et al.* 2012, Olodo *et al.* 2019, Benito & Fritz 2020). This type of knowledge assists in decision-making for species conservation, especially in a scenario of constantly threatened biodiversity (Garnett & Christidis 2018, Azevedo-Santos *et al.* 2021).

The organic layer surrounding the diatom frustule contains metals that are essential for diatom metabolism (Sunda *et al.* 2005), preventing, for example, the loss of silica to the aquatic environment (Round *et al.* 1990). However, metals are potential stressors depending on their concentrations and under specific conditions (Falasco *et al.* 2009b, 2021). Diatom species from metal-polluted streams may lose diversity (da Silva *et al.* 2009, Barral-Fraga *et al.* 2016, Leguay *et al.* 2016, Pandey *et al.* 2018a), suffer physiological changes, such as in cytoplasmic content, lipid bodies number, and nuclear abnormalities (Morin *et al.* 2012, Gautam *et al.* 2017, Pandey et al. 2017), as well as undergo morphological changes involving community structure or individual scale (Cantonati *et al.* 2014, Lavoie *et al.* 2017, Olenici *et al.* 2017, Su *et al.* 2018, Falasco *et al.* 2021).

Establishing relationships between metal contamination and deformities in diatoms is difficult due to the various environmental and anthropogenic factors that are potential drivers of teratologies (Falasco *et al.* 2009a, Lavoie *et al*. 2017). Further, low frequency of deformed valves is considered natural in unpolluted environments (see Cattaneo *et al.* 2004, Lavoie *et al.* 2012, Morin *et al.* 2012, Pandey *et al.* 2014). Based on this, floristic studies provide an initial insight into aquatic systems, extending the recognition of deformities in diatoms, thus indicating possible metal contamination (Morin *et al.* 2012, Park *et al.* 2020, Falasco *et al.* 2021). Conducting prior taxonomic investigations of diatom assemblages is crucial in ecological studies of aquatic environments, helping to identify the influence of metals on diatom abnormalities (see Yang & Duthie 1993, Szabó *et al.* 2005, Sgro *et al.* 2007, Tapia 2008, Falasco *et al.* 2009b, Ferreira da Silva *et al.* 2009, Pandey et al. 2018a). Although this type of approach is apparently becoming obsolete (Rimet 2012), the relationship between metals and teratologies in diatoms is underexplored in tropical environments as in Brazil. Detailed floristic studies would provide valuable information on aquatic systems for biomonitoring purposes using abnormalities in diatoms.

We conducted a taxonomic survey of epilithic diatoms from a hydrographic microbasin in southern Brazil, focusing on their teratological forms and characterizing the limnological conditions and metal concentrations where they were found.

Material & Methods

The Cascavel River is the principal source of water supply for the city of Cascavel, located in the Western Paraná State, and its tributaries are influenced by urbanized areas (FUNDETEC 1995). This subtropical region is characterized by the Cfa climate, with temperatures above 22 ºC in the summer and around 30 mm of rain in the driest month (Alvares *et al.* 2013). The soil of the hydrographic microbasin is classified as Distropheric Red Latosol, with low fertility, high iron and aluminum concentrations, and usually clayey texture (dos Santos *et al.* 2018). Regarding trace metals, high bioavailability of Pb, Cu, and Mn have already been registered for the initial portion of the microbasin, at Paulo Gorski Lake (Remor *et al.* 2018).

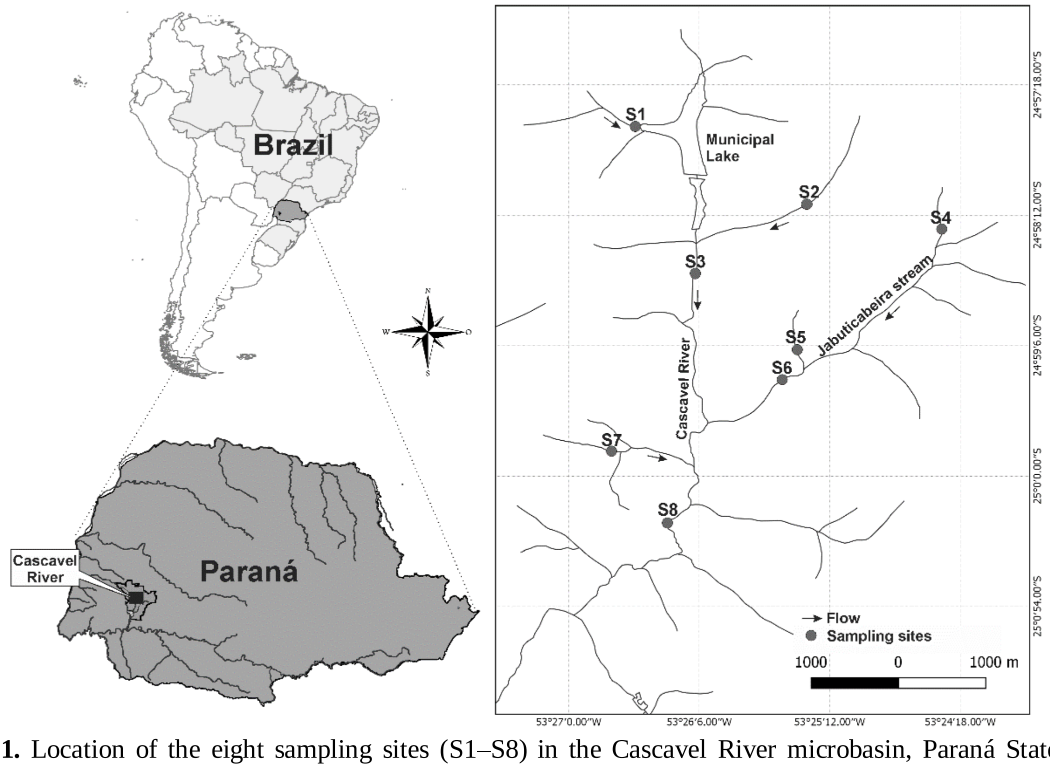

FIGURE 1. Location of the eight sampling sites (S1–S8) in the Cascavel River microbasin, Paraná State, Southern Brazil.

We analyzed the epilithic diatom flora collected from eight streams (Fig. 1), three of them located in the main channel of the Cascavel River, and five tributaries (see Table 1 in Appendix A for description of sampling sites), following the direction upstream to downstream of the river.

We performed 12 seasonal samplings from 2016 to 2019. Initially, we collected 60 rocky substrates at S1, S3 and S8, 10 per sampling site, during autumn and spring 2016 (see details in Medeiros *et al.* 2020). Starting in 2017, we have additionally collected 240 stones in triplicates at the eight sampling sites. A total of 300 qualitative samples were collected (Appendix B). The biofilm containing the diatoms was scraped from all the stones using a toothbrush and distilled water, and stored in *Transeau* 1:1 solution (Bicudo & Menezes 2017) at the Universidade Estadual do Oeste do Paraná Herbarium (UNOPA).

A multiparameter probe (HORIBA U-5000) was used for *in situ* measuring of water temperature (Temp), electrical conductivity (Cond), dissolved oxygen (DO), pH, and turbidity (Turb). We also collected one water sample per sampling site, using polyethylene bottles immersed in the subsurface of the water column. These samples were kept in the dark and cooled, and subsequently analyzed to verify the physical, chemical, and biological properties of the water (Chlorophyll *a*: CLa; Total coliforms: TC; Biochemical Oxygen Demand: BOD; Chemical Oxygen Demand: COD; *Escherichia coli*: *E. coli*; Ammoniacal nitrogen: N-NH_3; Nitrate: NO_3; pH; Orthophosphate: PO_4^-; Total phosphorus: TP; Dissolved solids: DS; Total solids: TS) (APHA 2012). The depth was manually measured by sinking a ruler to the bottom of the river. The flow was obtained by multiplying the length and the average speed of the displacement of a polystyrene object along a virtual transect in the river. The precipitation data was provided by the Paraná Meteorological System (SIMEPAR) (See Table 1 in Appendix C).

Three surface sediment samples were collected at each sampling site to form a composite sample, from which metals were extracted following CETESB & ANA (2011). Aluminum (Al) barium (Ba) cadmium (Cd), chromium (Cr), cobalt (Co), copper (Cu), Iron (Fe) lead (Pb), manganese (Mn), nickel (Ni), and zinc (Zn) were read (See table 1 in Appendix D), according to U.S. Environmental Protection Agency 3050B method (USEPA 1996).

Ecological variables and metals were submitted to principal component analysis (PCA) aiming to characterize the sampling stations, as well as identify the variables that best differentiate them (Wiegleb, 1980).

Permanent slides were prepared with subsamples oxidized according to Simonsen (1974), modified by Moreira-Filho & Valente-Moreira (1981). Light microscopy (LM) analyzes were performed at 1000× magnification, using an Olympus BX34 microscope equipped with a DP 71 capture camera and phase-contrast. Cleaned samples were also placed in aluminum stubs, sputter-coated with gold in Balzers Union SCD 030, and examined in Scanning Electron Microscopy (SEM) with JEOL JSM 6360LV, operated at 15–20 kV and a working distance of 5–8 mm.

We provide morphometric and meristic data, occurrences at sampling sites, and literature used for taxa identification (Table 1). Photomicrographs of identified taxa are provided in optical (Figs 3–11) and scanning electron microscopy (Figs 12–16). In taxa showing teratologies, we described the morphological changes, as well as the ecological characteristics of the environment where abnormal individuals were found. New records were commented, and are accompanied by asterisk symbols, one for the Paraná State (*) and two for Brazil (**). First records were considered when the species was not previously recorded in published taxonomic articles, with measurements and photomicrographs.

Results

We identified 221 infrageneric taxa (Table 1), belonging to 52 genera. Regarding species richness, *Pinnularia* Ehrenberg was the most representative genus (28 spp.), followed by *Eunotia* Ehrenberg (25 spp.), *Gomphonema* Ehrenberg (17 spp.), *Nitzschia* Hassall (14 spp.), and *Navicula* (11 spp.). *Fragilaria spectra*, *Fragilaria tenera* var. *nanana* and *Humidophila arcuatoides* represent new records for the state of Paraná, and *Pinnularia laucensis* represent a first record for Brazil.

TABLE 1. Epilithic diatom species identified from Cascavel River microbasin. Morphological measurements, occurrences (UNOPA), and consulted literature. (L: length; W: width; L/W: length/width ratio; D: diameter; MH: mantle height; S: striae; DS: dorsal striae; VS: ventral striae; TS: transapical striae; LS: longitudinal striae; AC: alar channels; F: fibulae; A: areolae).

Taxa	Figures	Morphometric (μm) and meristic (in 10 μm) data	Occurrence	Followed literature
STEPHANODISCACEAE				
Cyclotella distinguenda Hustedt	2A	D: 15–18.1; S: 12–17 (n= 8)	S3, S8	Houk & Klee (2010)
C. kingstonii Julius, Downey, Theriot, et al.	2E; 11A	D: 8.3–22.4; S: 17–21; A: 18–21 (n= 83)	S1, S3, S4, S5, S8	Johansen *et al.* (2008) Downey *et al.* (2021)
Discostella stelligera (Cleve & Grunow) Houk & Klee	2B–2D; 11B–11C	D: 6.3–16.7; S: 12–17 (n= 268)	S1, S2, S3, S4, S5, S6, S7, S8	Houk & Klee (2004)
MELOSIRACEAE				
Melosira varians Agardh	2F	D: 10.1–20.7 (n= 25)	S2, S3, S4, S5, S8	Krammer & Lange-Bertalot (1991)
ORTHOSEIRACEAE				
Orthoseira roeseana (Rabenhorst) Pfitzer	2G	D: 11.6–16.4; S: 12–14; A: 11–14 (n= 5)	S1, S2, S5	Krammer & Lange-Bertalot (1991)
AULACOSEIRACEAE				
Aulacoseira ambigua (Grunow) Simonsen	2H; 11D	D: 4.3–13.9; MH: 4.5–13.2; S: 14–20; A: 12–20 (n= 157)	S1, S3, S4, S8	Tremarin *et al.* (2013)
A. brasiliensis Tremarin, Torgan & Ludwig	2I	D: 11–11.1; MH: 5.9–6.4; S: 13–14; A: 11–12 (n= 2)	S3	Tremarin *et al.* (2012)
A. granulata var. *angustissima* (Müller) Simonsen	2J	D: 2.5–3.3; MH: 9.2–17.5; S: 12–19; A: 14–20 (n= 40)	S2, S3, S4, S8	Krammer & Lange-Bertalot (1991)
A. granulata (Ehrenberg) Simonsen	2K	D: 4.4–4.6; MH: 9.9–14.5; S: 12–14; A: 10–14 (n= 5)	S3, S6, S8	Krammer & Lange-Bertalot (1991)
A. pusilla (Meister) Tuji & Houki	2L–2N; 11G	D: 4.5–6.6; MH: 2.3–3.8; A: 17–20 (n= 95)	S3, S4, S8	Tuji & Houki (2004)
A. tenella (Nygaard) Simonsen	2O–2Q; 11E–11F	D: 5.7–6.9; MH: 3.6–4.3; S: 19–26 (n= 95)	S1, S3, S4, S5, S8	Siver & Kling (1997) Camburn & Charles (2000)
FRAGILARIACEAE				
Fragilaria fragilarioides (Grunow) Cholnoky	2R–2T	L: 16.9–47.2; W: 4.3–6; S: 10–12 (n= 22)	S6, S8	Cholnoky (1963) Ludwig & Flôres (1997)
F. gracilis Østrup	2U–2AA; 11H–11I	L: 22.6–45.9; W: 2–3.2; S: 18–22 (n= 82)	S1, S3, S4, S8	Tuji (2007) Lange-Bertalot & Ulrich (2014)
F. pectinalis (Müller) Lyngbye	2AB–2AH; 11J–11K	L: 25.9–31.1; W: 2.7–3.6; S: 15–16; A: 57–61 (n= 97)	S1, S3, S4, S6, S8	Tuji & Williams (2008) Wetzel & Ector (2015)
F. spectra Almeida, Morales, Wetzel, Ector & Bicudo	2AP–2AR	L: 42.7–70.1; W: 1.8–3.1; S: 19–24 (n= 12)	S3, S8	Almeida *et al.* (2016)

Taxa	Figures	Morphometric (μm) and meristic (in 10 μm) data	Occurrence	Followed literature
F. tenera var. *tenera* (Smith) Lange-Bertalot	2AI–2AK	L: 39.9–66.7; 2.5–2.9; S: 15–17 (n= 44)	S1, S3, S6, S8	Lange-Bertalot & Ulrich (2014)
F. tenera var. *nanana* (Lange-Bertalot) Lange-Bertalot & Ulrich	2L–2AO	L: 45.1–67.1; W: 1.9–3.1; S: 20–22 (n= 30)	S3, S4, S6, S7, S8	Lange-Bertalot & Ulrich (2014)
Fragilariforma javanica (Hustedt) Wetzel, Morales & Ector	2AS–2AT	L: 20.5–95.9; W: 5.2–6.4; S: 19–20 (n= 39)	S1, S4, S5	Metzeltin & Lange-Bertalot (1998) Wetzel *et al*. (2013)
Ulnaria contracta (Østrup) Morales & Vis	2AU	L: 38.8–122.2; W: 6.7–8.9; S: 9–11 (n= 30)	S3, S8	Patrick & Reimer (1966) Morales & Vis (2007)
U. delicatissima (W.Smith) Aboal & Silva	2AV	L: 159.5–233.2; W: 4–5.5; S: 10–12 (n= 4)	S3, S6, S8	Tuji & Houki (2004)
U. ulna (Nitzsch) Compère	2AW–2AZ	L: 56.9–301.5; W: 5–8.5; S: 9–11 (n= 106)	S1, S2, S3, S4, S6, S7, S8	Patrick & Reimer (1966) Lange-Bertalot & Ulrich (2014)
EUNOTIACEAE				
Actinella hermes-moreirae Ruwer, Ludwig & Rodrigues	3A–3C	L: 15.8–49.6; W: 2.9–3.8; S: 15–18 (n= 43)	S2, S5, S7, S8	Ruwer *et al*. (2019)
Eunotia bilunaris (Ehrenberg) Schaarschmidt	3D–3J; 12A	L: 15.4–123; W: 2.9–4.3; S: 14–18; A: 42–44 (n= 353)	S1, S2, S3, S4, S5, S6, S7, S8	Lange-Bertalot *et al*. (2011) Costa *et al*. (2017a)
E. botulitropica Wetzel & Costa	3K–3P; 12B–12C	L: 9.8–32.9; W: 2.4–3.5; S: 13–18; A: 38–44 (n= 481)	S1, S2, S3, S4, S5, S6, S7, S8	Costa *et al*. (2017a)
E. canicula Furey, Lowe & Johansen	3Q–3R	L: 32.2–47.3; W: 3.9–4.8; S: 12–16 (n= 7)	S3, S5, S8	Furey *et al*. (2011)
E. desmogonioides Metzeltin & Lange-Bertalot	3S–3T; 12F–12G	L: 58.5–144.7; W: 3.4–6.6; S: 15–17; A: 36–37 (n= 49)	S1, S3, S8	Metzeltin & Lange-Bertalot (2002) Costa *et al*. (2017a)
E. fallax Cleve	3Y–3Z	L: 14.5–31.8; W: 2.4–3.1; S: 15–19 (n= 14)	S1, S3, S4, S5, S6, S7	Lange-Bertalot *et al*. (2011)
E. formica Ehrenberg	3AA	L: 42.7; W: 9.6; S: 9 (n= 1)	S1	Costa *et al*. (2017a)
E. formicina Lange-Bertalot	3AB	L: 86.3–116.2; W: 7.6–9.3; S: 8–10 (n= 5)	S1, S4, S7	Costa *et al*. (2017a)
E. georgii Metzeltin & Lange-Bertalot	3AY; 12H	L: 28.7–92.4; W: 6.8–9.9; S: 10–14; A: 28–29; O: 15–20 (n= 58)	S1, S2, S4, S5, S6, S7, S8	Costa *et al*. (2017a)
E. intricans Lange-Bertalot & Metzeltin	3AD	L: 23.3–49; W: 4.1–5.4; S: 11–15 (n= 52)	S1, S2, S3, S4, S5, S6, S8	Costa *et al*. (2017a)
E. juettnerae Lange-Bertalot	3AH–3AJ	L: 25.6–41.9; W: 2.2–3.2; S: 15–21 (n = 17)	S3, S8	Lange-Bertalot *et al*. (2011) Costa *et al*. (2017a)
E. karenae Metzeltin & Lange-Bertalot	3AC	L: 97.4–128.2; W: 8.4; S: 8–10 (n= 5)	S1, S6	Costa *et al*. (2017a)
E. kruegeri Lange-Bertalot	3AK–3AM	L: 12.1–19.2; W: 2.4–3.2; S: 18–24 (n= 57)	S1, S2, S3, S4, S5, S6, S8	Costa *et al*. (2017a)
E. longicamelus Costa, Bicudo & Wetzel	3AE	L: 25.5–49; W: 6.2–8.2; S: 10–12 (n= 10)	S1, S3, S8	Costa *et al*. (2017a)

Taxa	Figures	Morphometric (μm) and meristic (in 10 μm) data	Occurrence	Followed literature
E. meridiana Metzeltin & Lange-Bertalot	3AR–3AX	L: 14.5–34.9; W: 4.2–6.6; S: 11–16; A: 39 (n= 179)	S1, S2, S3, S4, S5, S6, S7, S8	Metzeltin & Lange-Bertalot (1998) Costa *et al*. (2017a)
E. monodon Ehrenberg	3AP–3AQ	L: 37.2–120.9; W: 8.6–10; S: 8–11 (n= 36)	S1, S2, S3, S6, S7, S8	Lange-Bertalot *et al*. (2011) Costa *et al*. (2017a)
E. muscicola Krasske	3AN–3AO	L: 11.7–17.9; W: 3.1–3.8; S: 20–25 (n= 21)	S3, S6, S8	Lange-Bertalot *et al*. (2011) Costa *et al*. (2017a)
E. ossicula (Metzeltin & Lange-Bertalot) Costa	4A	L: 111,8; W: 8.6–12.3; S: 14–17 (n= 7)	S1, S3, S8	Costa *et al*. (2017a)
E. rabenhorstii var. *monodon* Cleve & Grunow	3AF	L: 16.5–24.5; W: 5.9–7.3; S: 12–16 (n= 11)	S3, S6, S8	Costa *et al*. (2017a)
E. rabenhorstii var. *triodon* Cleve & Grunow	3AG	L: 22.8–26; W: 6.2–7.2; S: 12–15 (n= 8)	S1, S3	Costa *et al*. (2017a)
E. rhomboidea Hustedt	4B–4G; 12D–12E	L: 12.4–45.3; W: 4.1–5.6; S: 11–16 (n= 287)	S1, S2, S3, S4, S5, S6, S7, S8	Costa *et al*. (2017a)
E. subarcuatoides Alles, Nörpel & Lange-Bertalot	3U–3X	L: 8.3–19.3; W: 2.5–4.3; S: 21–23 (n= 24)	S1, S3, S4, S5, S6, S8	Costa *et al*. (2017a)
E. tropico-arcus Metzeltin & Lange-Bertalot	4H	L: 28.8–53.5; W: 6.3–9; S: 10–14 (n= 8)	S5, S7	Metzeltin & Lange-Bertalot (2007) Costa *et al*. (2017a)
E. veneris (Kützing) De Toni	4I–4K	L: 18.2–53.1; W: 4.4–6.2; S: 15–19 (n= 30)	S1, S2, S3, S5, S8	Lange-Bertalot *et al*. (2011) Costa *et al*. (2017a)
E. yanomami Metzeltin & Lange-Bertalot	4L	L: 20.1–113.9; W: 12.3–22.6; S: 11–13; A: 22–24 (n= 35)	S1, S3, S5, S6, S7	Metzeltin & Lange-Bertalot (1998) Costa *et al*. (2017a)
E. yberai Frenguelli	4M–4P	L: 20.7–89.2; W: 6.2–10.7; E: 6–10 (n= 52)	S1, S3, S4, S8	Costa *et al*. (2017a)
CYMBELLACEAE				
Cymbopleura naviculiformis (Auerswald) Krammer	4Q	L: 25.4–34.4; W: 7.1–9; L/W: 3.6–4.3; S: 13–17 (n= 83)	S1, S3, S4, S6, S8	Krammer (2003)
Encyonema angustecapitatum Krammer	4R–4S	L: 11.4–25; W: 4.1–5.2; S: 13–15 (n= 9)	S1, S4, S8	Rumrich *et al*. (2000) Vouilloud *et al*. (2010)
E. exuberans Tremarin, Wetzel & Ludwig	4AC–4AE	L: 33.5–39.8; W: 7.3–10; L/W: 3.7–5.2; DS: 7–9; VS: 11–13 (n= 34)	S8	Tremarin *et al*. (2011)
E. minutiforme Krammer	4AB	L: 16.1–23; W: 4–5.7; S: 10–12 (n= 23)	S3, S8	Krammer (1997a)
E. neogracile Krammer	4U	L: 17.2–40.6; W: 4.5–7.1; L/W: 3.6–6.1 S: 12–16 (n= 64)	S1, S3, S4, S8	Krammer (1997a)
E. neomesianum Krammer	4V–4X	L: 21.1–41.8; W: 5.6–8.5; S: 10–12 (14) (n= 54)	S3, S8	Krammer (1997a)
E. perpusillum (Cleve-Euler) Mann	4T	L: 14.4–21.7; W: 4–5.4; S: 9–13 (n= 102)	S3, S6, S8	Krammer (1997a)
E. silesiacum (Bleisch) Mann	4AY–4AA	L: 18.3–35.5; W: 6.8–8.3; S: 9–12 (n= 146)	S1, S2, S3, S4, S5, S6, S7, S8	Krammer (1997a)

Taxa	Figures	Morphometric (µm) and meristic (in 10 µm) data	Occurrence	Followed literature
Geissleria punctifera (Hustedt) Metzeltin, Lange-Bertalot & García-Rodríguez	4AT–4AU; 12I	L: 12.5–26.4; W: 5.6–7.1; S: 16–18; A: 48 (n= 83)	S1, S3, S4, S8	Metzeltin *et al*. (2005)
Navigeia ignota (Krasske) Bukhtiyarova	4AF–4AH	L: 11.1–19.4; W: 4.7–5.2; S: 15–16 (n= 9)	S1, S2, S3, S7	Bukhtiyarova & Pomazkina (2013)
Placogeia kriegeri (Krasske) Bukhtiyarova	4AI–4AK	L: 15–20.4; W: 6.8–8; S: 16–19 (n= 4)	S3, S8	Lange-Bertalot & Metzeltin (1996)
GOMPHONEMATACEAE				
Encyonopsis difficilis (Krasske) Krammer	4AN–4AO	L: 20–27.4; W: 4.7–6.2; S: 9–10 (n= 7)	S1, S3, S6, S8	Krammer (1997b) Marquardt *et al*. (2014)
E. schubartii (Hustedt) Krammer	4AP	L: 29.2–31.9; W: 5.9–7.5; R L/W: 4.2–5; S: 9–12 (n= 17)	S3, S4	Krammer (1997b)
E. subminuta Krammer & Reichardt	4AL–4AM	L: 18.1–19.5; W: 4.1–4.2; L/W: 4.3–4.8; S: 23–26 (n= 8)	S3	Krammer (1997b)
E. thienemannii (Hustedt) Krammer	4AQ–4AS	L: 16.9–18.1; W: 4.1–4.2; L/W: 4.1–4.3; E: 23–25 (n= 3)	S3	Krammer (1997b)
Kurtkrammeria spicula (Hustedt) Ohtsuka	4AV	L: 33.1–56.5; W: 5.9–7.2; L/W: 5.5–8.2; S: 15–17 (n= 31)	S3, S4	Ohtsuka (2018)
Gomphonema affine Kützing	5A–5B	L: 39.9–54.9; W: 7.4–7.7; S: 11–12 (n= 4)	S3, S8	Reichardt (1999)
G. angustatum (Kützing) Rabenhorst	5C–5H	L: 17.9–40.9; W: 4.6–6.6; S: 13–17 (n= 172)	S1, S2, S3, S4, S5, S6, S7, S8	Rumrich *et al*. (2000) Metzeltin *et al*. (2005)
G. brasiliense Grunow	5I	L: 17.3–34.5; W: 4.4–6.8; S: 11–15 (n= 28)	S3, S6, S8	Medeiros *et al*. (2018)
G. brasiliense subsp. *pacificum* Moser, Lange-Bertalot & Metzeltin	5J–5K	L: 19.8–34.3; W: 4.1–5.8; S: 12–14 (n= 5)	S3, S8	Medeiros *et al*. (2018)
G. brasiliensoide Metzeltin, Lange-Bertalot & García-Rodríguez	5L	L: 29.6–36.1; W: 6.6–6.9; S: 11–12 (n= 8)	S6, S8	Metzeltin *et al*. (2005) Medeiros *et al*. (2018)
G. exilissimum (Grunow) Lange-Bertalot & Reichardt	5M–4O	L: 18.4–31.4; W: 4.5–6.1; S: 12–16 (n= 53)	S1, S2, S3, S4, S5, S6, S7, S8	Jüttner *et al*. (2013)
G. frequentiformis (Metzeltin & Krammer) Wetzel & Almeida	5S	L: 41.9–48.7; W: 8.9–10.1; S: 11–14 (n= 2)	S3, S8	Metzeltin & Lange-Bertalot (1998)
G. graciledictum Reichardt	5T–5Y	L: 24.3–67.7; W: 5.6–8.4; S: 11–15 (n= 222)	S1, S3, S4, S6, S8	Reichardt (2015)
G. guaraniarum Metzeltin & Lange-Bertalot	5AC	L: 44.5–56.9; W: 7.2–9.7; S: 11–14; A: 23–27 (n= 48)	S1, S2, S3, S6, S8	Metzeltin & Lange-Bertalot (2007)
G. hawaiiense Reichardt	5AA–5AB	L: 32.7–50.8; W: 5.8–8.5; S: 12–16 (n= 15)	S2, S3, S6, S8	Reichardt (2005)
G. lagenula Kützing	5AN–5AS; 12J	L: 9–26.8; W: 4.8–7.2; S: 13–18; A: 32–34 (n= 400)	S1, S2, S3, S4, S5, S6, S7, S8	Metzeltin & Lange-Bertalot (1998)

Taxa	Figures	Morphometric (µm) and meristic (in 10 µm) data	Occurrence	Followed literature
G. naviculoides Smith	5AT–5AU	L: 32.2–59.8; W: 7.7–10.6; S: 12–14; A: 23–26 (n= 128)	S1, S2, S3, S4, S6, S8	Reichardt (2015) Levkov *et al*. (2016)
G. parvulum (Kützing) Kützing	5P–5R	L: 11.5–23.2; W: 4.7–6.2; S: 13–17 (n= 430)	S1, S2, S3, S4, S5, S6, S7, S8	Abarca *et al*. (2014) Levkov *et al*. (2016)
G. perapicatum Metzeltin & Lange-Bertalot	5Z	L: 50.9; W: 11.7; S: 9 (n= 1)	S6	Metzeltin & Lange-Bertalot (2007)
G. pseudoaugur Lange-Bertalot	5AG–5AI	L: 22.4–38.1; W: 7.4–8.7; S: 12–15 (n= 58)	S1, S2, S3, S4, S6, S8	Krammer & Lange-Bertalot (1986)
G. pumilum (Grunow) Reichardt & Lange-Bertalot	5AJ–5AM; 12K–12L	L: 9.6–26.3; W: 3.4–4.5; S: 11–16; A: 47–49 (n= 104)	S1, S2, S3, S4, S6, S8	Reichardt (1997)
G. saprophilum (Lange-Bertalot & Reichardt) Abarca, Jahn, Zimmermann & Enke	5AD–5AF	L: 15.2–31; W: 4.8–7.5; S: 12–17 (n= 58)	S1, S3, S4, S6, S8	Abarca *et al*. (2014)
Placoneis elginensis (Gregory) Cox	6A	L: 21.2; W: 7.7; S: 14 (n= 1)	S3	Cox (2003)
P. hambergii (Hustedt) Bruder	6B	L: 12.2–23.2; W: 5.9–7.9; S: 14–17 (n= 45)	S1, S2, S3, S4, S5, S6, S7, S8	Bruder & Medlin (2007)
P. undulata (Østrup) Lange-Bertalot	6C	L: 19.5–24.7; W: 6.1–8.2; S: 14 (n= 3)	S3, S8	Rumrich *et al*. (2000)
ACHNANTHIDIACEAE				
Achnanthes inflata (Kützing) Grunow	6D	L: 58.8; W: 16.5; S: 11–12; A: 12–13 (n= 1)	S4	Patrick & Reimer (1966)
Achnanthidium caledonicum Lange-Bertalot	6E–6G; 13A	L: 16–23.9; W: 2.9–3.8; S: 26–30; A: 47–49 (n= 21)	S3, S6, S8	Wojtal *et al*. (2011)
A. macrocephalum (Hustedt) Round & Bukhtiyarova	6H–6P; 13B	L: 8.7–14.6; W: 2.5–3.7; S: 28; A: 46 (n= 59)	S1, S3, S4, S6, S7, S8	Potapova & Hamilton (2007) Morales *et al*. (2011)
A. minutissimum (Kützing) Czarnecki	6S–6Z; 13C–13E	L: 5.9–17.7; W: 2–3.8; S: 24–34; A: 40–56 (n= 471)	S1, S2, S3, S4, S5, S6, S7, S8	Krammer & Lange-Bertalot (1991) Potapova & Hamilton (2007)
A. modestiforme (Lange-Bertalot) Van de Vijver	6AD–6AH	L: 6–14.1; W: 3.5–5; S: 19–24 (n= 91)	S1, S2, S3, S4, S5, S6, S7, S8	Morales *et al*. (2011)
A. tropicocatenatum Marquardt, Wetzel & Ector	6Q–6T; 13F–13G	L: 12–18.1; W: 2.8–4; S: 35–38; A: 44–50 (n= 88)	S2, S3, S4, S6, S8	Marquardt *et al*. (2017)
Gogorevia constricta (Torka) Kulikovskiy & Kociolek	6I–6J	L: 10.5–16.3; W: 4.4–6.8; S: 19–22 (n= 32)	S1, S8	Kulikovskiy *et al*. (2020)
Planothidium bagualensis Wetzel & Ector	6AK	L: 13.9–21.2; W: 6.4–8.1; S: 11–15 (n= 4)	S1, S8	Wetzel *et al*. (2014)
P. frequentissimum (Lange-Bertalot) Lange-Bertalot	6AQ–6AR	L: 7.2–16.1–16.6; W: 3.7–5.6; S: 14–17 (n= 17)	S1, S2, S3, S4, S7, S8	Lange-Bertalot (1999) Jahn *et al*. (2017)
P. lagerheimii (Cleve) Wetzel & Ector	6AL	L: 24.7; W: 12.6; S: 8 (n= 1)	S8	Wetzel *et al*. (2014)
P. rostratum (Østrup) Round & Bukhtiyarova	6AM–6AP	L: 13.2–14.4; W: 5.2–5.8; S: 14–15 (n= 8)	S3, S8	Round & Bukhtiyarova (1996) Krammer & Lange-Bertalot (1991)

Taxa	Figures	Morphometric (μm) and meristic (in 10 μm) data	Occurrence	Followed literature
Psammothidium hustedtii (Krasske) Mayama	6AS–6AT	L: 10.1–14.9; W: 4.5–6.7; S: 16–22 (n= 80)	S1, S2, S5, S6, S7, S8	Hofmann *et al*. (2013) Mayama *et al*. (2002)
COCCONEIDACEAE				
Cocconeis fluviatilis Wallace	6AAD	L: 19.4–19.7; W: 12.3–12.4; S: 12–16; A: 9–10 (n= 2)	S3, S8	Patrick & Reimer (1966)
C. lineata Ehrenberg	6AAE	L: 16.9–24.7; W: 11.4–12.5; S: 24–25; A: 11–16 (n= 3)	S2, S3, S8	Patrick & Reimer (1966) Krammer & Lange-Bertalot (1991b)
DIADESMIDACEAE				
Humidophila arcuatoides Lange-Bertalot	6AU–6AV	L: 12.1–14.6; W: 2.9–3.2 (n= 2)	S2, S8	Lange-Bertalot (2004) Lowe *et al*. (2014)
H. contenta (Grunow) Lowe et al..	6AX–6AZ	L: 7.2–15.7; W: 2.1–3.3 (n= 115)	S1, S2, S3, S4, S5, S6, S7, S8	Metzeltin & Lange-Bertalot (2007) Lowe *et al*. (2014)
H. implicata (Moser, Lange-Bertalot & Metzeltin) Lowe et al.	6AW	L: 9.4–13.1; W: 2.8–3.5 (n= 4)	S1, S5, S6	Lowe *et al*. (2014)
H. subtropica (Metzeltin, Lange-Bertalot & García-Rodríguez) Lowe et al.	6AAA–6AAC	L: 9.6–15.8; W: 2.3–3.2 (n= 42)	S1, S2, S3, S4, S6, S7, S8	Lowe *et al*. (2014)
Luticola charlatii (Peragallo) Metzeltin & Lange-Bertalot	6AAH	L: 37.6–39; W: 10.6–12.1; S: 12–15; A: 12 (n= 2)	S1, S7	Metzeltin *et al*. (2005)
L. ectorii Levkov, Metzeltin & Pavlov	6AAF; 13I	L: 11.3–17.7; W: 5.2–7.1; S: 20–27; A: 26–28 (n= 20)	S1, S3, S8	Levkov *et al*. (2013)
L. goeppertiana (Bleisch) Mann	6AAL–6AAN	L: 10.3–34.8; W: 4.8–8.8; S: 18–22 (n= 68)	S2, S3, S4, S5, S6, S8	Levkov *et al*. (2013)
L. hustedtii Levkov, Metzeltin & Pavlov	6AAG	L: 15.6–22.4; W: 7–7.8; S: 22–24 (n= 10)	S1, S3, S4, S5, S6, S8	Levkov *et al*. (2013)
L. permuticoides Metzeltin & Lange-Bertalot	6AAI–AAJ	L: 11.2–18.2; W: 6.3–8.7; S: 21–25 (n= 26)	S1, S2, S3, S4, S5, S6, S7, S8	Levkov *et al*. (2013)
L. ventricosa (Kützing) Mann	6AAK	L: 17.5; W: 6; S: 18 (n= 1)	S1	Levkov *et al*. (2013)
AMPHIPLEURACEAE				
Amphipleura lindheimeri Grunow	7A	L: 175–194; W: 28–29 (n= 4)	S8	Metzeltin *et al*. (2005)
Frustulia acidophilissima Wydrzycka & Lange-Bertalot	7B	L: 39.2–57.4; W: 11.2–14.6; TS: 27–30; LS: 28–30 (n= 27)	S2, S3, S4, S5, S6, S7, S8	Metzeltin & Lange-Bertalot (2007
F. australocrassinervia Casa, Mataloni & Van de Vijver	7C; 13K–13L	L: 25–61.2; W: 7.7–11.8; TS: 28–35; LS: 28–37 (n= 223)	S1, S2, S3, S4, S5, S6, S7, S8	Casa *et al*. (2018)
F. guayanensis Metzeltin & Lange Bertalot	7D	L: 36.9–56.1; W: 8.8–9.2 (n= 4)	S3, S5, S8	Metzeltin & Lange-Bertalot (1998)
F. neomundana Lange-Bertalot & Rumrich	7E; 13M	L: 29.2–39.7; W: 6.4–9.1; S: 36; A: 31 (n= 64)	S1, S2, S3, S4, S5, S6, S7, S8	Rumrich *et al*. (2000)
F. pumilio Lange-Bertalot & Rumrich	7K–7L	L: 14–27.5; W: 4.5–6.1 (n= 35)	S1, S2, S3, S4, S6, S7, S8	Rumrich *et al*. (2000)

Taxa	Figures	Morphometric (μm) and meristic (in 10 μm) data	Occurrence	Followed literature
F. saxonica Rabenhorst	7I–7J	L: 46.1–71.6; W: 10.9–14.9; TS: 24–30; LS: 23–30 (n= 105)	S1, S2, S3, S4, S5, S6, S7, S8	Lange-Bertalot (2001)
F. undosa Metzeltin & Lange-Bertalot	7F	L: 33.4–43.8; W: 7.6–10 (n= 32)	S1, S2, S3, S4, S5, S6, S7, S8	Lange-Bertalot (2001)
F. vulgaris (Thwaites) De Toni	7H	L: 41.2–46.9; W: 7.5–9.1 (n= 30)	S1, S2, S3, S4, S6, S7, S8	Lange-Bertalot (2001)
F. weinholdii Hustedt	7G; 13J	L: 24.6–37.9; W: 6.8–8.3; S: 32; A: 29 (n= 65)	S1, S2, S3, S4, S6, S7, S8	Lange-Bertalot (2001)
BRACHYSIRACEAE				
Brachysira brebissonii Ross	7N	L: 18.3–25; W: 5.1–6.9; S: 27–28 (n= 14)	S3, S4, S5, S6, S8	Lange-Bertalot & Moser (1994) Kennedy & Allott (2017)
B. microcephala (Grunow) Compère	7O; 13H	L: 11.3–26.4; W: 3.8–5.2; S: 34–36 (n= 116)	S2, S3, S4, S6, S7, S8	Lange-Bertalot & Moser (1994) Kennedy & Allott (2017)
B. serians var. *acuta* (Hustedt) Vyverman	7M	L: 37.4–62.5; W: 8.7–11.4; S: 21–26; A: 13–14 (n= 6)	S1, S3, S8	Vyverman (1991)
N. praecipuoides Tremarin & Ludwig	7P	L: 15.4–18.7; W: 4.7–6 (n= 38)	S1, S3, S8	Tremarin *et al.* (2015)
N. semifasciata Amaral, Ludwig & Bueno	7Q–7R	L: 6.7–16.4; W: 3.2–4.8; L/W: 1.7–3.7 (n= 222)	S1, S2, S3, S4, S5, S6, S7, S8	Amaral *et al.* (2021)
NEIDIACEAE				
Neidium affine var. *amphirhynchus* (Ehrenberg) Cleve	7U	L: 36.3–51.7; W: 9.9–11.9; S: 22–25; A: 18–24 (n= 10)	S3, S8	Patrick & Reimer (1966)
N. catarinense (Krasske) Lange-Bertalot	7Y	L: 18.8–23.5; W: 4.2–4.7; S: 21–23 (n= 5)	S1, S6, S8	Metzeltin & Lange-Bertalot (1998)
N. essequiboanum Metzeltin & Krammer	7W–7X	L: 31.6–40.2; W: 5.4–6.5 (n= 5)	S5	Metzeltin & Lange-Bertalot (1998, 2007)
N. gracile f. *aequale* Hustedt	7S	L: 48.2–49.8; W: 10–10.6; S: 21–23 (n= 4)	S3	Patrick & Reimer (1966)
N. iridis (Ehrenberg) Cleve	7T	L: 44–57.6; W: 12.1–13.6; S: 22–23; A: 19–20 (n= 2)	S3	Patrick & Reimer (1966) Krammer & Lange-Bertalot (1986)
N. tenuissimum Hustedt	7V	L: 15–19.8; W: 3.8–4.9 (n= 8)	S1, S2, S3, S4, S5, S8	Hustedt (1943) Patrick & Reimer (1966)
PINNULARIACEAE				
Pinnularia acoricola Hustedt	7Z–7AA; 14A	L: 15.3–25.5; W: 3.7–5; S: 16–19 (n= 53)	S1, S2, S3, S4, S5, S7, S8	Hustedt (1935) Tremarin *et al.* (2010)
P. acrosphaeria (Brébisson) Smith	7AB	L: 49–54.5; W: 10.2–11.9; S: 12–14 (n= 4)	S2, S3	Krammer (2000)
P. borealis var. *rectangularis* Carlson	7AD	L: 23–42; W: 6.4–8.2; S: 5–6 (n= 7)	S1, S3, S6, S7, S8	Krammer (2000)
P. borealis var. *sublinearis* Krammer	7AE	L: 19.6–44.5; W: 6–9.7; S: 5–7 (n= 2)	S1, S3	Krammer (2000)

Taxa	Figures	Morphometric (µm) and meristic (in 10 µm) data	Occurrence	Followed literature
P. brauniana (Grunow) Studnicka	7AF	L: 34.6–55.8; W: 6.3–8.9; S: 10–13 (n= 19)	S1, S2, S3, S5	Krammer (1992)
P. butantanum (Krasske) Metzeltin	7AH	L: 63.6–102; W: 12–13.5; S: 15–17 (n= 13)	S3, S6, S8	Metzeltin & Lange-Bertalot (1998)
P. certa Krammer & Metzeltin	8L–8M	L: 38.2–41.9; W: 7.7–8.5; S: 11–12 (n= 3)	S3	Metzeltin & Lange-Bertalot (1998)
P. decrescens var. *ignorata* (Krammer) Krammer	7AK	L: 41.7–52.1; W: 11.4–12.8; S: 11–12 (n= 4)	S3	Krammer (2000)
P. divergens Smith	7I–7J	L: 41.8–73.9; W: 9.2–12.2; S: 9–12 (n= 20)	S1, S2, S3, S4, S5, S6	Krammer (1992)
P. divergens var. *media* Krammer	7AG	L: 39.6–72.8; W: 8.9–13.3; S: 10–13 (n= 85)	S1, S2, S3, S4, S6	Krammer (2000)
P. divergens var. *mesoleptiformis* Krammer & Metzeltin	7AL	L: 63.2–89.2; W: 12.1–13.9; S: 11–12 (n= 9)	S1, S3, S4, S8	Metzeltin & Lange-Bertalot (1998)
P. gaiserae Metzeltin & Lange-Bertalot	7AC	L: 46.6–56.2; W: 7.3–8.9; S: 11 (n= 7)	S1, S5, S8	Metzeltin & Lange-Bertalot (2007)
P. graciloides var. *latecapitata* Metzeltin & Krammer	8A–8B	L: 38.6–65.4; W: 6.7–9.4; S: 11–13 (n= 45)	S1, S2, S3, S4, S5, S6, S8	Metzeltin & Lange-Bertalot (1998)
P. graciloides var. *triundulata* (Fontell) Krammer	8C	L: 65.3; W: 9.1; S: 12 (n= 1)	S8	Krammer (2000)
P. joculata (Manguin) Krammer	8V	L: 18.6–19.4; W: 3.8; S: 18–20 (n= 2)	S1, S2	Krammer (2000)
P. laucensis Lange-Bertalot	8J–8K	L: 15.5–26.3; W: 3.6–4.5; S: 12–15 (n= 23)	S1, S3, S5, S7, S8	Rumrich *et al*. (2000)
P. meridiana Metzeltin & Krammer	8Q	L: 32.2–45.; W: 8.8–10; S: 11–13 (n= 12)	S1, S2, S3, S4	Metzeltin & Lange-Bertalot (1998)
P. microstauron var. *rostrata* Krammer	8N	L: 24.6–34.7; W: 5.2–8; S: 12–14 (n= 21)	S1, S2, S3, S4, S5, S6, S8	Krammer (2000)
P. obscura Krasske	8T–8U	L: 16.8–30.1; W: 4.6–6.2; S: 13–16 (n= 37)	S1,S2, S3, S4, S5, S7, S8	Krasske (1932) Krammer (2000)

Taxa	Figures	Morphometric (µm) and meristic (in 10 µm) data	Occurrence	Followed literature
P. rumrichae Krammer	8R	L: 27.6–40,7; W: 5.1–6.8; S: 11–13 (n= 17)	S1, S2, S3	Krammer (2000)
P. schoenfelderi Krammer	8S	L: 24.8–40.9; W: 5.6–7.9; S: 13–15 (n= 10)	S1, S2, S3, S5, S6	Krammer (1992)
P. stidolphii Krammer	8I	L: 150.2; W: 24; S: 12 (n= 1)	S4	Krammer (2000)
P. subanglica Krammer	8P	L: 30.4–47.8; W: 7.5–9.9; S: 11–13 (14) (n= 98)	S1, S2, S3, S4, S5, S6, S8	Krammer (2000)
P. subcapitata W.Gregory	8O	L: 33.3–44; W: 5.5–7.2; S: 13–15 (n= 29)	S1, S2, S3, S4, S5, S8	Krammer (2000)
P. subgibba Krammer	8H	L: 61.9–78.7; W: 9.4–11.6; S: 9 (n= 2)	S1, S3	Krammer (1992)
P. subgibba var. *undulata* Krammer	8F–8G	L: 35.7–83.3; W: 8.1–11; S: 10–12 (n= 80)	S1, S2, S3, S4, S5, S6, S7, S8	Krammer (2000)
P. tabellaria Ehrenberg	8E	L: 70.6–75.3; W: 10.3–12.1; S: 13–15 (n= 3)	S3	Krammer (2000)
P. viridiformis Krammer	8D	L: 72–79.5; W: 12.5–13.2; S: 10–11 (n= 2)	S3	Krammer (2000)
SELLAPHORACEAE				
Fallacia insociabilis (Krasske) Mann	8W	L: 8.8–13; W: 5.4–6.6; S: 22–24 (n= 5)	S1, S3	Krammer & Lange-Bertalot (1986)
Sellaphora laevissima (Kützing) Mann	8Z	L: 33.4–39.8; W: 6.8–10.2; S: 22–25 (n= 7)	S2, S3, S6	Mann *et al*. (2008)
S. nigri (De Notaris) Wetzel & Ector	8X–8Y; 14C–14D	L: 6.5–11.3; W: 3.4–4.5; S: 23–30; A: 42–54 (n= 192)	S1, S2, S3, S4, S5, S6, S7, S8	Wetzel *et al*. (2015)
S. pupula (Kützing) Mereschkowsky	8AB	L: 14.7–39.4; W: 5.6–8.7; S: 20–26 (n= 55)	S1, S2, S3, S5, S6, S8	Mann *et al*. (2004)
S. rhombicarea Metzeltin, Lange-Bertalot & García-Rodríguez	8AA	L: 36.3; W: 9.8; S: 16 (n= 1)	S8	Metzeltin *et al*. (2005)
S. sassiana (Metzeltin & Lange-Bertalot) Wetzel	8AG	L: 12.1–15.4; W: 4.3–5.2; S: 23–26 (n= 71)	S1, S3, S4, S8	Metzeltin & Lange-Bertalot (1998)
S. saugerresii (Desmazières) Wetzel & Mann	8AC–8AF; 14E	L: 5.2–16.6; W: 3–5.2; 19–23 (n= 291)	S1, S2, S3, S4, S5, S6, S7, S8	Wetzel *et al*. (2015)
S. tridentula (Krasske) Wetzel	8AH	L: 13.8–20.2; W: 3.8–4.9 (n= 8)	S1, S3	Wetzel *et al*. (2015)
DIPLONEIDACEAE				
Diploneis subovalis Cleve	8AI	L: 17–34.4; W: 10.1–19.1; S: 10–13; A: 18–22 (n= 27)	S1, S2, S3, S4, S6, S7, S8	Krammer & Lange-Bertalot (1986)
NAVICULACEAE				
Caloneis bacillum (Grunow) Cleve	8AL–8AM	L: 25.7–37.3; W: 4.7–7.3; S: 19–23 (n= 57)	S1, S2, S3, S4, S7, S8	Krammer & Lange-Bertalot (1986)
C. hyalina Hustedt	8AJ	L: 14.8–21.4; W: 4.5–5.7 (n= 61)	S1, S2, S3, S4, S5, S6, S7, S8	Patrick & Reimer (1966)
C. westii (Smith) Hendey	8AK	L: 49.6–59.8; W: 12.1; S: 14–15 (n= 3)	S1, S2, S3, S5	Hendey (1964)

Taxa	Figures	Morphometric (μm) and meristic (in 10 μm) data	Occurrence	Followed literature
Capartogramma crucicula (Grunow) Ross	9A	L: 30.5–30.7; W: 8.4–8.5; S: 23–25 (n= 2)	S3	Patrick & Reimer (1966)
Gyrosigma acuminatum (Kützing) Rabenhorst	9B	L: 100.4; W: 12.8; S: 21 (n= 1)	S1	Metzeltin *et al*. (2005)
G. obtusatum (Sullivant & Wormley) Boyer	9C	L: 56.4–65.8; W: 9.5–10.1; S: 24–25 (n= 28)	S1, S2, S3, S4, S6, S7, S8	Patrick & Reimer (1966) Metzeltin *et al*. (2005)
Navicula angusta Grunow	9J	L: 36.9–49.8; W: 5.7–6.6; S: 12–14 (n= 101)	S1, S2, S3, S4, S5, S6, S7, S8	Krammer & Lange-Bertalot (1997)
N. cryptocephala Kützing	9F–9I; 14F	L: 21.2–43.9; W: 4.7–7.1; S: 15–18; A: 40 (n= 280)	S1, S2, S3, S4, S5, S6, S7, S8	Lange-Bertalot (2001) Jüttner *et al*. (2020)
N. cryptotenella Lange-Bertalot	9L–9M	L: 15.4–36; W: 5–6.7; S: 14–17; A: 37 (n= 108)	S1, S2, S3, S4, S5, S6, S7, S8	Krammer & Lange-Bertalot (1997) Lange-Bertalot (2001)
N. eichhorniaephila Manguin ex Kociolek & Reviers	9D–9E	L: 29.8–34.7; W: 4.9–6.1; 12–14 (n= 36)	S1, S2, S3, S4, S6, S7, S8	Rumrich *et al*. (2000) Metzeltin *et al*. (2007)
N. leptostriata Jørgensen	9K	L: 47.2–55.8; W: 6.8–9.3; S: 13–14 (n= 27)	S2, S6, S7, S8	Lange-Bertalot (2001) Metzeltin & Lange-Bertalot (2007)
N. radiosa Kützing	9N	L: 49.6–85.4; W: 8.3–10; S: 9–11 (n= 42)	S1, S2, S3, S4, S6, S8	Lange-Bertalot (2001)
N. rostellata Kützing	9S	L: 35.3–42.8; W: 8.6–10.7; S: 12–15 (n= 49)	S1, S2, S3, S6, S8	Rumrich *et al*. (2000) Lange-Bertalot (2001)
N. salinicola Hustedt	9T–9U; 14G	L: 10–18.9; W: 3.1–4.4; S: 17–20; A: 38–43 (n= 125)	S1, S2, S3, S4, S5, S6, S7, S8	Krammer & Lange-Bertalot (1997) Lange-Bertalot (2001)
N. schwabei Krasske	9R	L: 53.3; W: 9.9; S: 21–22; A: 22–23 (n= 1)	S3	Lange-Bertalot *et al*. (1996)
N. symmetrica Patrick	9Q; 14H–14I	L: 24.8–40.9; W: 5.9–7.9; S: 13–15; A: 23–29 (n= 148)	S1, S2, S3, S4, S6, S7, S8	Lange-Bertalot (2001)
N. tenelloides Hustedt	9O–9P	L: 11.5–18.3; W: 2.9–4; S: 18–21 (n= 8)	S1, S8	Krammer & Lange-Bertalot (1997) Lange-Bertalot (2001)
STAURONEIDACEAE				
Craticula ambigua (Ehrenberg) Mann	9X	L: 54.8–82.1; W: 14.6–21.5; S: 16–20; A: 27–29 (n= 3)	S1, S3	Lange-Bertalot (2001) Levkov *et al*. (2016)
C. riparia (Hustedt) Lange-Bertalot	9Y–9Z	L: 32.7–48.1; W: 7.6–10.6; S: 18–22 (n= 25)	S3, S4, S8	Lange-Bertalot (2001)
C. submolesta (Hustedt) Lange-Bertalot	9V–9W	L: 14.2–23.2; W: 4.1–5.8; S: 18–24 (n= 27)	S1, S2, S3, S4, S5	Lange-Bertalot (2001)
Stauroneis gracilis Ehrenberg	9AC	L: 54–78.3; W: 9.9–14.8; S: 19–25; A: 20–23 (n= 3)	S3, S6	Reichardt (1995) Bahls (2010)
S. neohyalina Lange-Bertalot & Krammer	9AD	L: 44.4–50.2; W: 8.8–9.1 (n= 2)	S3, S4	Lange-Bertalot & Genkal (1999)

Taxa	Figures	Morphometric (μm) and meristic (in 10 μm) data	Occurrence	Followed literature
S. phoenicenteron (Nitzsch) Ehrenberg	9AE	L: 112–160; W: 21.7–28.9; S: 16–18; A: 15–19 (n= 3)	S3, S8	Krammer & Lange-Bertalot (1986) Patrick & Reimer (1966)
S. smithii Grunow	9AA–9AB	L: 21.1–21.7; W: 3.7–4.1 (n= 7)	S2, S4, S5, S6	Bahls (2010) Levkov *et al.* (2016)
NAVICULALES *INCERTAE SEDIS*				
Chamaepinnularia brasilianopsis Metzeltin & Lange-Bertalot	9AF–9AG; 14B	L: 8.5–13.3; W: 3–4.1; S: 23–26 (n= 22)	S2, S3, S4, S5, S7	Metzeltin & Lange-Bertalot (1998)
Kobayasiella parasubtilissima (Kobayasi & Nagumo) Lange-Bertalot	9AI–AJ	L: 16.8–30.9; W: 3.7–5.5 (n= 40)	S1, S3, S8	Kobayasi & Nagumo (1988) Buczkó *et al.* (2009)
Pseudofallacia monoculata (Hustedt) Liu, Kociolek & Wang	9AH	L: 12.8–16.2; W: 4.8–5; S: 22–24 (n= 2)	S3	Hustedt (1945) Krammer & Lange-Bertalot (1985)
CATENULACEAE				
Amphora copulata (Kützing) Schoeman & Archibald	9AM	L: 28.1–33.9; W: 6.2–7.8; S: 14 (n= 2)	S3	Schoeman & Archibald (1986) Levkov (2009)
Halamphora montana (Krasske) Levkov	9AK	L: 12.9–18.2; W: 2.9–4.2 (n= 61)	S1, S2, S3, S4, S6, S7, S8	Krammer e Lange-Bertalot (1997) Hofmann *et al.* (2013)
H. normanii (Rabenhorst) Levkov	9AL	L: 21.6–31.7; W: 4.5–6.2; S: 17–19 (n= 40)	S1, S3, S4, S6, S7, S8	Levkov (2009)
BACILLARIACEAE				
Hantzschia amphioxys (Ehrenberg) Grunow	10A	L: 19.4–38.7; W: 3.6–7.5; S: 8–12 (14); S: 22–27 (n= 48)	S1, S2, S3, S4, S5, S6, S7, S8	Krammer & Lange-Bertalot (1988) Siver & Hamilton (2011)
Nitzschia amphibia Grunow	10U–10V	L: 9–27.4; W: 3.2–4.1; F: 8–11; S: 16–19 (n= 23)	S1, S4, S8	Rumrich *et al.* (2000)
N. brevissima Grunow	10Q	L: 27.7–31.6; W: 5.5–5.6; F: 8 (n= 2)	S4, S7	Krammer & Lange-Bertalot (1988)
N. clausii Grunow	9AJ; 15A–15B	L: 22.4–42.1; W: 3.6–5.1; F: 9–14; S: 37; A: 38 (n= 58)	S1, S2, S3, S4, S5, S6, S7, S8	Krammer & Lange-Bertalot (1988) Hofmann *et al.* (2013)
N. dissipata (Kützing) Rabenhorst	10B	L: 29.1–33.5; W: 4.3–4.9; F: 13 (n= 3)	S3	Krammer & Lange-Bertalot (1988)
N. inconspicua Grunow	10N–10P; 15C–15D	L: 8.5–18.3; W: 2.5–3.3; F: 9–13; S: 23–25; A: 28 (n= 17)	S1, S2, S3, S4, S7, S8	Trobajo *et al.* (2013)
N. intermedia Hantzsch ex Cleve & Grunow	10I	L: 23.5–71; W: 2.9–6; F: 10–16 (n= 73)	S1, S2, S3, S6, S8	Krammer & Lange-Bertalot (1988)
N. linearis (Agardh) Smith	10K	L: 49–119.2; W: 5.7–6; F: 7–13 (n= 29)	S2, S3, S4, S6, S8	Krammer & Lange-Bertalot (1988)
N. lorenziana Grunow	10J	L: 49.3–79.6; W: 3–3.8; F: 8–10; S: 17–18 (n= 9)	S2, S3, S4, S6, S8	Rumrich *et al.* (2000)

Taxa	Figures	Morphometric (µm) and meristic (in 10 µm) data	Occurrence	Followed literature
N. palea (Kützing) Smith	10C–10F	L: 15.7–44.4; W: 3–5.1; F: 10–16 (n= 155)	S1, S2, S3, S4, S5, S6, S7, S8	Rumrich *et al*. (2000) Levkov *et al*. (2007)
N. palea var. *debilis* (Kützing) Grunow	10L–10M	L: 13.1–53.6; W: 2.3–3.6; F: 11–14 (n= 29)	S1, S2, S3, S4, S6	Krammer & Lange-Bertalot (1988)
N. perminuta Grunow in Van Heurck	10R–10S; 15E–15F	L: 10.5–19.1; W: 2.6–3.4; F: 10–13; S: 22–33; A: 47 (n= 36)	S1, S2, S3, S4, S6, S7, S8	Krammer & Lange-Bertalot (1988) Levkov *et al*. (2007)
N. recta Hantzsch ex Rabenhorst	10H	L: 24–63.4; W: 3.3–5.5; F: 5–9 (n= 56)	S1, S2, S3, S4, S5, S6, S7, S8	Krammer & Lange-Bertalot (1988)
N. semirobusta Lange-Bertalot	10W	L: 16–24.7; W: 3.4–4.2; F: 7–8; S: 17 (n= 2)	S1	Lange-Bertalot (1993)
N. terrestris (Petersen) Hustedt	10T	L: 38.3–55.9; W: 4.3–4.4; F: 6–7 (n= 2)	S3	Krammer & Lange-Bertalot (1988)
Tryblionella debilis Arnott ex O'Meara	10X	L: 20.5–21.6; W: 8.7–9.1; S: 17–18 (n= 2)	S3, S4	Krammer & Lange-Bertalot (1988)
RHOPALODIACEAE				
Epithemia gibberula (Ehrenberg) Kützing	10Y	L: 29.4–34; W: 7.8–8.2; AC: 3–4; S: 18–20; A: 14–20 (n= 7)	S2, S3, S6	Cocquyt *et al*. (2018)
SURIRELLACEAE				
Iconella curvula (Smith) Ruck & Nakov	10Z–10AA; 15G–15H	L: 166.3–214; W: 5.6–6.8; AC: 5–6; S: 23–25 (n= 2)	S3	Metzeltin & Lange-Bertalot (1998)
I. delicatissima (Lewis) Ruck & Nakov	10AB; 15I	L: 37.4–65.6; W: 4.9–6.4; AC: 6–7 (n= 2)	S3, S5	Metzeltin & Lange-Bertalot (1998)
I. splendida (Ehrenberg) Kützing	10AC	L: 83.5–86.3; W: 34.4–38; AC: 2 (n= 5)	S1, S3, S6, S8	Krammer & Lange-Bertalot (1988)
I. tenuissima (Hustedt) Kapustin & Kulikovskiy	10AD	L: 12–31.2; W: 5.2–10; AC: 4–6 (n= 99)	S1, S2, S3, S4, S5, S6, S7, S8	Krammer & Lange-Bertalot (1988) Kapustin & Kulikovskiy (2018)
Surirella angusta Kützing	10AF	L: 16.9–35.4; W: 7.2–8.3; AC: 5–7; S: 27 (n= 23)	S1, S2, S3, S4, S7, S8	Krammer & Lange-Bertalot (1988)
S. biseriata var. *constricta* Grunow ex Hustedt	10AG	L: 74.3–97.9; W: 15.5–18.7; AC: 2–3 (n= 2)	S3	Hustedt (1930)
S. grunowii Kulikovskiy, Lange-Bertalot & Witkovski	10AH	L: 60.6; W: 13.1–16.8; AC: 3 (n= 2)	S3	Kulikovskiy *et al*. (2010)
S. stalagma Hohn & Hellerman	10AE	L: 12.8; 4.7; AC: 9 (n= 1)	S4	Hohn & Hellerman (1963)

[1]Van Dam *et al*. (1994); [2]Lobo *et al*. (2015); [3]Faustino *et al*. (2016); [4]Marra *et al*. (2016); [5]Hofmann (1994); [6]Yang & Dickman (1993); [7]Levkov *et al*. (2016); [8]Costa *et al*. (2017a); [9]Jüttner *et al*. (2013); [10]Lange-Bertalot (2001); [11]Wojtal *et al*. (2011); [12]Krammer & Lange-Bertalot (1991a); [13]Krammer & Lange-Bertalot (1997); [14]Lange-Bertalot & Ulrich (2014); [15]Tuji & Williams (2007); [16]Wetzel *et al*. (2002); [17]Lepskaya *et al*. (2010); [18]Liu *et al*. (2011); [19]Taylor *et al*. (2007); [20]Almeida *et al*. (2016); [21]Silva *et al*. (2010); [22]Moro & Fürstenberger (1997); [23]Krammer (1997a); [24]Krammer (1997b); [25]Wetzel *et al*. (2014); [26]Potapova & Charles (2007); [27]Stenger-Kovács *et al*. (2007); [28]Krammer (2000); [29]Ferreira &

Bicudo (2017); [30]Levkov *et al*. (2013); [31]Moresco *et al*. (2011); [32]Reichardt (2015); [33]Morales & Vis (2007); [34]Hofmann *et al*. (2011); [35]Patrick & Reimer (1966); [36]Silva-Lehmkuhl *et al*. (2019); [37]Bicudo *et al*. (2016); [38]Wengrat *et al*. (2015); [39]Faria *et al*. (2010); [40]Lange-Bertalot & Metzeltin (1996); [41]Bertolli *et al*. 2010; [42]Luchini & Verona (1972); [43]Bartozek *et al*. (2018); [44]Nardelli *et al*. (2016); [45]Metzeltin *et al*. (2005); [46]Marquardt *et al*. (2014); [47]Weiler *et al*. (2016); [48]Kapetanovic *et al*. (2011); [49]Wunsam *et al*. (1995); [50]Udovic *et al*. (2017); [51]Costa *et al*. (2017b); [52]Almeida *et al*. (2020); [53]Marquardt *et al*. (2017); [54]Medeiros *et al*. (2018); [55]Lobo *et al*. (2004); [56]Heinrich *et al*. (2014); [57]da Silva *et al*. (2016); [58]Lobo *et al*. (2016); [59]Levkov *et al*. (2016); [60]Morais *et al*. (2018); n.d.: no data.

The Principal Component Analysis (PCA) for the ecological variables accounted for 52.52% of the total variability in the data in the first two axes (Fig 2a). The first axis of the PCA explains the variability primary related to total phosphorus positively (correlation value: 0.54), and pH negatively (-0.51). The distribution of these scores tends to cluster points S5, S6, S7 and S8 to the negative side of the axis, relating to higher values of pH. The second axis is positively related with orthophosphate (0.39) and negatively with nitrate (-0.63), and electrical conductivity (-0.54). The distribution of these scores tends to separate sampling sites S2 and S4 from S5, S6, S7, and S8.

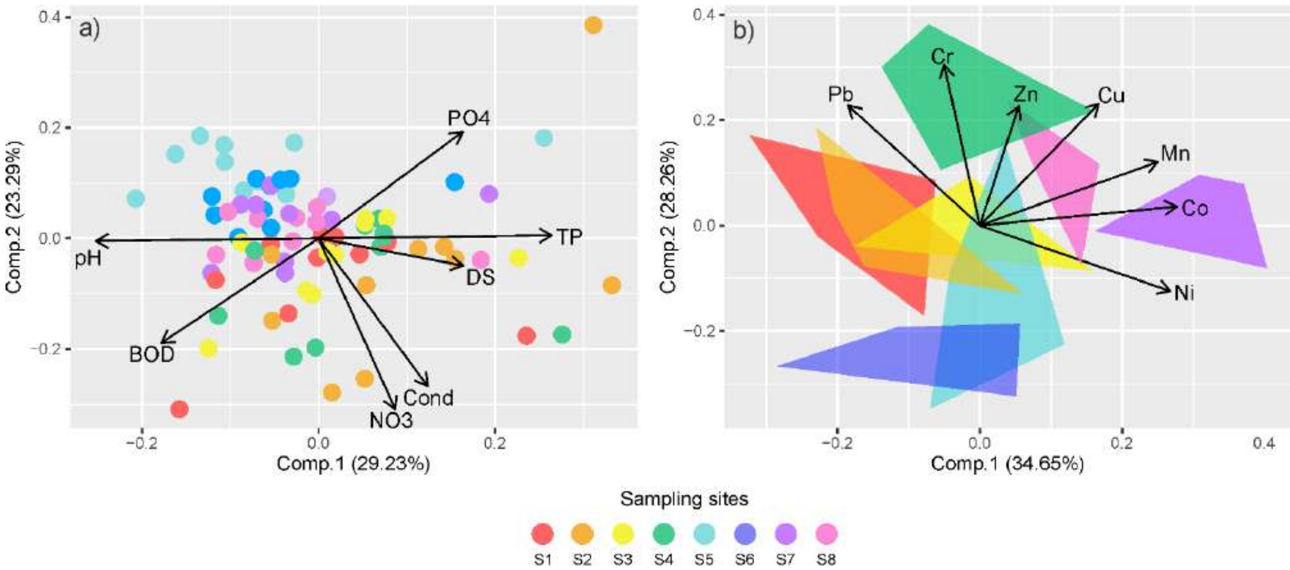

FIGURE 2. Variability of environmental data for the eight sampling sites in the Cascavel River microbasin, Paraná State, Brazil. a) Principal Component Analysis for abiotic data analyzed from water samples (BOD: Biochemical Oxygen Demand; NO_3: nitrate; Cond: electrical conductivity; DS: dissolved solids; TP: total phosphorus; PO_4^-: orthophosphate). b) Principal Component Analysis for metals data analyzed in the surface sediment (Co: cobalt, Cr: chromium, Cu: copper, Mn: manganese, Ni: nickel, Pb: lead, Zn: zinc). The sampling sites for surface sediment were represented by polygons.

Principal Component Analysis for the metals accounted for 62.91% of the total variability in the data in the first two axes (Fig 2b). The first axis of the PCA explains the variability primary related to cobalt (correlation value: 0.53), nickel (0.51), and manganese (0.47) positively, and lead negatively (-0.35). The distribution of these scores demonstrates a separation of sampling sites S7 and S8 from S1 and S2. Moreover, the second axis is positively related with chromium (0.58), copper (0.44), lead (0.43), and zinc (0.42) positively, and nickel negatively (-0.24). The distribution of these scores demonstrates a separation of sampling sites S5 and S6 from the others.

During our study, we identified diatoms with deformed valve outlines, changes concerning the striae pattern, and with doubled central area in the eight sampling sites (Table 2). Teratological valves were found in 34 taxa, belonging to 15 genera, with *Eunotia* containing the greater number of altered taxa (8 spp.). Mixed teratologies (deformed valve outline + unusual striae pattern) were found only in *Ulnaria ulna*, *Encyonema neomesianum*, and *Gomphonema graciledictum*. In SEM, we found only *Eunotia bilunaris* (n = 1) and *Gomphonema lagenula* (n = 1) with teratologies, showing a deformed valve outline. Teratological taxa are described below, showing morphological changes and ecological characteristics of the environment where abnormal individuals were found.

TABLE 2. Teratological diatoms found in Cascavel river microbasin, with occurrences in sampling sites, and related metals.

Taxa	Figures	Type of teratology*	Occurrence	Metals	
				Literature*	Our study
Discostella stelligera	2D–2E	Type 3	S3	x	Undefined
Fragilaria gracilis	2X–2AA	Type 1	S3, S8	As, Cd, Cu, Hg, Pb, Zn	Cu, Mn, Ni
F. pectinalis	2AE–2AH	Type 1	S3	x	Undefined
F. tenera var. *nanana*	2AL–2AO	Type 1	S3	x	Undefined
Ulnaria ulna	2AX–2AZ	Type 1 Type 7	S1, S2, S3, S6, S8	Cd, Cr, Cu, Fe, Sr, Zn	Undefined
Eunotia bilunaris	3G–3J; 12A	Type 1	S1, S2, S3, S4, S6, S8	x	Undefined
E. botulitropica	3P	Type 1	S5	x	Ni, Zn
E. desmogonioides	3T	Type 1	S3, S8	x	Cu, Mn, Ni
E. meridiana	3AV–3AX	Type 1	S3, S8	x	Cu, Mn, Ni
E. monodon	3AQ	Type 1	S2	x	Pb
E. rhomboidea	4E–4G	Type 1	S2	x	Pb
E. subarcuatoides	3W–3X	Type 1	S3, S8	Al, Ba, Mn	Cu, Mn, Ni
E. yberai	4N–4P	Type 1 Type 2	S1, S4	x	Cr, Pb
Encyonema neomesianum	4X	Type 7	S3	x	Undefined
E. silesiacum	4AA	Type 1	S2	Cd, Cu, Pb, Zn	Pb
Gomphonema angustatum	5F–5H	Type 1	S2, S3, S6	x	Pb
G. graciledictum	5W–5X	Type 2 Type 7	S3	x	Undefined
G. lagenula	5AQ–5AS; 12J	Type 1	S1, S2, S3, S4, S6, S7, S8	x	Undefined
G. naviculoides	5AU	Type 2	S3	x	Undefined
G. pumilum	5AM	Type 1	S8	x	Cu, Mn
Achnanthidium macrocephalum	6L–6P	Type 1	S3, S4, S8	Cu, Zn	Cr, Zn
A. minutissimum	6X–6AC	Type 1	S1, S2, S3, S4, S6, S7	Cd, Cr, Cu, Pb, Sr, Zn	Undefined
A. modestiforme	6AF–AH	Type 1	S3, S5, S7	x	Ni
Planothidium rostratum	6AO–AP	Type 1	S3	x	Undefined
Frustulia saxonica	7I	Type 1	S1, S2	x	Pb
Pinnularia divergens	7AJ	Type 1	S1	x	Pb
P. graciloides var. *latecapitata*	8B	Type 1	S2, S4, S7	x	Cr, Ni, Pb
Sellaphora saugerresii	8AD–8AF	Type 1	S1, S2, S7, S8	As, Cd, Pb, Zn	Ni, Pb
Caloneis bacillum	8AM	Type 1	S8	Cd, Cu, Pb, Zn	Cu, Mn
Navicula cryptocephala	9G–9I	Type 1	S2	x	Pb
N. cryptotenella	9M	Type 1	S2, S3	Cd, Cu, Pb, Zn	Pb
Craticula riparia	9Z	Type 1	S3	x	Undefined
C. submolesta	9W	Type 1	S3	x	Undefined
Nitzschia palea	10D–10F	Type 1	S3	As, Cd, Cu, Hg, Ni, Pb, Zn	Undefined

* See Falasco *et al.* (2021) and references therein.

Family STEPHANODISCACEAE

Discostella stelligera (Figs 3D–3E)

Duplication of the stellate pattern of the alveoli in the central area (n = 2).

Ecological characteristics: Cond: 47.00 µS cm^{-1}; BOD: 3.00 mg L^{-1}; COD: 15.50 mg L^{-1}; $N\text{-}NH_3$: 200 µg L^{-1}; NO_3: 1.40 mg L^{-1}; DO: 16.30 mg L^{-1}; pH: 6.05; PO_4^-: 0.022 mg L^{-1}; TP: 0.05 mg L^{-1}; TS: 58.00 mg L^{-1}; Temp: 18.31 °C; Turb: 7.26; Flow: 0.93 m^3 s; Average depth: 0.15 m; Prec: 2.73 mm.

Metal Concentrations: Co: 33.57 mg L^{-1}; Cr: 27.33 mg L^{-1}; Cu: 197.55 mg L^{-1}; Mn: 398.50 mg L^{-1}; Ni: 31.80 mg L^{-1}; Pb: 46.56 mg L^{-1}; Zn: 93.81 mg L^{-1}.

Family FRAGILARIACEAE

Fragilaria gracilis (Figs 3X–3AA)

Deformed valve outline, undulated, containing protrusions, or bent apices (n = 6).

Ecological characteristics: Cond: 39.00–40.00 µS cm^{-1}; BOD: 1.19–2.38 mg L^{-1}; COD: 5.95–13.60 mg L^{-1}; $N\text{-}NH_3$: 58.00–37.80 µg L^{-1}; NO_3: 0.34–0.37 mg L^{-1}; DO: 14.27–14.80 mg L^{-1}; pH: 6.19–6.26; PO_4^-: 0.004–0.006 mg L^{-1}; TP: 0.007–0.016 mg L^{-1}; TS: 10.00–48.00 mg L^{-1}; Temp: 17.37–17.90 °C; Turb: 7.96–10.70; Flow: 0.47–1.16 m^3 s; Average depth: 0.19–0.29 m; Prec: 9.96 mm.

Metal Concentrations: Co: 23.91–39.39 mg L^{-1}; Cr: 27.33–85.31 mg L^{-1}; Cu: 170.55–264.18 mg L^{-1}; Mn: 398.50–606.73 mg L^{-1}; Ni: 31.80–73.27 mg L^{-1}; Pb: 31.05–46.56 mg L^{-1}; Zn: 79.00–172.60 mg L^{-1}.

F. pectinalis (Figs 3AE–3AH)

Abnormal valve outline, undulated (n = 11).

Ecological characteristics: Cond: : 39.00–40.00 µS cm^{-1}; BOD: 0.89– 2.38 mg L^{-1}; COD: 8.08–13.60 mg L^{-1}; $N\text{-}NH_3$: 323–378 µg L^{-1}; NO_3: 0.34–0.37 mg L^{-1}; DO: 14.62–14.80 mg L^{-1}; pH: 6.04–6.26; PO_4^-: 0.005–0.006 mg L^{-1}; TP: 0.009–0.016 mg L^{-1}; TS: 10.00–38.00 mg L^{-1}; Temp: 17.37–17.68 °C; Turb: 9.25–10.70; Flow: 0.47–0.62 m^3 s; Average depth: 0.23–0.31 m; Prec: 9.96 mm.

Metal Concentrations: Co: 23.91–33.57 mg L^{-1}; Cr: 27.33–78.86 mg L^{-1}; Cu: 197.55–235.49 mg L^{-1}; Mn: 398.50–444.52 mg L^{-1}; Ni: 31.80–69.89; Pb: 35.58–46.56 mg L^{-1}; Zn: 93.81–167.31 mg L^{-1}.

F. spectra (Figs 3AP–3AR)

Length: 42.7–70.1; width: 1.8–3.1; striae: 19–24 in 10 µm

The individuals found in our samples presented greater width (1.8–3.1 × 1.5–2.5 µm) and lower striae density (19–24 × 24–25 in 10 µm) in comparison to the original description (Almeida *et al.* 2016), however, the delicate appearance of the valves are similar. In our samples, *Fragilaria tenera* var. *tenera* was distinguished by lower striae density (15–16 in 10 µm) and *F. tenera* var. *nanana* by the capitate apices (Lange-Bertalot & Ulrich 2014, Almeida *et al.* 2020).

F. tenera* var. *nanana (Figs 3AL–3AO)

Length: 45.1–67.1 µm; width: 1.9–3.1 µm; striae: 20–22 in 10 µm

The individuals from Cascavel river microbasin contain a higher striae number (18.5–20 in 10 µm) than the original description. However, the authors pointed out that their specimens had lower striae density compared to the protologue provided by Meister (Lange-Bertalot & Ulrich 2014).

Deformed valve outline, undulated (n = 3).

Ecological characteristics: Cond: 38.00–40.00 µS cm^{-1}; BOD: 1.49–3.27 mg L^{-1}; COD: 7.23–8.08 mg L^{-1}; N-NH_3: 316–378 µg L^{-1}; NO_3: 0.37 mg L^{-1}; DO: 11.42–14.57 mg L^{-1}; pH: 5.79–6.19; PO_4^-: 0.006–0.008 mg L^{-1}; TP: 0.010–0.017 mg L^{-1}; TS: 38.00–66.00 mg L^{-1}; Temp: 17.37–17.50 °C; Turb: 7.03–10.70; Flow: 0.47 m^3 s; Average depth: 0.19–0.23 m; Prec: 9.96 mm.

Metal Concentrations: Co: 23.91–33.57 mg L^{-1}; Cr: 27.33–78.86 mg L^{-1}; Cu: 197.55–235.49 mg L^{-1}; Mn: 398.50–444.52 mg L^{-1}; Ni: 31.80–69.89; Pb: 35.58–46.56 mg L^{-1}; Zn: 93.81–167.31 mg L^{-1}.

Ulnaria ulna (Figs 3AX–3AZ)

Deformed valve outline, undulated or with strong constriction in the median portion of the valve. Slight alteration in the striae pattern (n = 18).

Ecological characteristics: Cond: 38.00–78.00 µS cm^{-1}; BOD: 0.1–9.9 mg L^{-1}; COD: 1.22–24.32 mg L^{-1}; N-NH_3: 8–316 µg L^{-1}; NO_3: 0.34–17.20 mg L^{-1}; DO: 5.84–22.80 mg L^{-1}; pH: 5.31–7.09; PO_4^-: 0.005–0.030 mg L^{-1}; TP: 0.005–0.82 mg L^{-1}; TS: 10.00–72.00 mg L^{-1}; Temp: 17.37–23.24 °C; Turb: 1.93–10.7; Flow: 0.027–4.17 m^3 s; Average depth: 0.02–0.29 m; Prec: 2.36–9.98 mm.

Metal Concentrations: Co: 18.10–55.52 mg L^{-1}; Cr: 24.51–85.01 mg L^{-1}; Cu: 170.45–245.83 mg L^{-1}; Mn: 345.77–639.87 mg L^{-1}; Ni: 32.41–78.27 mg L^{-1}; Pb: 24.07–52,76 mg L^{-1}; Zn: 123.32–412.52.

Family EUNOTIACEAE

Eunotia bilunaris (Figs 4G–4J; 13A)

Deformed valve outline, undulated, with protrusion, slight or strong constriction in the median portion of the valve, or strong bent ventrally or near the apices (n = 49).

Ecological characteristics: Cond: 41.00–70.00 µS cm^{-1}; BOD: 0.89–9.35 mg L^{-1}; COD: 1.20–20.32 mg L^{-1}; N-NH_3: 18–316 µg L^{-1}; NO_3: 0.32–9.31 mg L^{-1}; DO: 7.70–19.50 mg L^{-1}; pH: 5.79–6.99; PO_4^-: 0.003–0.022 mg L^{-1}; TP: 0.007–0.040 mg L^{-1}; TS: 10.00–174.00 mg L^{-1}; Temp: 17.37–23.56 °C; Turb: 2.47–37.50; Flow: 0.07–5.49 m^3 s; Average depth: 0.04–0.42 m; Prec: 2.37–11.17 mm.

Metal Concentrations: Co: 17.50–47.24 mg L^{-1}; Cr: 21.98–81.32 mg L^{-1}; Cu: 160.64–263.62 mg L^{-1}; Mn: 349.80–502.78 mg L^{-1}; Ni: 27.57–66.65 mg L^{-1}; Pb: 33.49–66.21 mg L^{-1}; Zn: 78.97–170.48 mg L^{-1}.

E. botulitropica (Fig 4P)

Deformed valve outline, with constriction in the median portion of the valve (n = 1).

Ecological characteristics: Cond: 10.00 µS cm^{-1}; BOD: 1.19 mg L^{-1}; COD: 4.28 mg L^{-1}; N-NH_3: 200 µg L^{-1}; NO_3: 0.10 mg L^{-1}; DO: 18.64 mg L^{-1}; pH: 7.18; PO_4^-: 0.005 mg L^{-1}; TP: 0.005 mg L^{-1}; TS: 13.00 mg L^{-1}; Temp: 21.27 °C; Turb: 0.96; Flow: 0.03 m^3 s; Average depth: 0.02 m; Prec: 3.81 mm.

Metal Concentrations: Co: 26.94 mg L^{-1}; Cr: 72.40 mg L^{-1}; Cu: 234.78 mg L^{-1}; Mn: 312.44 mg L^{-1}; Ni: 91.80 mg L^{-1}; Pb: 25.81 mg L^{-1}; Zn: 162.55 mg L^{-1}.

E. desmogonioides (Fig 4T)

Deformed valve outline, undulated (n = 34)

Ecological characteristics: Cond: 6.00–53.00 µS cm^{-1}; BOD: 0.89–5.83 mg L^{-1}; COD: 4.68–17.50 mg L^{-1}; N-NH_3: 200–680 µg L^{-1}; NO_3: 0.32–7.50 mg L^{-1}; DO: 7.66–14.62 mg L^{-1}; pH: 5.79–7.09; PO_4^-: 0.004–0.030 mg L^{-1}; TP: 0.007–0.017 mg L^{-1}; TS: 11.00–66.00 mg L^{-1}; Temp: 17.40–23.53 °C; Turb: 7.03–13.70; Flow: 0.45–1.06 m^3 s; Average depth: 0.19–0.34 m; Prec: 3.48–9.96 mm.

Metal Concentrations: Co: 23.73–60.76 mg L^{-1}; Cr: 27.33–88.85 mg L^{-1}; Cu: 160.64–264.18 mg L^{-1}; Mn: 398.50–606.73 mg L^{-1}; Ni: 27.57–73.27 mg L^{-1}; Pb: 31.05–66.21 mg L^{-1}; Zn:78.97–173.12 mg L^{-1}.

E. meridiana (Figs 4AV–4AX)

Deformed valve outline, with protrusion or constriction near the apices (n = 4)

Ecological characteristics: Cond: 47.00–52.00 µS cm^{-1}; BOD: 0.89–5.05 mg L^{-1}; COD: 10.20–11.05 mg L^{-1}; N-NH_3: 363–448 µg L^{-1}; NO_3: 0.37 mg L^{-1}; DO: 11.15–14.62 mg L^{-1}; pH: 6.04–6.47; PO_4^-: 0.005–0.006 mg L^{-1}; TP: 0.009 mg L^{-1}; TS: 21.00–49.00 mg L^{-1}; Temp: 17.35–17.40 °C; Turb: 7.79–9.25; Flow: 0.47–1.32 m^3 s; Average depth: 0.19–0.33 m; Prec: 9.96 mm.

Metal Concentrations: Co: 23.73–60.76 mg L^{-1}; Cr: 27.33–88.85 mg L^{-1}; Cu: 160.64–264.18 mg L^{-1}; Mn: 398.50–606.73 mg L^{-1}; Ni: 27.57–73.27 mg L^{-1}; Pb: 31.05–66.21 mg L^{-1}; Zn:78.97–173.12 mg L^{-1}.

E. monodon (Fig 4AQ)

Deformed valve outline, undulated (n = 1).

Ecological characteristics: Cond: 70.00 µS cm^{-1}; BOD: 1.00 mg L^{-1}; COD: 2.62 mg L^{-1}; N-NH_3: 200 µg L^{-1}; NO_3: 3.30 mg L^{-1}; DO: 15.81 mg L^{-1}; pH: 6.30; PO_4^-: 0.05 mg L^{-1}; TP: 0.005 mg L^{-1}; TS: 174.00 mg L^{-1}; Temp: 18.23 °C; Turb: 2.47; Flow: 0.88 m^3 s; Average depth: 0.14 m; Prec: 2.37 mm.

Metal Concentrations: Co: 17.50 mg L^{-1}; Cr: 79.78 mg L^{-1}; Cu: 244.29 mg L^{-1}; Mn: 370.99 mg L^{-1}; Ni: 66.65 mg L^{-1}; Pb: 33.49 mg L^{-1}; Zn:146.17 mg L^{-1}.

E. rhomboidea (Figs 5E–5G)

Deformed valve outline, with protrusion or bent of the valve (n = 9).

Ecological characteristics: Cond: 1.00–76.00 µS cm^{-1}; BOD: 2.03–3.50 mg L^{-1}; COD: 4.79–27.60 mg L^{-1}; N-NH_3: 200–310 µg L^{-1}; NO_3: 2.00–2.53 mg L^{-1}; DO: 11.62–17.23 mg L^{-1}; pH: 5.11–5.79; PO_4^-: 0.05–0.323 mg L^{-1}; TP: 0.17–0.35 mg L^{-1}; TS: 61.00–83.00 mg L^{-1}; Temp: 19.44–21.55 °C; Turb: 1.09–4.73; Flow: 0.33–0.82 m^3 s; Average depth: 0.07–0.15 m; Prec: 2.73–3.81 mm.

Metal Concentrations: Co: 19.52–23.11 mg L^{-1}; Cr: 25.92–78.24 mg L^{-1}; Cu: 196.71–253.92 mg L^{-1}; Mn: 329.01–434.49 mg L^{-1}; Ni: 33.21–84.74 mg L^{-1}; Pb: 24.42–38.28 mg L^{-1}; Zn: 78.35–182.64 mg L^{-1}.

E. subarcuatoides (Figs 4W–4X)

Deformed valve outline, undulated in the ventral side of the valve (n = 3).

Ecological characteristics: Cond: 44.00–53.00 µS cm^{-1}; BOD: 1.49–5.66 mg L^{-1}; COD: 8.08–16.67 mg L^{-1}; N-NH_3: 200–378 µg L^{-1}; NO_3: 0.37–5.46 mg L^{-1}; DO: 10.60–14.57 mg L^{-1}; pH: 6.19–6.58; PO_4^-: 0.006–0.030 mg L^{-1}; TP: 0.006–0.010 mg L^{-1}; TS: 38.00–44.00 mg L^{-1}; Temp: 17.35–21.57 °C; Turb: 10.70–24.40; Flow: 0.47–6.34 m^3 s; Average depth: 0.19–0.37 m; Prec: 3.48–9.96 mm.

Metal Concentrations: Co: 23.91–60.76 mg L^{-1}; Cr: 27.33–88.85 mg L^{-1}; Cu: 163.45–241.67 mg L^{-1}; Mn: 398.50–557.50 mg L^{-1}; Ni: 31.80–69.89 mg L^{-1}; Pb: 35.58–48.63 mg L^{-1}; Zn:83.42–173.12 mg L^{-1}.

E. yberai (Figs 5N–5P)

Deformed valve outline, with depression in the ventral region of the valve. Some individuals presented valves more curved ventrally. Unusual striae pattern (n = 5).

Ecological characteristics: Cond: 58.00–78.00 mS cm^{-1}; BOD: 1.10–5.50 mg L^{-1}; COD: 1.00–18.10 mg L^{-1}; N-NH_3: 200 µg L^{-1}; NO_3: 2.10–14.30 mg L^{-1}; DO: 6.17–19.50 mg L^{-1}; pH: 6.09–6.75;

PO_4^-: 0.004–0.046 mg L^{-1}; TP: 0.009–0.943 mg L^{-1}; TS: 32.00–104.00 mg L^{-1}; Temp:18.01–20.93 °C; Turb: 2.81–6.38; Flow: 0.10–0.45 m^3 s; Average depth: 0.04–0.12 m; Prec: 2.39–11.17 mm.

Metal Concentrations: Co: 23.67–44.91 mg L^{-1}; Cr: 23.67–83.01 mg L^{-1}; Cu: 210.07–273.01 mg L^{-1}; Mn: 349.80–523.81 mg L^{-1}; Ni: 28.58–58.71 mg L^{-1}; Pb: 35.17–61.04 mg L^{-1}; Zn: 81.88–239.18 mg L^{-1}.

Family CYMBELLACEAE

Encyonema neomesianum (Fig 5X)

Deformed valve outline, slight constriction in the median portion of the valve, on the ventral side. Slight change in striae pattern in the dorsal margin (n = 2).

Ecological characteristics: Cond: 41.00–52.00 µS cm^{-1}; BOD: 2.32–4.16 mg L^{-1}; COD: 5.10–17.43 mg L^{-1}; N-NH_3: 313–316 mg L^{-1}; NO_3: 0.32–1.70 mg L^{-1}; DO: 7.24–12.72 mg L^{-1}; pH: 6.03–6.90; PO_4^-: 0.004–0.006 mg L^{-1}; TP: 0.010–0.012 mg L^{-1}; TS: 10.00–16.00 mg L^{-1}; Temp: 17.90–23.23 °C; Turb: 8.84–9.60; Flow: 0.45–0.75 m^3 s; Average depth: 0.19–0.29 m; Prec: 9.96 mm.

Metal Concentrations: Co: 23.73–47.24 mg L^{-1}; Cr: 27.33–80.86 mg L^{-1}; Cu: 160.64–235.49 mg L^{-1}; Mn: 398.05–444.52 mg L^{-1}; Ni: 27.57–69.89 mg L^{-1}; Pb: 35.58–66.21 mg L^{-1}; Zn: 78.97–167.31 mg L^{-1}.

E. silesiacum (Fig 5AA)

Deformed valve outline, with slight constriction in the median portion of the valve, on the ventral side (n = 1).

Ecological characteristics: Cond: 70.00 µS cm^{-1}; BOD: 1.00 mg L^{-1}; COD: 2.62 mg L^{-1}; N-NH_3: 200 µg L^{-1}; NO_3: 3.30 mg L^{-1}; DO: 15.81 mg L^{-1}; pH: 6.30; PO_4^-: 0.05 mg L^{-1}; TP: 0.005 mg L^{-1}; TS: 174.00 mg L^{-1}; Temp: 18.28 °C; Turb: 2.47; Flow: 0.88 m^3 s; Average depth: 0.14 m; Prec: 2.37 mm.

Metal Concentrations: Co: 17.50 mg L^{-1}; Cr: 79.78 mg L^{-1}; Cu: 244.29 mg L^{-1}; Mn: 370.99 mg L^{-1}; Ni: 66.65 mg L^{-1}; Pb: 33.49 mg L^{-1}; Zn:146.17 mg L^{-1}.

Family GOMPHONEMATACEAE

Gomphonema angustatum (Figs 6F–6H)

Deformed valve outline, with protrusion, or bent apices. Unusual striae pattern, usually becoming more radiate (n = 6).

Ecological characteristics: Cond: 21.00–53.00 µS cm^{-1}; BOD: 1.49–10.03 mg L^{-1}; COD: 8.08–24.32 mg L^{-1}; N-NH_3: 200–378 µg L^{-1}; NO_3: 0.37–9.69 mg L^{-1}; DO: 8.98–14.57 mg L^{-1}; pH: 6.02–6.80; PO_4^-: 0.002–0.030 mg L^{-1}; TP: 0.01–0.04 mg L^{-1}; TS: 20.00–72.00 mg L^{-1}; Temp:

17.37–21.82 °C; Turb: 1.93–14.57; Flow: 0.31–2.78 m^3 s; Average depth: 0.09–0.29 m; Prec: 3.48–9.96 mm.

Metal Concentrations: Co: 17.50–58.28 mg L^{-1}; Cr: 23.10–85.16 mg L^{-1}; Cu: 153.45–259.07 mg L^{-1}; Mn: 370.99–622.76 mg L^{-1}; Ni: 31.80–69.89 mg L^{-1}; Pb: 33.49–57.94 mg L^{-1}; Zn: 71.00–412.52 mg L^{-1}.

G. graciledictum (Figs 6W–6X)

Deformed valve outline, with bent apices. Unusual striae pattern, throughout the valve or strongly radiate in the median portion of the valve (n = 7).

Ecological characteristics: Cond: 50.00–53.00 µS cm^{-1}; BOD: 0.89–3.27 mg L^{-1}; COD: 7.23–13.60 mg L^{-1}; N-NH_3: 316–378 µg L^{-1}; NO_3: 0.34–0.37 mg L^{-1}; DO: 11.42–14.80 mg L^{-1}; pH: 5,79–6.26; PO_4^-: 0.005–0.008 mg L^{-1}; TP: 0.009–0.017 mg L^{-1}; TS: 10.00–66.00 mg L^{-1}; Temp: 17.40–17.68 °C; Turb: 7.03–10.70; Flow: 0.47–0.62 m^3 s; Average depth: 0.19–0.24 m; Prec: 9.96 mm.

Metal Concentrations: Co: 23.91–33.57 mg L^{-1}; Cr: 27.33–78.86 mg L^{-1}; Cu: 197.55–235.49 mg L^{-1}; Mn: 398.50–444.52 mg L^{-1}; Ni: 31.80–69.89; Pb: 35.58–46.56 mg L^{-1}; Zn: 93.81–167.31 mg L^{-1}.

G. lagenula (Figs 6AQ–6AS; 13J)

Deformed valve outline, undulated, or with bent apices. Unusual striae pattern, usually strongly radiate in the median portion of the valve (n = 23).

Ecological characteristics: Cond: 1.00–63.00 µS cm^{-1}; BOD: 1.19–13.96 mg L^{-1}; COD: 1.23–24.65 mg L^{-1}; N-NH_3: 3–448 µg L^{-1}; NO_3: 0.32–13.60 mg L^{-1}; DO: 7.18–26.24 mg L^{-1}; pH: 5.28–6.79; PO_4^-: 0.002–0.050 mg L^{-1}; TP: 0.005–0.036 mg L^{-1}; TS: 4.00–84.0 mg L^{-1}; Temp: 16.60–21.82 °C; Turb: 1.93–10.70 ; Flow: 0.06–5.88 m^3 s; Average depth: 0.02–1.32 m; Prec: 2.39–11.17 mm.

Metal Concentrations: Co: 17.50–60.76 mg L^{-1}; Cr: 23.10–79.78 mg L^{-1}; Cu: 163.45–301.34 mg L^{-1}; Mn: 370.99–809.37 mg L^{-1}; Ni: 29.18–87.39 mg L^{-1}; Pb: 33.49–57.94 mg L^{-1}; Zn: 71.00–296.79 mg L^{-1}.

G. naviculoides (Fig 6AU)

Unusual striae pattern, strongly radiate in the middle portion of the valve (n = 3).

Ecological characteristics: Cond: 52.00–53.00 µS cm^{-1}; BOD: 0.89–3.27 mg L^{-1}; COD: 7.23–11.05 mg L^{-1}; N-NH_3: 316–378 mg L^{-1}; NO_3: 0.37 mg L^{-1}; DO: 11.42–14.62 mg L^{-1}; pH: 5.79–6.19; PO_4^-: 0.005–0.008 mg L^{-1}; TP: 0.009–0.017 mg L^{-1}; TS: 21.00–66.00 mg L^{-1}; Temp: 17.37–17.50 °C; Turb: 7.03–10.70; Flow: 0.66–0.78 m^3 s; Average depth: 0.22–0.34 m; Prec: 9.96 mm.

Metal Concentrations: Co: 23.91–33.57 mg L^{-1}; Cr: 27.33–78.86 mg L^{-1}; Cu: 197.55–235.49 mg L^{-1}; Mn: 398.50–444.52 mg L^{-1}; Ni: 31.80–69.89; Pb: 35.58–46.56 mg L^{-1}; Zn: 93.81–167.31 mg L^{-1}.

G. pumilum (Fig 6AM)

Deformed valve outline, with bent of the valve (n = 1)

Ecological characteristics: Cond: 44.00 µS cm^{-1}; BOD: 3.27 mg L^{-1}; COD: 11.05 mg L^{-1}; $N\text{-}NH_3$: 18 µg L^{-1}; NO_3: 0.32 mg L^{-1}; DO: 13.39 mg L^{-1}; pH: 6.43; PO_4^-: 0.004 mg L^{-1}; TP: 0.007 mg L^{-1}; TS: 42.00 mg L^{-1}; Temp: 17.71 °C; Turb: 8.27; Flow: 1.12 m^3 s; Average depth: 0.33 m; Prec: 9.96 mm.

Metal Concentrations: Co: 34.35–39.39 mg L^{-1}; Cr: 28.18–85.31 mg L^{-1}; Cu: 170.55–264.18 mg L^{-1}; Mn: 503.78–606.73 mg L^{-1}; Ni: 32.81–73.27 mg L^{-1}; Pb: 31.05–39.31 mg L^{-1}; Zn: 79.00–172.60 mg L^{-1}.

Family ACHNANTHIDIACEAE

Achnanthidium macrocephalum (Figs 7L–7P)

Deformed valve outline, usually with constriction near the apices (n = 6).

Ecological characteristics: Cond: 22.00–64.00 µS cm^{-1}; BOD: 1.49–4.57 mg L^{-1}; COD: 5.53–18.10 mg L^{-1}; $N\text{-}NH_3$: 130–378 µg L^{-1}; NO_3: 0.37–2.20 mg L^{-1}; DO: 7.71–19.35 mg L^{-1}; pH: 5.51–6.19; PO_4^-: 0.006–0.046 mg L^{-1}; TP: 0.010–0.060 mg L^{-1}; TS: 4.00–104.00 mg L^{-1}; Temp: 17.37–23.00 °C; Turb: 6.38–10.70; Flow: 0.44–1.20 m^3 s; Average depth: 0.09–0.34 m; Prec: 2.73–9.96 mm.

Metal Concentrations: Co: 23.91–60.76 mg L^{-1}; Cr: 23.67–88.85 mg L^{-1}; Cu: 163.45–241.67 mg L^{-1}; Mn: 393.75–557.50 mg L^{-1}; Ni: 31.80–69.89; Pb: 35.58–48.63 mg L^{-1}; Zn: 83.42–173.12 mg L^{-1}.

A. minutissimum (Figs 7X–7AC)

Deformed valve outline, usually with constriction or bent apices. Sometimes with strong constriction in the median portion of the valve. Sigmoid shape, or unidentified (n = 38).

Ecological characteristics: Cond: 25.00–91.00 µS cm^{-1}; BOD: 0.77–9.90 mg L^{-1}; COD: 1.00–24.32 mg L^{-1}; $N\text{-}NH_3$: 200–540 µg L^{-1}; NO_3: 0.37–13.60 mg L^{-1}; DO: 6.54–19.35 mg L^{-1}; pH: 5.01–6.92; PO_4^-: 0.005–0.050 mg L^{-1}; TP: 0.005–0.922 mg L^{-1}; TS: 19.00–174.00 mg L^{-1}; Temp: 17.40–23.56 °C; Turb: 0.06–37.50; Flow: 0.10–5.09 m^3 s; Average depth: 0.04–0.41 m; Prec: 2.37–11.17 mm.

Metal Concentrations: Co: 16.73–58.28 mg L^{-1}; Cr: 21.98–85.31 mg L^{-1}; Cu: 160.64–292.30 mg L^{-1}; Mn: 347.86–745.82 mg L^{-1}; Ni: 27.57–85.63 mg L^{-1}; Pb: 33.49–66.21 mg L^{-1}; Zn: 73.15–412.52 mg L^{-1}.

A. modestiforme (Figs 7AF–7AH)

Deformed valve outline, with constriction near the apices (n = 8).

Ecological characteristics: Cond: 11.00–50.00 µS cm^{-1}; BOD: 2.49–9.90 mg L^{-1}; COD: 7.57–24.32 mg L^{-1}; N-NH_3: 200 µg L^{-1}; NO_3: 0.40–9.69 mg L^{-1}; DO: 8.98–19.93 mg L^{-1}; pH: 6.70–6.92; PO_4^-: 0.002–0.050 mg L^{-1}; TP: 0.005–0.019 mg L^{-1}; TS: 23.00–48.00 mg L^{-1}; Temp: 20.12–21.23 °C; Turb: 0.06–8.40; Flow: 0.13–2.78 m^3 s; Average depth: 0.05–0.29 m; Prec: 3.76–4.96 mm.

Metal Concentrations: Co: 26.05–57.56 mg L^{-1}; Cr: 19.44–85.16 mg L^{-1}; Cu: 149.34–268.89 mg L^{-1}; Mn: 234.22–745.82 mg L^{-1}; Ni: 33.21–85.63 mg L^{-1}; Pb: 33.84–61.04 mg L^{-1}; Zn: 68.52–258.21 mg L^{-1}.

Planothidium rostratum (Figs 7AO–7AP)

Deformed valve outline, with loss of transapical symmetry (n = 2).

Ecological characteristics: Cond: 42.00–50.00 µS cm^{-1}; BOD: 1.43–2.38 mg L^{-1}; COD: 4.68–13.68 mg L^{-1}; N-NH_3: 323–680 mg L^{-1}; NO_3: 0.34–1.00 mg L^{-1}; DO: 7.79–14.80 mg L^{-1}; pH: 6.26–6.28; PO_4^-: 0.005–0.006 mg L^{-1}; TP: 0.007–0.016 mg L^{-1}; TS: 10.00–11.00 mg L^{-1}; Temp: 17.68–23.25 °C; Turb: 10.30–10.40; Flow: 0.62–0.66 m^3 s; Average depth: 0.22–0.24 m; Prec: 9.96 mm.

Metal Concentrations: Co: 23.73–47.24 mg L^{-1}; Cr: 27.33–80.86 mg L^{-1}; Cu: 160.64–235.49 mg L^{-1}; Mn: 398.05–444.52 mg L^{-1}; Ni: 27.57–69.89 mg L^{-1}; Pb: 35.58–66.21 mg L^{-1}; Zn: 78.97–167.31 mg L^{-1}.

Family DIADESMIDACEAE

Humidophila arcuatoides (Figs 7AU–7AV)

Length: 12.1–14.6 µm; width: 2.9–3.2 µm

Humidophila arcuatoides (= *Diadesmis arcuatoides*), described originally by Werum & Lange-Bertalot (2004), has 16–26 µm in length and 5–6 µm in width, however, the taxon has been already registered with 8–14 µm in length and 2.6–4 µm in width by Wetzel (2011). *Humidophila arcuata* Lange-Bertalot is easily differentiated by the less inflated central portion of the valve (Werum & Lange-Bertalot 2004).

Family AMPHIPLEURACEAE

Frustulia saxonica (Fig 8I)

Deformed valve outline, slightly undulated in one side of the valve (n = 2).

Ecological characteristics: Cond: 60.00–94.00 µS cm^{-1}; BOD: 6.62–13.63 mg L^{-1}; COD: 7.14–25.30 mg L^{-1}; N-NH_3: 200 µg L^{-1}; NO_3: 11.80–12.70 mg L^{-1}; DO: 7.52–9.50 mg L^{-1}; pH: 6.18–6.78; PO_4^-: 0.002–0.055 mg L^{-1}; TP: 0.01–0.09 mg L^{-1}; TS: 44.00–47.00 mg L^{-1}; Temp: 19.10–20.91 °C; Turb: 2.82–3.32; Flow: 0.06–0.61 m^3 s; Average depth: 0.03–0.10 m; Prec: 3.48–9.96 mm.

Metal Concentrations: Co: 16.73–47.67 mg L^{-1}; Cr: 25.08–85.31 mg L^{-1}; Cu: 206.13–238.31 mg L^{-1}; Mn: 347.86–406.12 mg L^{-1}; Ni: 28.58–70.77 mg L^{-1}; Pb: 26.51–43.45 mg L^{-1}; Zn: 81.88–364.96 mg L^{-1}.

Family PINNULARIACEAE

Pinnularia divergens (Fig 8AJ)

Deformed valve outline, with bent of the apex (n = 1).

Ecological characteristics: Cond: 60.00 µS cm^{-1}; BOD: 13.63 mg L^{-1}; COD: 25.30 mg L^{-1}; N-NH_3: 200 µg L^{-1}; NO_3: 11.80 mg L^{-1}; DO: 9.50 mg L^{-1}; pH: 6.78; PO_4^-: 0.002 mg L^{-1}; TP: 0.01 mg L^{-1}; TS: 44.00 mg L^{-1}; Temp: 19.10 °C; Turb: 2.82; Flow: 0.06 m^3 s; Average depth: 0.03 m; Prec: 4.96 mm.

Metal Concentrations: Co: 30.30 mg L^{-1}; Cr: 59.68 mg L^{-1}; Cu: 263.28 mg L^{-1}; Mn: 410.09 mg L^{-1}; Ni: 45.89 mg L^{-1}; Pb: 40.73 mg L^{-1}; Zn: 139.68 mg L^{-1}.

P. graciloides var. ***latecapitata*** (Fig 9B)

Deformed valve outline, with sigmoid shape (n = 3).

Ecological characteristics: Cond: 65.00 µS cm^{-1}; BOD: 1.00 mg L^{-1}; COD: 2.55 mg L^{-1}; N-NH_3: 200 µg L^{-1}; NO_3: 2.90 mg L^{-1}; DO: 12.12 mg L^{-1}; pH: 6.40; PO_4^-: 0.05 mg L^{-1}; TP: 0.02 mg L^{-1}; TS: 95.00 mg L^{-1}; Temp: 17.93 °C; Turb: 3.78; Flow: 0.94 m^3 s; Average depth: 0.24 m; Prec: 2.37–4.96 mm.

Metal Concentrations: Co: 17.50–57.56 mg L^{-1}; Cr: 24.23–83.01 mg L^{-1}; Cu: 195.31–273.01 mg L^{-1}; Mn: 370.99–745.82 mg L^{-1}; Ni: 33.62–85.63 mg L^{-1}; Pb: 33.49–54.83 mg L^{-1}; Zn: 78.88–258.21 mg L^{-1}.

****Pinnularia laucensis*** (Figs 9J–9K)

Length: 15.5–26.3 µm; width: 3.6–4.5; striae: 12–15 in 10 µm

This taxon was originally described from high-altitude (4000 m) and acidic (pH = 5) river samples from Chile (Rumrich *et al.* 2000). The individuals found in Cascavel river microbasin are similar to *P. laucensis*, except for being slightly larger than the original description (length: 13–20 µm; width: 3.3–4 µm), but similar striae density (11–14 in 10 µm). *Pinnularia sinistra* Krammer, the most similar taxon, can be differentiated by the subrostrate apices and more radiate striae (Krammer 1992).

Family SELLAPHORACEAE

Sellaphora saugerresii (Figs 9AD–9AF)

Deformed valve outline, usually undulated, with asymmetry of the apical axis (n = 33).

Ecological characteristics: Cond: 1.00–70.00 µS cm^{-1}; BOD: 1.00–10.3 mg L^{-1}; COD: 1.22–27.60 mg L^{-1}; N-NH_3: 110–500 µg L^{-1}; NO_3: 2.00–6.88 mg L^{-1}; DO: 8.18–15.81 mg L^{-1}; pH: 5.11–7.42; PO_4^-: 0.002–0.323 mg L^{-1}; TP: 0.005–0.350 mg L^{-1}; TS: 7.00–174.00 mg L^{-1}; Temp: 18.28–22.27 °C; Turb: 1.93–41.90; Flow: 0.05–6.34 m^3 s; Average depth: 0.02–0.37 m; Prec: 2.37–9.96 mm.

Metal Concentrations: Co: 17.50–65.84 mg L^{-1}; Cr: 25.92–85.01 mg L^{-1}; Cu: 163.45–273.45 mg L^{-1}; Mn: 329.01–642.36 mg L^{-1}; Ni: 27.57–72.54 mg L^{-1}; Pb: 31.05–52.76 mg L^{-1}; Zn:78.35–287.28 mg L^{-1}.

Family NAVICULACEAE

Caloneis bacillum (Fig 9AM)

Deformed valve outline, with asymmetry of the apical axis (n = 1).

Ecological characteristics: Cond: 44.00 µS cm^{-1}; BOD: 4.59 mg L^{-1}; COD: 6.79 mg L^{-1}; N-NH_3: 200 µg L^{-1}; NO_3: 1.60 mg L^{-1}; DO: 26.24 mg L^{-1}; pH: 6.81; PO_4^-: 0.05 mg L^{-1}; TP: 0.02 mg L^{-1}; TS: 50.00 mg L^{-1}; Temp: 20.30 °C; Turb: 0.00; Flow: 5.88 m^3 s; Average depth: 0.34 m; Prec: 2.73 mm.

Metal Concentrations: Co: 60.76 mg L^{-1}; Cr: 33.25 mg L^{-1}; Cu: 163.45 mg L^{-1}; Mn: 538.54 mg L^{-1}; Ni: 32.81 mg L^{-1}; Pb: 48.63 mg L^{-1}; Zn: 83.42 mg L^{-1}.

Navicula cryptocephala (Figs 10G–10I)

Deformed valve outline, with loss of transapical symmetry (n = 3).

Cond: 52.00 µS cm^{-1}; BOD: 4.16 mg L^{-1}; COD: 17.43 mg L^{-1}; N-NH_3: 316 µg L^{-1}; NO_3: 0.32 mg L^{-1}; DO: 14.62 mg L^{-1}; pH: 6.04; PO_4^-: 0.004 mg L^{-1}; TP: 0.012 mg L^{-1}; TS: 16.00 mg L^{-1}; Temp: 17.90 °C; Turb: 9.25; Flow: 0.45 m^3 s; Average depth: 0.19 m; Prec: 9.96 mm.

Metal Concentrations: Co: 19.28–23.11 mg L^{-1}; Cr: 25.92–83.62 mg L^{-1}; Cu: 196.71–241.52 mg L^{-1}; Mn: 400.50–955.89 mg L^{-1}; Ni: 33.21–59.59 mg L^{-1}; Pb: 36.28–38.28 mg L^{-1}; Zn: 78.35–169.95 mg L^{-1}.

Navicula cryptotenella (Figs 10M)

Deformed valve outline, with loss of transapical symmetry (n = 3).

Ecological characteristics: Cond: 50.0–53.00 µS cm^{-1}; BOD: 1.49–2.38 mg L^{-1}; COD: 8.08–13.60 mg L^{-1}; N-NH_3: 323–378 mg L^{-1}; NO_3: 0.34–0.37 mg L^{-1}; DO: 14.57–14.80 mg L^{-1}; pH: 6.19–6.26; PO_4^-: 0.005–0.006 mg L^{-1}; TP: 0.010–0.016 mg L^{-1}; TS: 10.00–38.00 mg L^{-1}; Temp: 17.37–17.68 °C; Turb: 10.40–10.70; Flow: 0.47–0.62 m^3 s; Average depth: 0.19–0.24 m; Prec: 9.96–11.17 mm.

Metal Concentrations: Co: 22.67–33.57 mg L^{-1}; Cr: 23.67–78.86 mg L^{-1}; Cu: 197.55–235.49 mg L^{-1}; Mn: 291.12–444.52 mg L^{-1}; Ni: 31.80–69.89; Pb: 35.58–46.56 mg L^{-1}; Zn: 93.81–167.31 mg L^{-1}.

Family STAURONEIDACEAE

Craticula riparia (Figs 10Z)

Deformed valve outline, slightly undulated (n = 4).

Ecological characteristics: Cond: 53.00 µS cm^{-1}; BOD: 1.49–3.27 mg L^{-1}; COD: 7.23–8.08 mg L^{-1}; N-NH_3: 316–378 mg L^{-1}; NO_3: 0.37 mg L^{-1}; DO: 11.42–14.57 mg L^{-1}; pH: 5.79–6.19; PO_4^-: 0.006–0.008 mg L^{-1}; TP: 0.010–0.017 mg L^{-1}; TS: 38.00–66.00 mg L^{-1}; Temp: 17.37–17.50 °C; Turb: 7.03–10.70; Flow: 0.47 m^3 s; Average depth: 0.19–0.23 m; Prec: 9.96 mm.

Metal Concentrations: Co: 23.73–47.24 mg L^{-1}; Cr: 27.33–80.86 mg L^{-1}; Cu: 160.64–235.49 mg L^{-1}; Mn: 398.05–444.52 mg L^{-1}; Ni: 27.57–69.89 mg L^{-1}; Pb: 35.58–66.21 mg L^{-1}; Zn: 78.97–167.31 mg L^{-1}.

C. submolesta (Figs 10W)

Deformed valve outline, slightly undulated in one side of the valve (n = 1).

Ecological characteristics: Cond: 53.00 µS cm^{-1}; BOD: 1.49 mg L^{-1}; COD: 8.08 mg L^{-1}; N-NH_3: 378 µg L^{-1}; NO_3: 0.37 mg L^{-1}; DO: 14.57 mg L^{-1}; pH: 6.19; PO_4^-: 0.006 mg L^{-1}; TP: 0.010 mg L^{-1}; TS: 38.00 mg L^{-1}; Temp: 17.37 °C; Turb: 10.70; Flow: 0.47 m^3 s; Average depth: 0.19 m; Prec: 4.96–9.96 mm.

Metal Concentrations: Co: 23.91–37.79 mg L^{-1}; Cr: 27.33–85.16 mg L^{-1}; Cu: 197.55–259.07 mg L^{-1}; Mn: 398.50–465.70 mg L^{-1}; Ni: 31.80–69.89; Pb: 35.58–49.66 mg L^{-1}; Zn: 93.81–167.31 mg L^{-1}.

Family BACILLARIACEAE

Nitzschia palea (Figs 11D–11F)

Deformed valve outline, with asymmetry of the apical axis, or constriction near the apex (n = 3).

Ecological characteristics: Cond: 50.00–52.00 µS cm^{-1}; BOD: 0.77–9.90 mg L^{-1}; COD: 1.70–24.32 mg L^{-1}; N-NH_3: 200–540 µg L^{-1}; NO_3: 1.00–9.69 mg L^{-1}; DO: 8.19–8.98 mg L^{-1}; pH: 6.80–6.93; PO_4^-: 0.007–0.010 mg L^{-1}; TP: 0.010–0.015 mg L^{-1}; TS: 41.00–48.00 mg L^{-1}; Temp: 20.35–23.62 °C; Turb: 8.40–10.6; Flow: 0.66–2.78 m^3 s; Average depth: 0.25–0.29 m; Prec: 4.96–9.96 mm.

Metal Concentrations: Co: 23.73–47.24 mg L^{-1}; Cr: 28.46–85.16 mg L^{-1}; Cu: 160.64–259.07 mg L^{-1}; Mn: 419.46–465.70 mg L^{-1}; Ni: 27.57–69.89 mg L^{-1}; Pb: 35.93–66.21 mg L^{-1}; Zn: 78.97–151.46 mg L^{-1}.

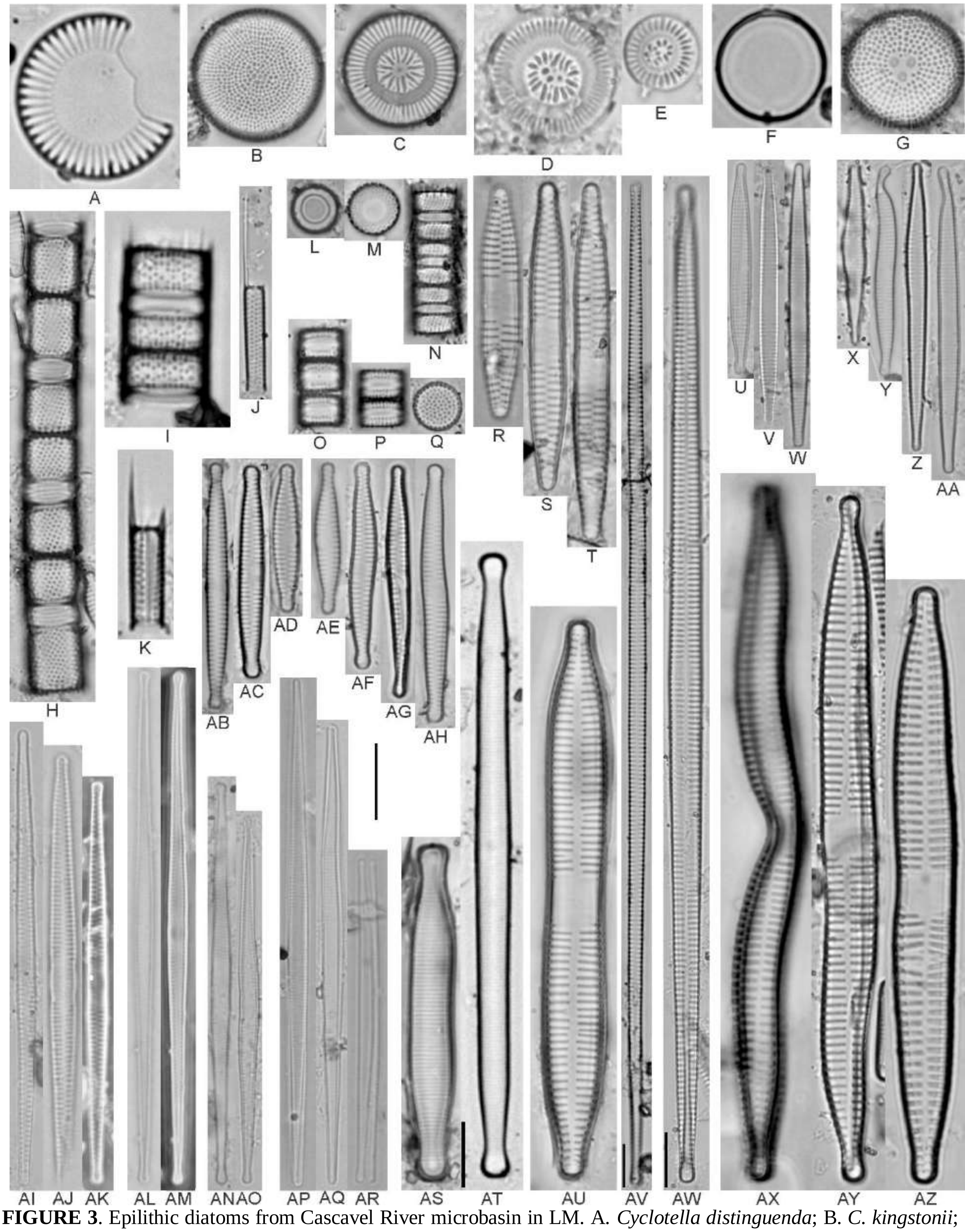

FIGURE 3. Epilithic diatoms from Cascavel River microbasin in LM. A. *Cyclotella distinguenda*; B. *C. kingstonii*; C–E. *Discostella stelligera*. D–E. Teratological valves; F. *Melosira varians*; G. *Orthoseira roeseana*; H. *Aulacoseira ambigua*; I. *A. brasiliensis*; J. *A. granulata* var. *angustissima*; K. *A. granulata*; L–N. *A. pusilla*; O–Q. *A. tenella*. R–T. *Fragilaria fragilarioides*; U–AA. *F. gracilis*. X–AA. Teratological valves; AB–AH. *F. pectinalis*. AE–AH. Teratological valves; AI–AK. *F. tenera* var. *tenera*; AL–AO. *F. tenera* var. *nanana*. AN–AO. Teratological valves; AP–AR. *F. spectra*; AS–AT. *Fragilariforma javanica*; AU. *Ulnaria contracta*; AV. *U. delicatissima*; AW–AZ. *U. ulna*; AX–AZ. Teratological valves. Scale bars represent 10 µm.

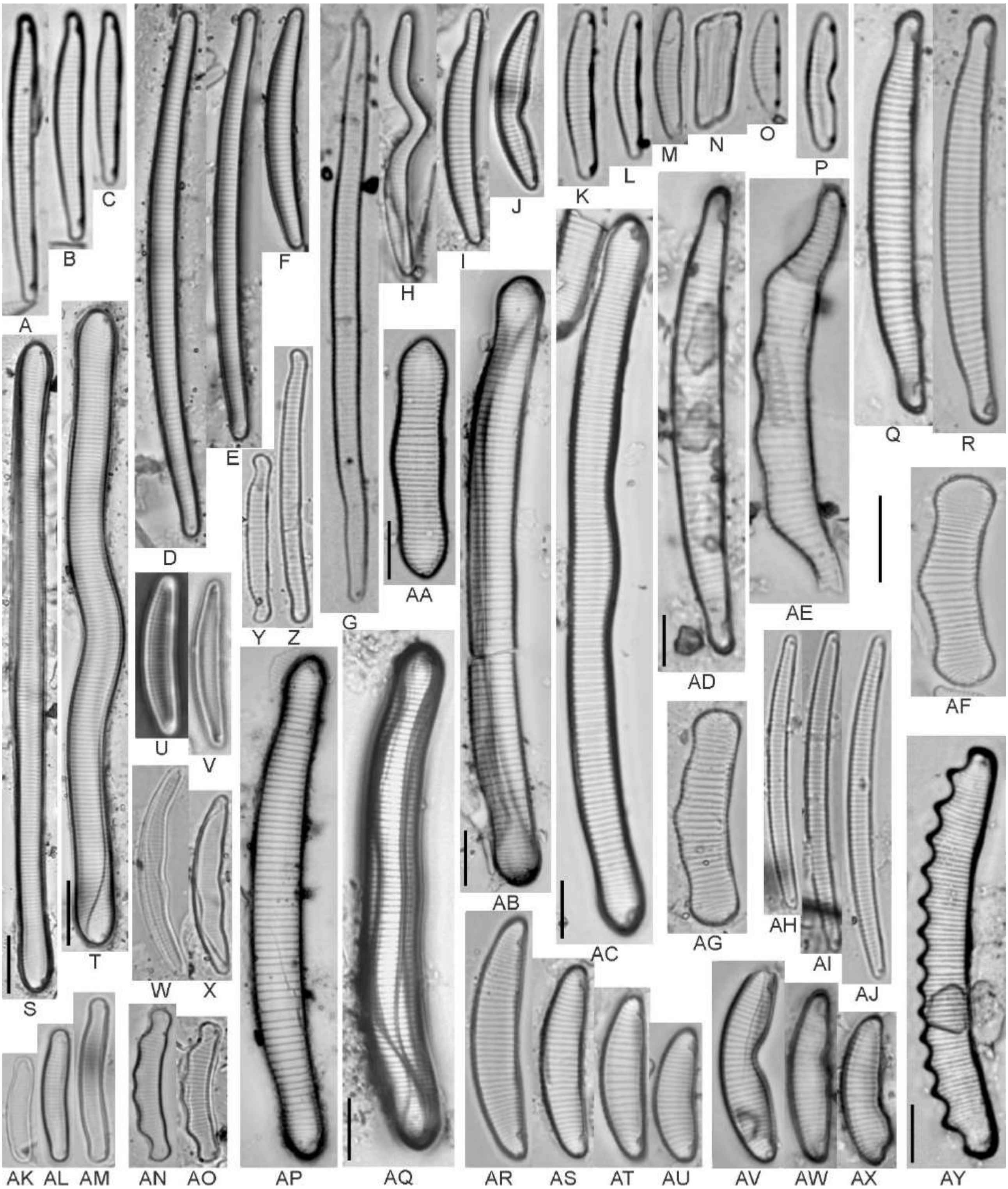

FIGURE 4. Epilithic diatoms from Cascavel River microbasin in LM. A–C. *Actinella hermes-moreirae*; D–J. *Eunotia bilunaris*. G–J. Teratological valves; K–P. *E. botulitropica*. P. Teratological valve; Q–R. *E. canicula*; S–T. *E. desmogonioides*. T. Teratological valve; U–X. *E. subarcuatoides*; W–X. Teratological valves; Y–Z. *E. fallax*; AA. *E. formica*; AB. *E. formicina*; AC. *E. karenae*; AD. *E. intricans*; AE. *E. longicamelus*; AF. *E. rabenhorstii* var. *monodon*; AG. *E. rabenhorstii* var. *triodon*; AH–AJ. *E. juettnerae*; AK–AM. *E. kruegeri*; AN–AO. *E. muscicola*; AP–AQ. *E. monodon*. AQ. Teratological valve; AR–AX. *E. meridiana*. AV–AX. Teratological valves; AY. *E. georgii*. Scale bars represent 10 µm.

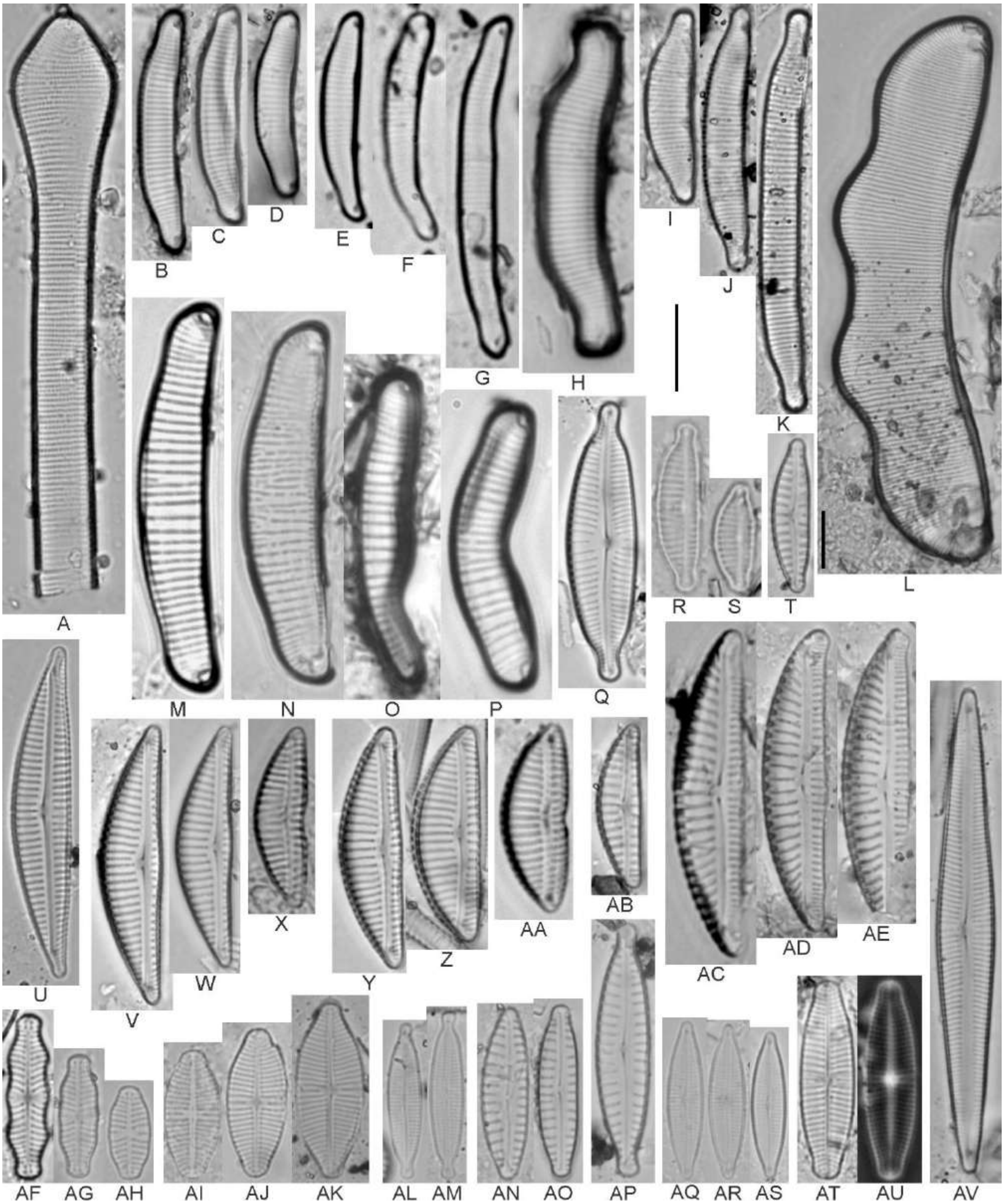

FIGURE 5. Epilithic diatoms from Cascavel River microbasin in LM. A. *Eunotia ossicula*; B–G. *E. rhomboidea*. E–G. Teratological valves; H. *E. tropico-arcus*; I–K. *E. veneris*; L. *E. yanomami*; M–P. *E. yberai*. N–P. Teratological valves; Q. *Cymbopleura naviculiformis*; R–S. *Encyonema angustecapitatum*; T. *E. perpusillum*; U. *E. neogracile*; V–X. *E. neomesianum*. X. Teratological valve; Y–AA. *E. silesiacum*. AA. Teratological valve; AB. *E. minutiforme*; AC–AE. *E. exuberans*; AF–AH. *Navigeia ignota*; AI–AK. *Placogeia kriegeri*; AL–AM. *Encyonopsis subminuta*; AN–AO. *E. difficilis*; AP. *E. schubartii*; AQ–AS. *E. thienemannii*; AT–AU. *Geissleria punctifera*; AV. *Kurtkrammeria spicula*. Scale bars represent 10 µm.

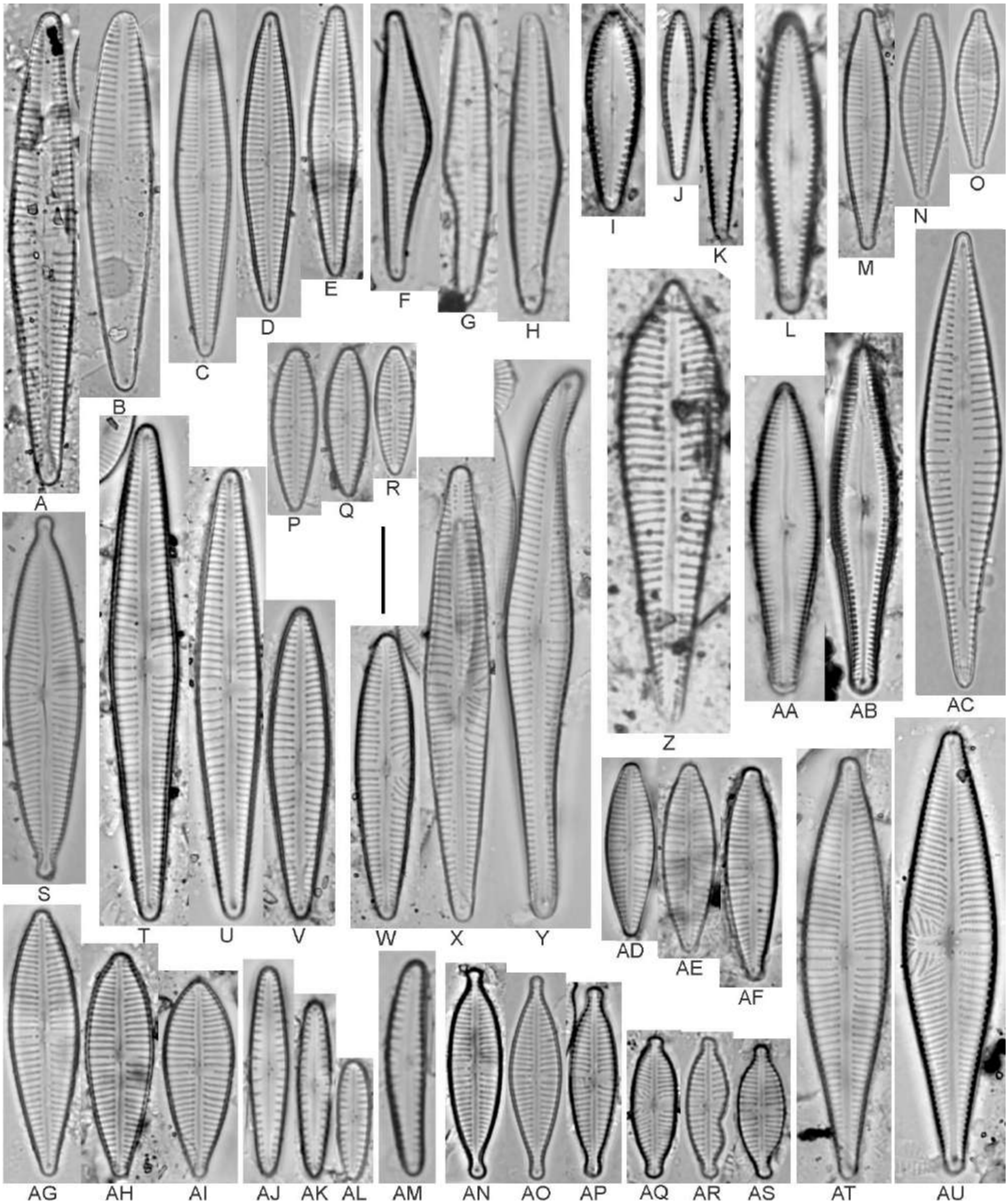

FIGURE 6. Epilithic diatoms from Cascavel River microbasin in LM. A–B. *Gomphonema affine*; C–H. *G. angustatum*. F–H. Teratological valves; I. *G. brasiliense*; J–K. *G. brasiliense* subsp. *pacificum*; L. *G. brasiliensoide*; M–O. *G. exilissimum*; P–R. *G. parvulum*; S. *G. frequentiformis*; T–Y. *G. gracilededictum*. W–Y. Teratological valves; Z. *G. perapicatum*; AA–AB. *G. hawaiiense*; AC. *G. guaraniarum*; AD–AF. *G. saprophilum*; AG–AI. *G. pseudoaugur*; AJ–AM. *G. pumilum*. AM. Teratological valve; AN–AS. *G. lagenula*. AQ–AS. Teratological valves; AT–AU. *G. naviculoides*. AU. Teratological valve. Scale bars represent 10 µm.

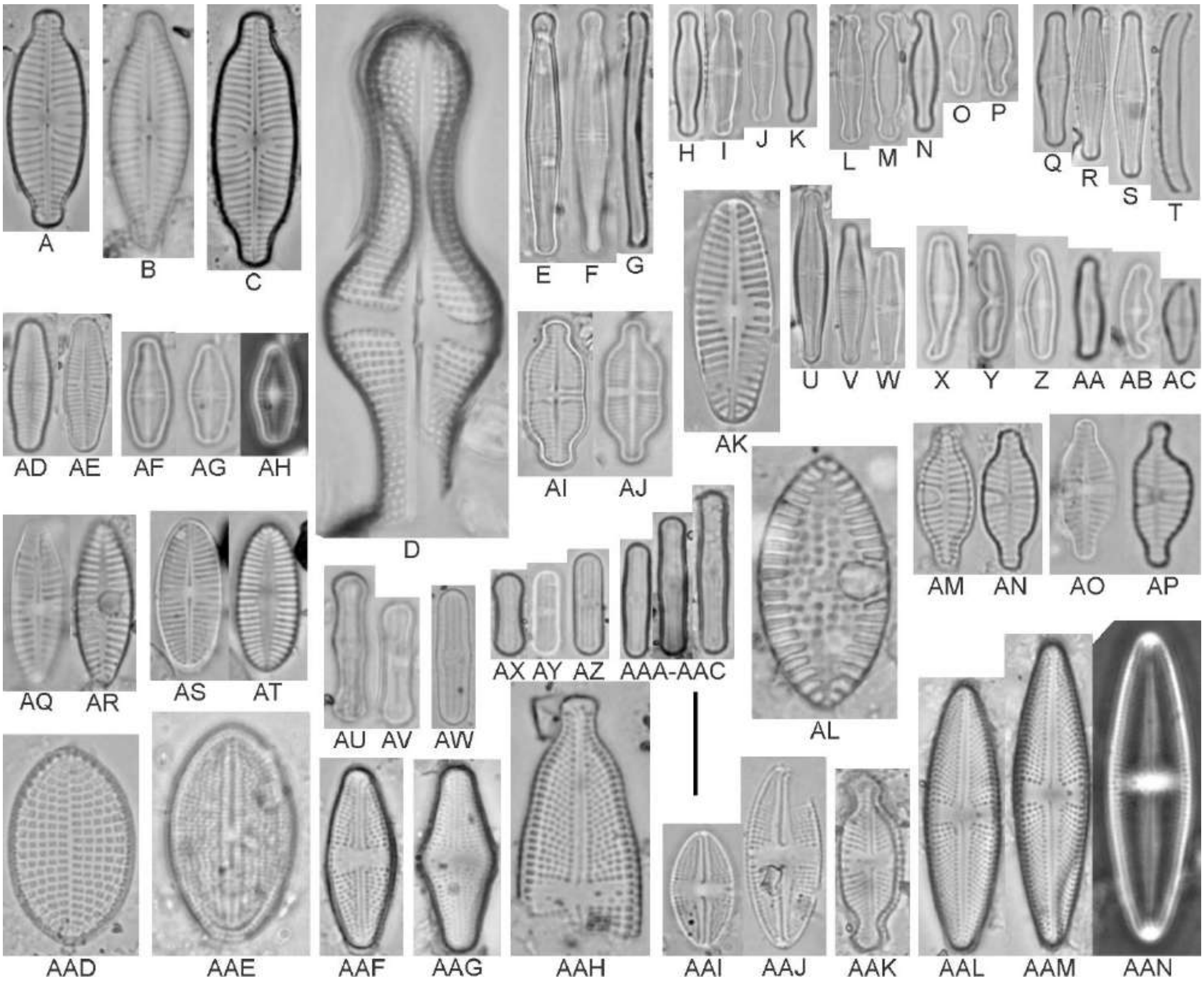

FIGURE 7. Epilithic diatoms from Cascavel River microbasin in LM. A. *Placoneis elginensis*; B. *P. hambergii*; C. *P. undulata*; D. *Achnanthes inflata*; E–G. *Achnanthidium caledonicum*; H–P. *A. macrocephalum*. L–P. Teratological valves; Q–T. *A. tropicocatenatum*; U–AC. *A. minutissimum*. X–AC. Teratological valves; AD–AH. *A. modestiforme*. AF–AH. Teratological valves; AI–AJ. *Gogorevia constricta*; AK. *Planothidium bagualensis*; AL. *P. laghereimii*; AM–AP. *P. rostratum*. AO–AP. Teratological valves; AQ–AR. *P. frequentissimum*; AS–AT. *Platessa hustedtii*; AU–AV. *Humidophila arcuatoides*; AW. *H. implicata*; AX–AZ. *H. contenta*; AAA–AAC. *H. subtropica*; AAD. *Cocconeis fluviatilis*; AAE. *C. lineata*; AAF. *Luticola ectorii*; AAG. *L. hustedtii*; AAH. *L. charlatii*; AAI–AAJ. *L. permuticoides*; AAK. *L. ventricosa*; AAL–AAN. *L. goeppertiana*. Scale bars represent 10 μm.

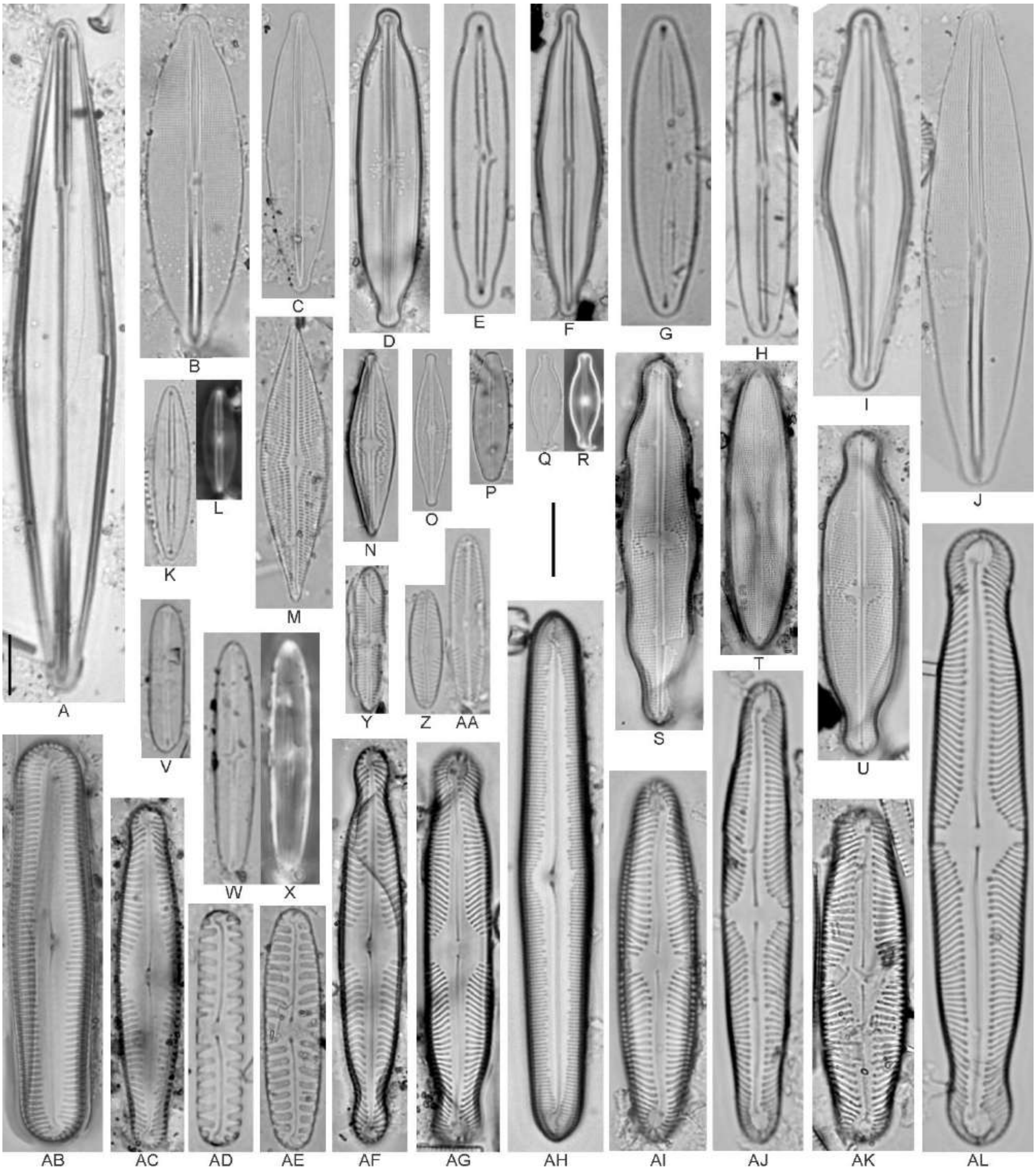

FIGURE 8. Epilithic diatoms from Cascavel River microbasin in LM. A. *Amphipleura lindheimeri*; B. *Frustulia acidophilissima*; C. *F. australocrassinervia*; D. *F. guayanensis*; E. *F. neomundana*; F. *F. undosa*; G. *F. weinholdii*; H. *F. vulgaris*; I–J. *F. saxonica*. I. Teratological valve; K–L. *F. pumilio*; M. *Brachysira serians* var. *acuta*; N. *B. brebissonii*; O. *B. microcephala*; P. *Nupela praecipuoides*; Q–R. *N. semifasciata*; S. *Neidium gracile* f. *aequale*; T. *N. iridis*; U. *N. affine* var. *amphirhynchus*; V. *N. tenuissimum*; W–X. *N. essequiboanum*; Y. *N. catarinense*; Z–AA. *Pinnularia acoricola*; AB. *P. acrosphaeria*; AC. *P. gaiserae*; AD. *P. borealis* var. *rectangularis*; AE. *P. borealis* var. *sublinearis*; AF. *P. brauniana*; AG. *P. divergens* var. *media*; AH. *P. butantanum*; AI–AJ. *P. divergens*. AJ. Teratological valve; AK. *P. decrescens* var. *ignorata*; AL. *P. divergens* var. *mesoleptiformis*. Scale bars represent 10 µm.

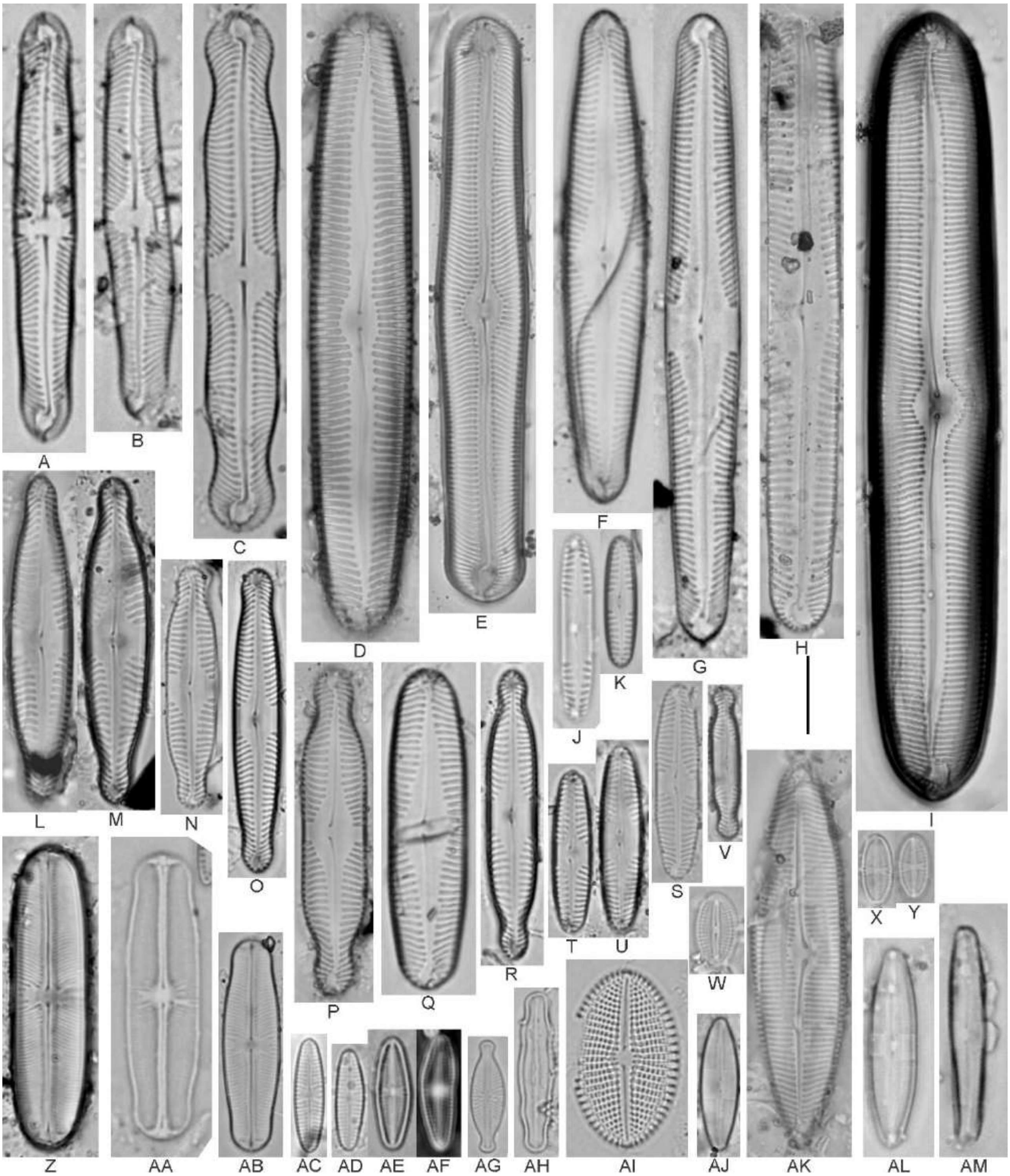

FIGURE 9. Epilithic diatoms from Cascavel River microbasin in LM. A–B. *Pinnularia graciloides* var. *latecapitata*. B. Teratological valve; C. *P. graciloides* var. *triundulata*; D. *P. viridiformis*; E. *P. tabellaria*; F–G. *P. subgibba* var. *undulata*; H. *P. subgibba*; I. *Pinnularia stidolphii*; J–K. *P. laucensis*; L–M. *P. certa*; N. *P. microstauron* var. *rostrata*; O. *P. subcapitata*; P. *P. subanglica*; Q. *P. meridiana*; R. *P. rumrichae*; S–T. *P. obscura*; U. *P. schoenfelderi*; V. *P. joculata*; W. *Fallacia insociabilis*; X–Y. *Sellaphora nigri*; Z. *S. laevissima*; AA. *S. rhombicarea*; AB. *S. pupula*; AC–AF. *S. saugerresii*. AD–AF. Teratological valves; AG. *S. sassiana*; AH. *S. tridentula*; AI. *Diploneis subovalis*; AJ. *Caloneis hyalina*; AK. *C. westii*; AL–AM. *C. bacillum*. AM. Teratological valve. Scale bars represent 10 µm.

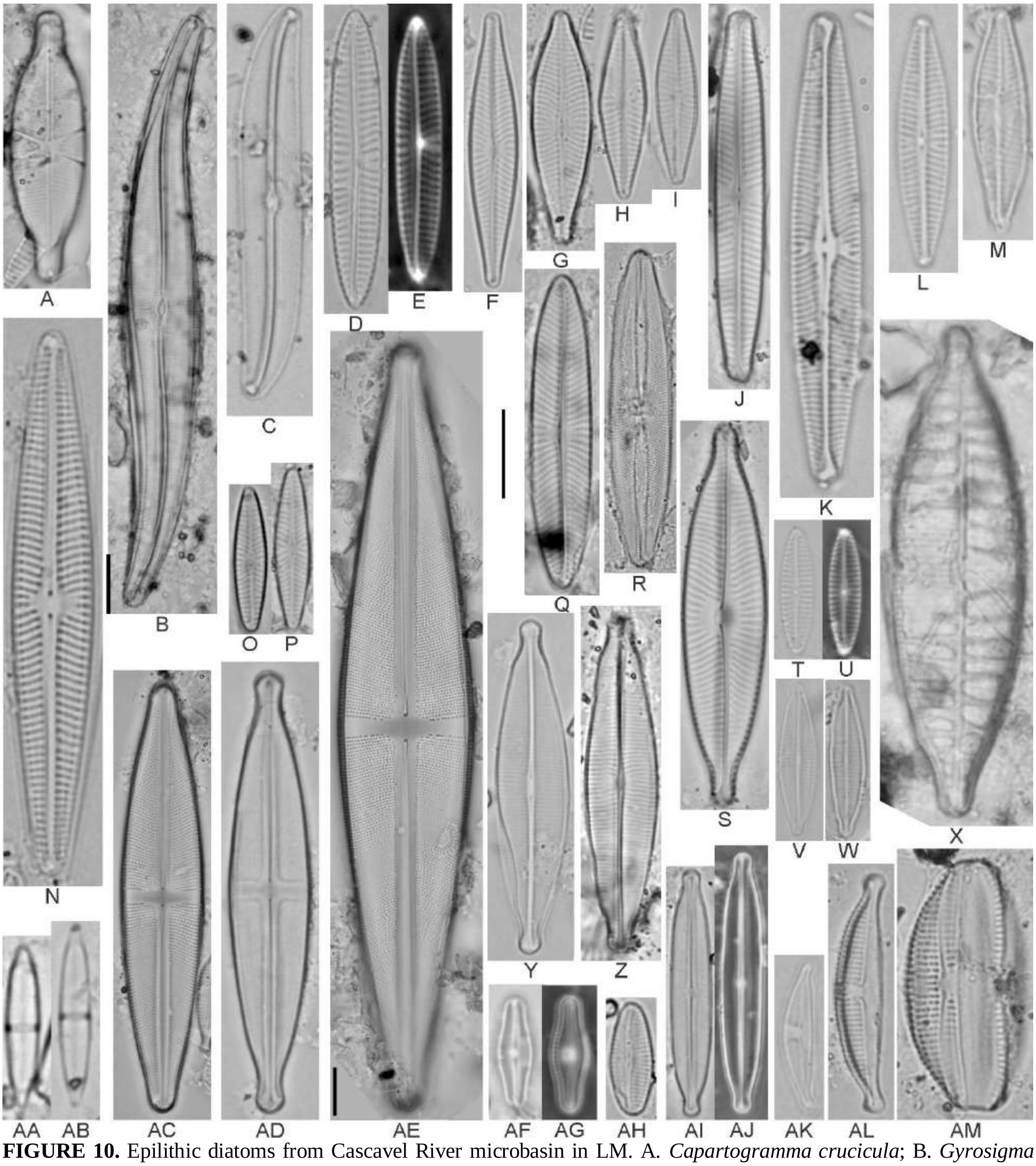

FIGURE 10. Epilithic diatoms from Cascavel River microbasin in LM. A. *Capartogramma crucicula*; B. *Gyrosigma acuminatum*; C. *G. obtusatum*; D–E. *Navicula eichhorniaephila*; F–I. *N. cryptocephala*. G–I. Teratological valves; J. *N. angusta*; K. *N. leptostriata*; L–M. *N. cryptotenella*. M. Teratological valve; N. *N. radiosa*; O–P. *N. tenelloides*; Q. *N. symmetrica*; R. *N. schwabei*; S. *N. rostellata*; T–U. *N. salinicola*; V–W. *Craticula submolesta*. W. Teratological valve; X. *C. ambigua*; Y–Z. *C. riparia*. Z. Teratological valve; AA–AB. *Stauroneis smithii*; AC. *S. gracilis*; AD. *S. neohyalina*; AE. *S. phoenicenteron*; AF–AG. *Chammaepinnularia brasilianopsis*; AH. *Pseudofallacia monoculata*; AI–AJ. *Kobayasiella parasubtilissima*; AK. *Halamphora montana*; AL. *H. normanii*; AM. *Amphora copulata*. Scale bars represent 10 µm.

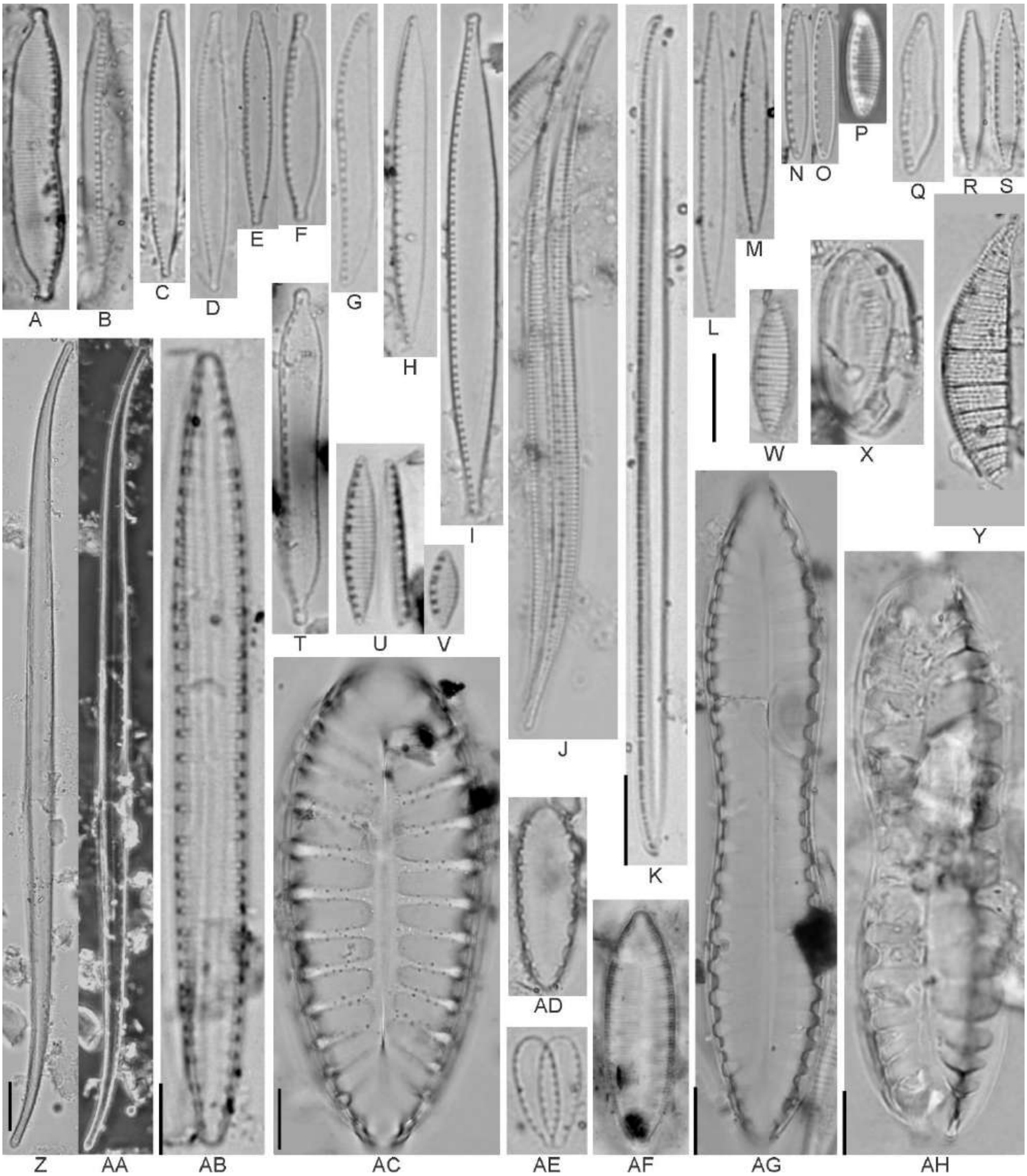

FIGURE 11. Epilithic diatoms from Cascavel River microbasin in LM. A. *Hantzschia amphioxys*; B. *Nitzschia dissipata*; C–F. *N. palea*. D–F. Teratological valves; G. *N. clausii*; H. *N. recta*; I. *N. intermedia*; J. *N. lorenziana*; K. *N. linearis*; L–M. *N. palea* var. *debilis*; N–P. *N. inconspicua*; Q. *N. brevissima*; R–S. *N. perminuta*; T. *N. terrestris*; U–V. *N. amphibia*; W. *N. semirobusta*; X. *Tryblionella debilis*; Y. *Epithemia gibberula*; Z–AA. *Iconella curvula*; AB. *I. delicatissima*; AC. *I. splendida*; AD. *I. tenuissima*; AE. *Surirella stalagma*; AF. *S. angusta*; AG. *S. biseriata* var. *constricta*; AH. *S. grunowii*. Scale bars represent 10 µm.

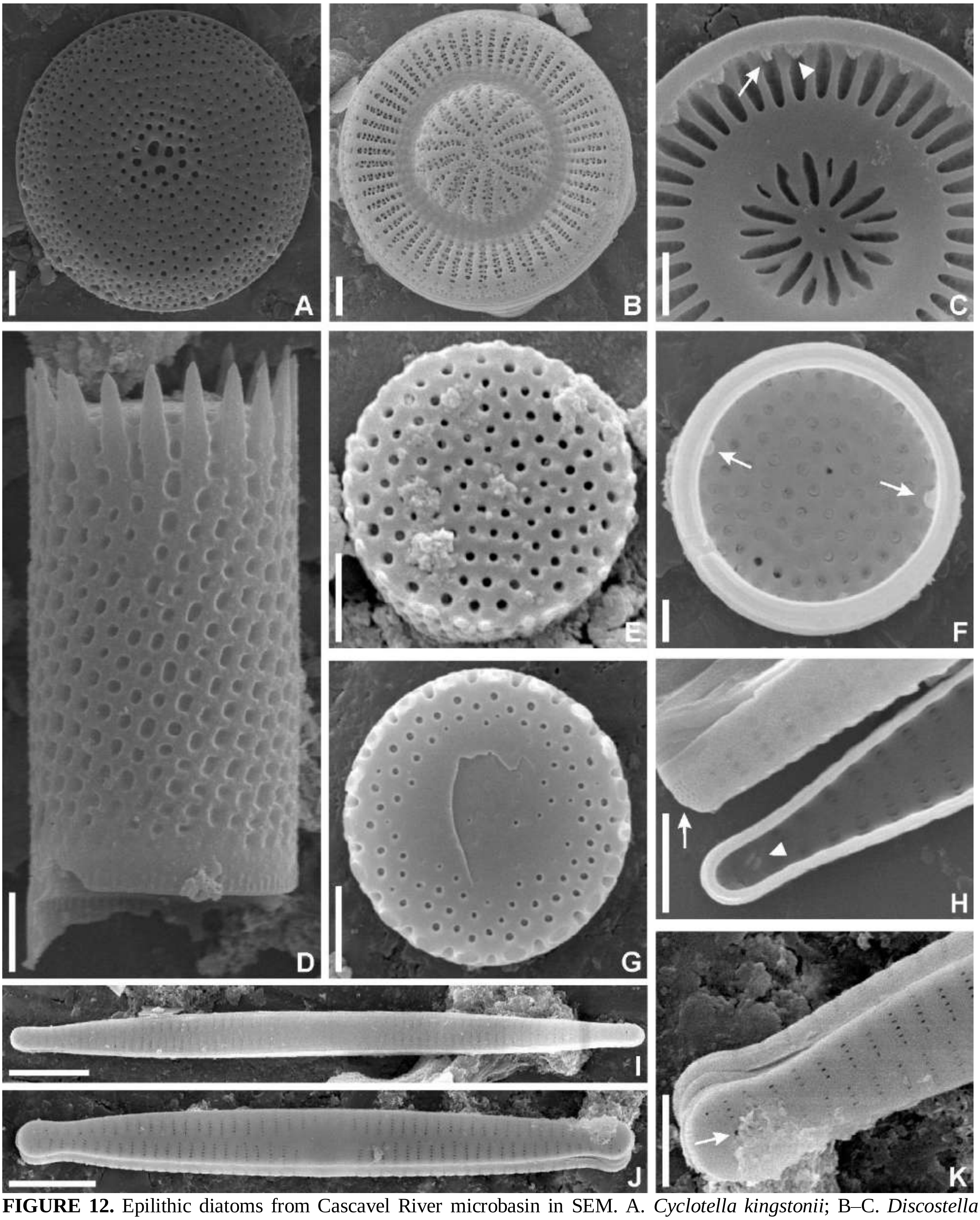

FIGURE 12. Epilithic diatoms from Cascavel River microbasin in SEM. A. *Cyclotella kingstonii*; B–C. *Discostella stelligera*. C. Internal view showing rimoportula (arrow) and fultoportula (arrowhead); D. *Aulacoseira ambigua*; E–F. *A. tenella*. F. Internal view showing rimoportulae (arrows); G. *A. pusilla*; H–I. *Fragilaria gracilis*. H. Internal valve view showing apical pore field (arrow) and rimoportula (arrowhead); J–K. *F. pectinalis*. K. External view showing rimoportula (arrow). Scale bars represent 2 µm; 5 µm (I, J).

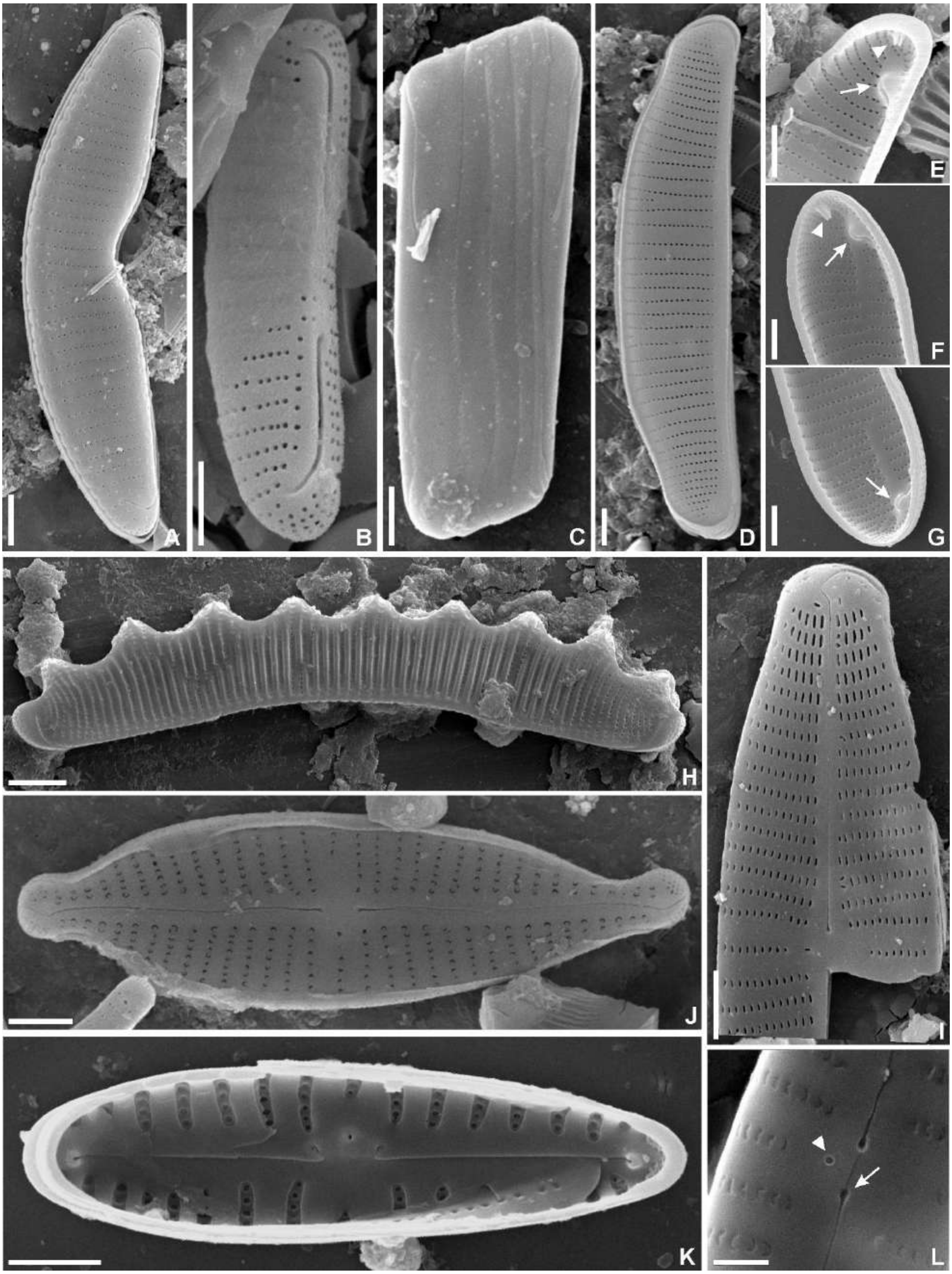

FIGURE 13. Epilithic diatoms from Cascavel River microbasin in SEM. A. *Eunotia bilunaris*, teratological valve; B–C. *E. botulitropica*. C. Girdle view; D–E. *E. rhomboidea*. E. Internal view showing helictoglossa (arrow) and rimoportula (arrowhead); F–G. *E. desmogonioides*. Internal view showing rimoportula (arrow) and helictoglossa (arrowhead); H. *E. georgii*; I. *Geissleria punctifera*; J. *G. lagenula*, teratological valve; K–L. *G. pumilum*. L. External view showing pore-like stigma (arrow), proximal raphe ends (arrow) and C-like areolae. Scale bars represent 2 µm, 5 µm (H), 1 µm (L).

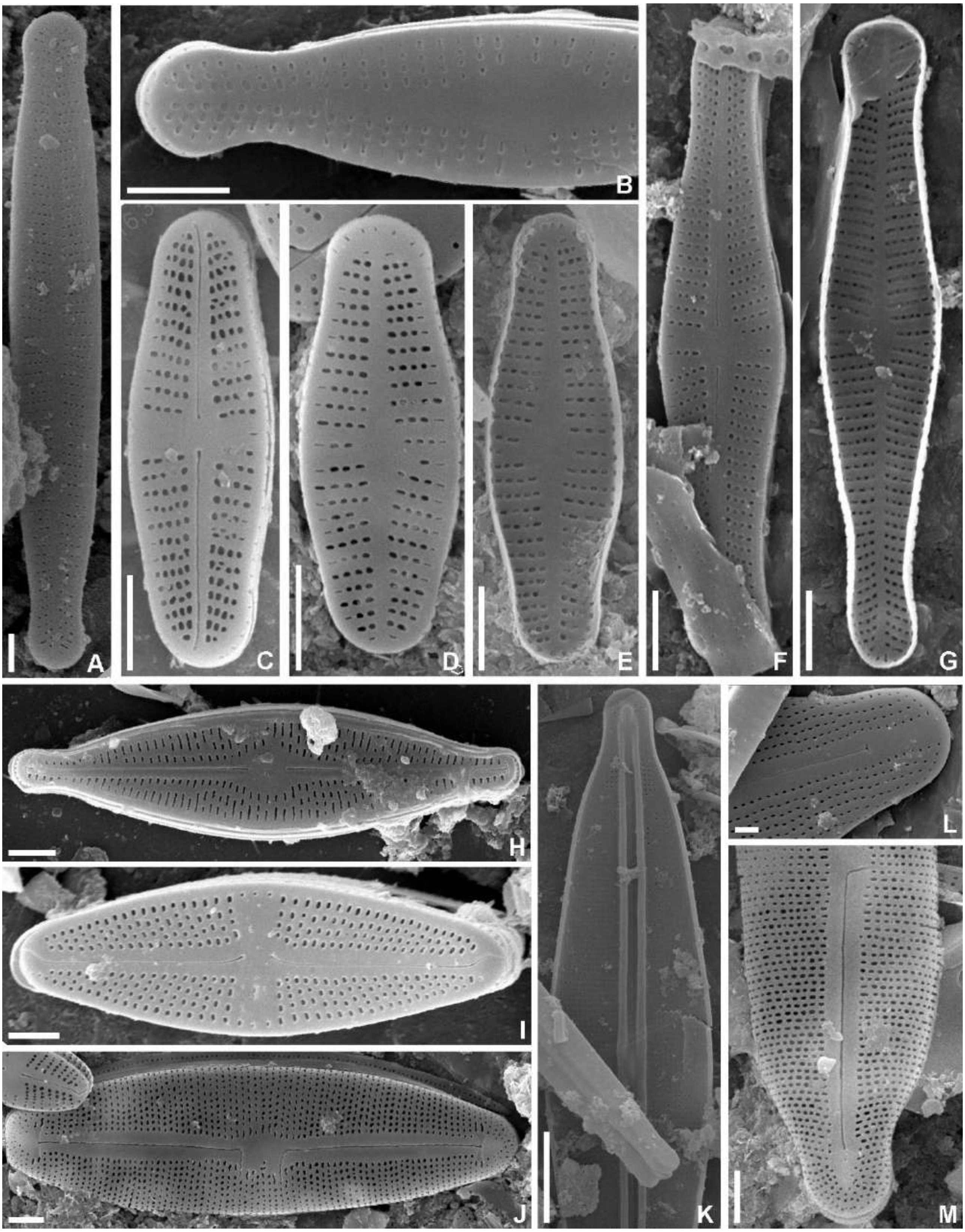

FIGURE 14. Epilithic diatoms from Cascavel River microbasin in SEM. A. *Achnanthidium caledonicum*, rapheless valve; B. *A. macrocephalum*, rapheless valve; C–E. *A. minutissimum*. C–D. Raphid and rapheless valve in external view; E. Internal view of rapheless valve; F–G. *A. tropicocatenatum*, raphid and rapheless valve; H. *Brachysira microcephala*; I. *Luticola ectorii*; J. *Frustulia weinholdii*. K–L. *Frustulia australocrassinervia*. L. External view showing proximal raphe ends T-shaped; M. *F. neomundana*. Scale bars represent 2 µm, 5 µm (K), 1 µm (L).

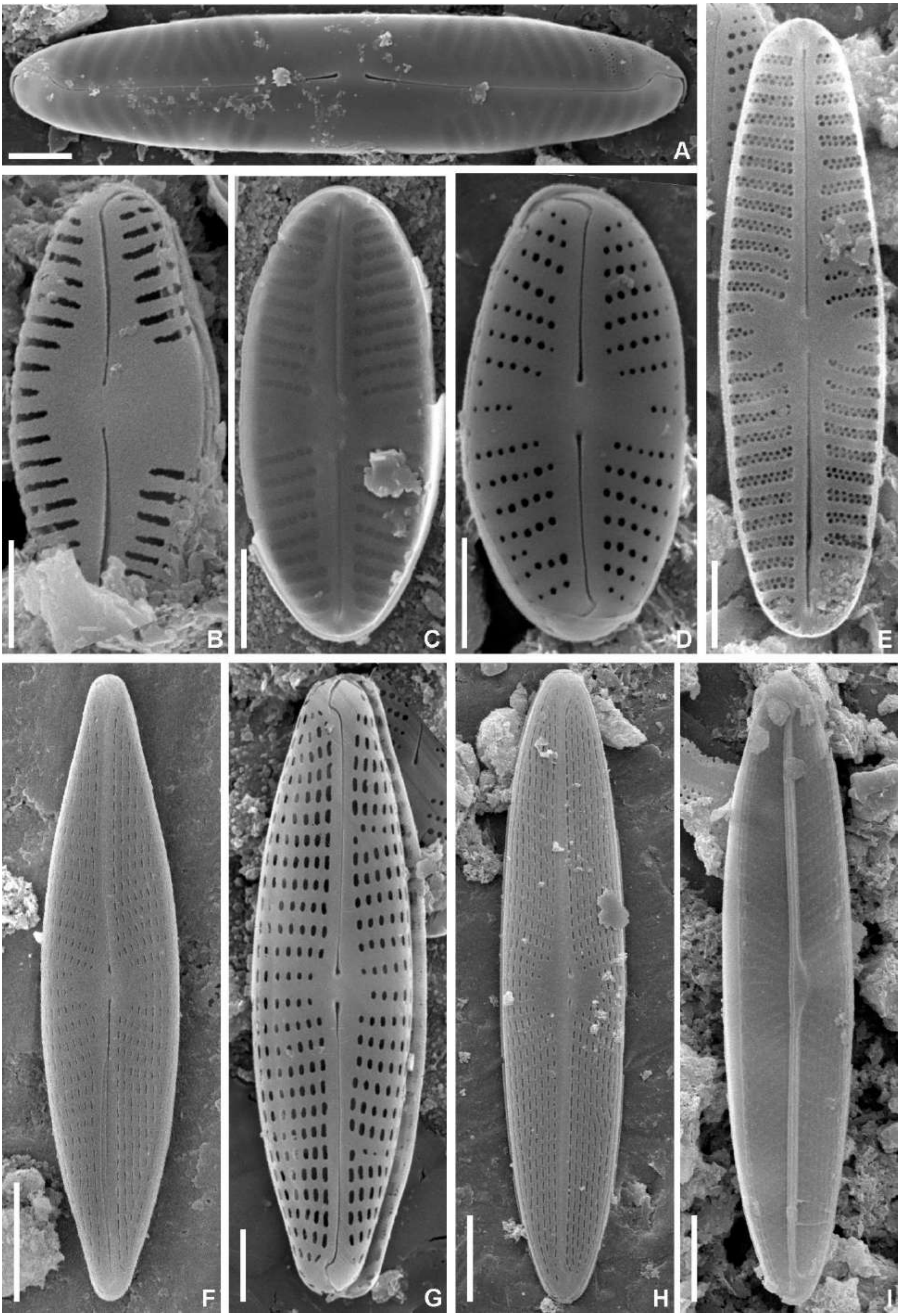

FIGURE 15. Epilithic diatoms from Cascavel River microbasin in SEM. A. *Pinnularia acoricola*; B. *Chamaepinnularia brasilianopsis*; C–D. *Sellaphora nigri*, internal and external views; E. *S. saugerresii*; F. *Navicula cryptocephala*; G. *N. salinicola*; H–I. *N. symmetrica*, external and internal views. Scale bars represent 2 µm, 5 µm (F, H, I).

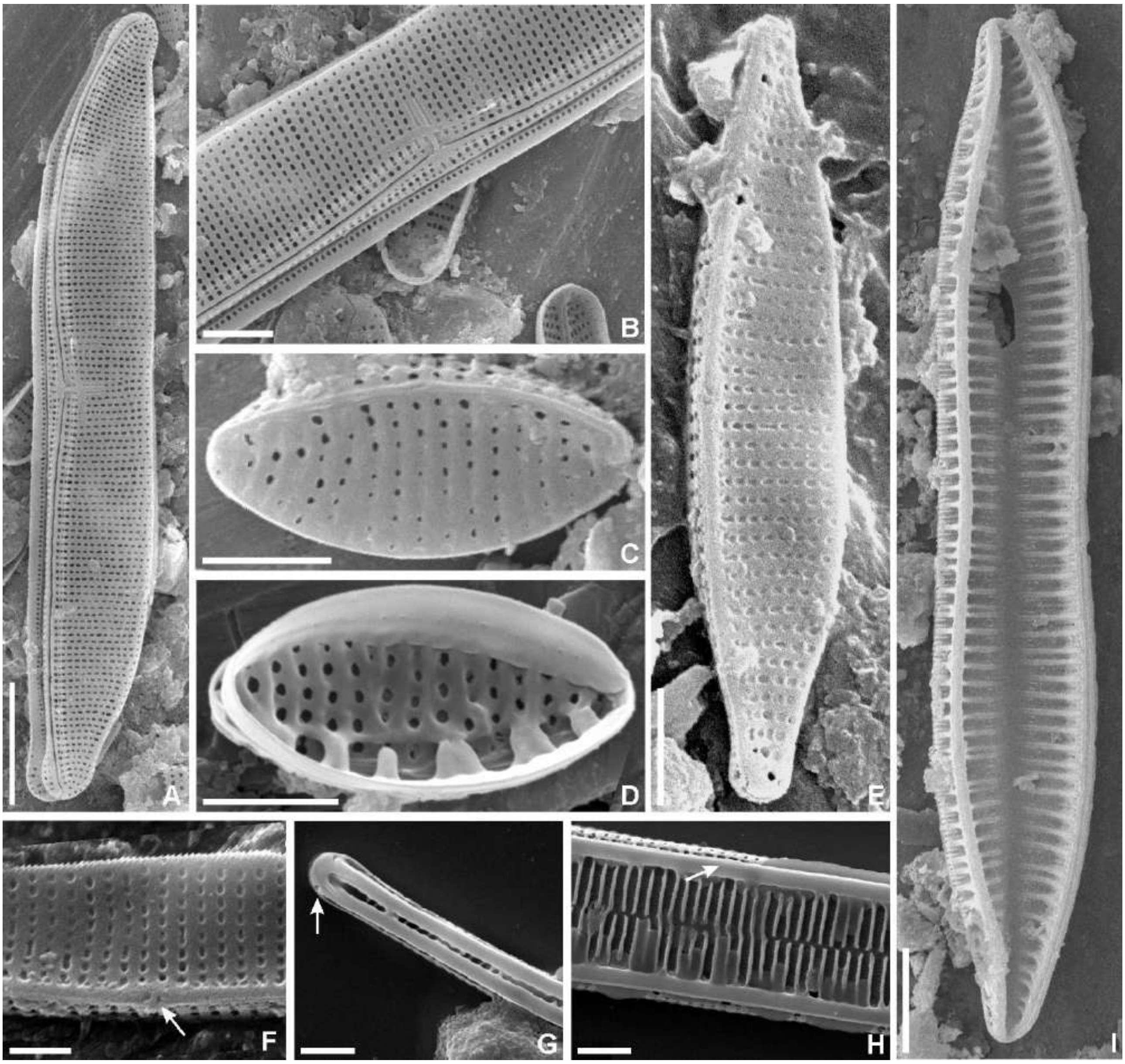

FIGURE 16. Epilithic diatoms from Cascavel River microbasin in SEM. A–B. *Nitzschia clausii*. B. External view showing the raphe and mantle ornamentation. C–D. *N. inconspicua*. D. Internal view showing fibulae; E–F. *N. perminuta*. F. External view showing proximal raphe ends (arrow); G–H. *Iconella curvula*. G. External view showing distal raphe ends (arrow). H. External view showing raphe (arrow) and striae. I. *I. delicatissima*. Scale bars represent 2 µm, 5 µm (A), 10 µm (I).

Discussion

Our taxonomic work provided morphological and meristic data on 221 epilithic taxa found in subtropical streams in Brazil. Three species were recorded for the first time in Paraná State, and one represented a new record for Brazil.

Belonging to a predominantly urban microbasin, and located in a region of red distropheric latosol (rich in Fe and Al), the studied streams were characterized by distinct metals, predominantly acidic pH, and high conductivity (dos Santos *et al.* 2018). Sampling sites connected to urban headwaters showed higher metal concentrations than sites with considerable riparian vegetation, such as S5 and S6, for example (Corbi *et al.* 2018, Khan *et al.* 2021). Further, the absence of riparian vegetation generates silting in several stretches of the basin, which favors the accumulation of sediment and increases the concentration of metals (Martins *et al.* 2021). Despite the conservation unit in the headwaters of the watershed, the region suffers from diffuse pollution sources from the urban center, as it is an open visitation area with uncontrolled capybara populations, contributing to high nitrate and conductivity values (Figure 2a) (Remor *et al.* 2018, Medeiros *et al.* 2020).

The slightly acid pH found in the Cascavel River microbasin could explain the high species richness of *Eunotia* and *Pinnularia*, although these genera are associated with streams with oligotrophic conditions and low conductivity (Round *et al.* 1990, Metzeltin & Lange-Bertalot 1998, Silva-Lehmkuhl *et al.* 2019). Furthermore, the Cascavel River microbasin was composed of many small diatom species of the genera *Achnanthidium* Kützing, *Brachysira* Kützing, *Humidophila* (Lange-Bertalot & Werum) Lowe *et al.*, *Nupela* Vyverman and Compère, *Planothidium* Round & Bukhtiyarova, and *Sellaphora* Mereschowsky, which may be related to the high availability of rocky substrates (Richards *et al.* 2020), or indicate selection of adnate species, which are tolerant to carryover by water flow and also to metal pollution (Morin *et al.* 2008, 2012, Barral-Fraga *et al.* 2016, Pandey *et al.* 2018a).

Polluted urban and rural streams also tend to suffer a reduction in the number of diatom species (Fernández *et al.* 2018), highlighting acidified and high conductivity environments (Luís *et al.* 2009, Moresco *et al.* 2011). However, the number of taxa found in our study (221 spp.) is higher when compared to other floras in the State (see Bertolli *et al.* 2010, Faria *et al.* 2010, Silva *et al.* 2010, Moresco *et al.* 2011, Santos *et al.* 2011, Marra *et al.* 2016, Silva-Lehmkuhl *et al.* 2019). This might be explained by the higher sampling effort in our study, and the fact that these studies have mostly evaluated reservoir floras, using artificial and epiphytic substrates.

Diatoms exposed to metal-contaminated environments may undergo modifications in community structure, such as alteration in colonization/growth form or turnover from sensitive to tolerant species (da Silva *et al.* 2009, Morin *et al.* 2012, Pandey *et al.* 2018a), or modifications on an individual scale, such as reduction in valve size or emergence of teratologies (Lavoie *et al.* 2012, Su *et al.* 2018, Olenici *et al.* 2017, 2019, Pandey *et al.* 2019). Although naturally high in the Cascavel River microbasin (see Table 1 in Appendix D), morphological abnormalities have previously been associated with Fe (McFarland *et al.* 1997, Dickman 1998, Cattaneo *et al.* 2004, Sienkiewicz & Gasiorowski 2016, Pandey *et al.* 2018b), and Al (Furey *et al.* 2009, Soleimani *et al.* 2020), affecting the valve outline, striae pattern, and areolae shape.

Considering other metals evaluated in our study, Cd, Cu and Zn are recorded in the literature as causing teratology in diatoms (Falasco *et al.* 2009a, 2021), increasing the number of deformed valves in water bodies (Pandey & Bergey 2016, Pandey *et al.* 2018b). Deformed valve outline (type 1 teratology) is common in diatoms exposed to copper (Pandey *et al.* 2014), which may explain the several species with abnormalities at S3 and S8 (see Table 2) (Moir *et al.* 2022). Centrally bent valves of *Eunotia* and bent apices in *Achnanthidium*, for example, also represent an effect of copper exposure (Cantonati *et al.* 2014, Olenici *et al.* 2017). Cadmium and zinc also contribute to the appearance of teratological valves, causing deformed valve outline in *Achnanthidium*, *Fragilaria*, *Gomphonema* (Morin & Coste 2006, Morin *et al.* 2007, de Jonge *et al.* 2008), abnormal striae pattern in *Encyonema*, *Gomphonema*, *Nitzschia*, *Planothidium*, and *Ulnaria* (Morin & Coste 2006, Morin *et al.* 2007, Falasco *et al.* 2009b), and duplicated central area in *Planothidium* (Morin *et al.* 2007). Anthropized environments, such as S4 and S7, are subject to receiving harmful concentrations of these metals to diatoms (see Table 1 in Appendix B and Figure 2b), suggesting their contribution as drivers of abnormalities in numerous species in our study (Table 2).

Other metals evaluated in our study may have contributed to the morphologically abnormal valves, such as Ba and Mn in *Eunotia subarcuatoides* (Furey *et al.* 2009), Cr in *Ulnaria ulna* (Pandey *et al.* 2018b), and Ni in *Achnanthidium minutissimum* and *Nitzschia palea* (Gómez *et al.* 2008, Morin *et al.* 2014, Sienkiewicz & Gasiorowski 2016, Lavoie *et al.* 2018), although not always related to specific sampling sites (see Table 1 in Appendix D and Figure 2b). Other species, however, showed a close relationship with these metals, such as *Gomphonema pumilum*, *Caloneis bacillum* (manganese) *Eunotia yberai*, *Achnanthidium macrocephalum*, *Pinnularia graciloides* var. *latecapitata* (chromium), *Eunotia desmogonioides*, *Achnanthidium modestiforme*, *Sellaphora saugerresii* (nickel) (Table 2), possibly indicating synergistic effects of metals on altered valve formation. The initial portion of the microbasin has a strong influence of Pb, especially S1 and S2, as previously indicated by Remor *et al.* (2018) and in our study (see Figure 2b), suggesting relationships with the occurrence of teratological forms in *Eunotia*, *Encyonema*, *Frustulia*, *Pinnularia*, and *Navicula* (Table 2). Lead is known to cause deformed valves in numerous diatom species, usually in association with other metals (Gómez *et al.* 2008, Pandey *et al.* 2014, Simic *et al.* 2018) or high concentrations of nutrients, especially phosphorus and nitrogen (Mora *et al.* 2015, Pandey *et al.* 2018b). Environmental factors combined with metal pollution also contribute to modify diatom frustules (Millan *et al.* 2019, Olenici *et al.* 2020), such as low pH ((Luís *et al.* 2011, 2016, Leguay *et al.* 2016, Olenici *et al.* 2020), high conductivity (Pandey *et al.* 2018a), low flow (Al-Handal & Abdullah 2010), and high nutrient concentrations (Gómez & Licurs 2003), which can be related to the characteristics found in the Cascavel River microbasin (see Table 1 in Appendix C and Figure 2a). Eutrophic conditions, for example, may have contributed to the duplicate pattern of alveoli in *Discostella stelligera* recorded by Silva *et al.* (2010). Different abiotic conditions lead to teratological forms in different species, such as high temperature, conductivity, total nitrogen, and coliforms for *U. ulna* (Morin *et al.* 2008, Pandey *et al.* 2018a, 2019), low pH for *E. bilunaris* (Grabowska *et al.* 2014), phosphorus and nitrogen for *A. minutissimum* (Pandey *et al.* 2018b).

These factors are recurrent in the Cascavel River microbasin, especially due to the lack of riparian vegetation and diffuse urban or agricultural pollution (see Table 1 in Appendix A and Figure 2a). Additionally, we point out that teratological valves of *Gomphonema lagenula* were recorded in almost all sampled sites, but there are no specific data on teratologies in this species. In general, teratologies associated with the genus *Gomphonema* arise from high metal concentrations and acidic pH (Gómez *et al.* 2008, Falasco *et al.* 2009b, Fernández *et al.* 2018).

It is interesting to note that some individuals of *Eunotia desmogonioides*, *E. monodon*, *E. subarcuatoides*, *Achnanthidium macrocephalum*, *Pinnularia brauniana*, *P. subgibba* var. *undulata*, and *Craticula riparia* (see Figs 4T, 4W, 4X, 3AQ, 7I, 8AF, 9F, 10Y) possibly presented cingulum teratology (type 8), since this type of abnormality was described in epilithic samples from metal-polluted environments, but further analysis are needed, especially observation in SEM.

Floristic studies are crucial for better understanding the biodiversity of algae, as well as their geographic distribution, ecological preferences, in addition to providing insights into ecosystem dynamics. Further studies including SEM images are needed to verify whether morphological abnormalities occur at a lower scale, such as in the raphe system, areolae pattern, and cingulum bands. The influence of metals on specific taxa and the other factors driving morphological abnormalities in diatom communities (e.g., flow, shading, substrate availability, nutrient content) should be better investigated, especially metal concentrations and their bioavailability.

Conclusion

Our work contributes to the taxonomic knowledge of epilithic diatoms in the region by extending measurements and occurrences. Three species were registered for the first time in the state of Paraná, and one species was recorded for the first time in Brazil, which helps to understand ecological and biogeographical aspects of diatoms. The numerous diatom valves with teratological characteristics suggest that the concentrations of metals in the river sediment, added to the other environmental variables in the microbasin, disturb this periphytic community. In fact, 34 diatom species presented deformed valve outline or unusual striae pattern. In this sense our study also contributes to avoid teratological populations from being described as new taxa. Further studies are needed, increasing the number of sampling sites, SEM analyses, and ecological characteristics, in order to contribute to the taxonomy of the group, as well as to the understanding of the effects of metals on freshwater diatom communities.

Acknowledgments

We acknowledge the Fundação Araucária (FA) and the Coordenação de Aperfeiçoamento Pessoal de Nível Superior (CAPES) for master and doctoral scholarships granted to Mailor Wellinton Wedig Amaral and Gabriela Medeiros. We also thank the Electron Microscopy Center (CME) of Universidade Federal do Paraná for technical assistance and to Acquasollus laboratory for the water chemical analyzes. We acknowledge the Conselho Nacional de Desenvolvimento Científico e Tecnológico (CNPq) for scientific productivity grant of T.A.V. Ludwig (311876/2019-6).

References

Abarca, N., Jahn, R., Zimmermann, J. & Enke, N. (2014) Does the Cosmopolitan Diatom *Gomphonema parvulum* (Kützing) Kützing Have a Biogeography? *PLoS ONE* 9: e86885. https://doi.org/10.1371/journal.pone.0086885

Agostinho, A.A., Thomaz, S.M. & Gomes, L.C. (2005) Conservation of the biodiversity of Brazil's inland waters. *Conservation Biology* 19: 646–652. https://doi.org/10.1111/j.1523-1739.2005.00701.x

AL-Handal, A.Y. & Abdullah, D.S. (2010) Diatoms from the restored Mesopotamian marshes, South Iraq. *Algological Studies* 133: 65–103. https://doi.org/10.1127/1864-1318/2010/0133-0065

Algarte, V.M., Dunck, B., Leandrini, J.A. & Rodrigues, L. (2016) Periphytic diatom ecological guilds in floodplain: Ten years after dam. *Ecological Indicators* 69: 407–414. https://doi.org/10.1016/j.ecolind.2016.04.049

de Almeida, F.F., Ector, L., Silva, E.S. & Wetzel, C.E. (2020) *Gomphonema frequentiformis* (Metzeltin & krammer) *comb. nov.* (Bacillariophyta): Ecology and taxonomy of a neotropical diatom. *Phytotaxa* 439: 265–275. https://doi.org/10.11646/PHYTOTAXA.439.3.8

Almeida, P.D., Morales, E.A., Wetzel, C.E., Ector, L. & Bicudo, D. de C. (2016) Two new diatoms in the genus *Fragilaria* Lyngbye (Fragilariophyceae) from tropical reservoirs in Brazil and comparison with type material of *F. tenera*. *Phytotaxa* 246: 163–183. https://doi.org/10.11646/phytotaxa.246.3.1

Alvares, C.A., Stape, J.L., Sentelhas, P.C., Gonçalves, J.L. de M. & Sparovek, G. (2013) Köppen's climate classification map for Brazil. *Meteorologische Zeitschrift* 22: 711–728. https://doi.org/10.1127/0941-2948/2013/0507

Amaral, M.W.W., Medeiros, G., Daufenbach, V., Gonçalves, M.S., Ludwig, T.A.V. & Bueno, N.C. (2021) *Nupela semifasciata* (Bacillariophyceae), a new species from subtropical lotic environments in western Paraná state, Brazil. *Fottea* 21: 152–163. https://doi.org/10.5507/FOT.2021.002

APHA (2012) *Standard Methods for the Examination of Water and Wastewater*. 22nd ed. American Public Health Association, Washington, 541 pp.

Azevedo-Santos, V.M., Brito, M.F.G., Manoel, P.S., Perroca, J.F., Rodrigues-Filho, J.L., Paschoal, L.R.P., Gonçalves, G.R.L., Wolf, M.R., Blettler, M.C.M., Andrade, M.C., Nobile, A.B., Lima, F.P., Ruocco, A.M.C., Silva, C. V., Perbiche-Neves, G., Portinho, J.L., Giarrizzo, T., Arcifa, M.S. & Pelicice, F.M. (2021) Plastic pollution: A focus on freshwater biodiversity. *Ambio* 50: 1313–1324. https://doi.org/10.1007/s13280-020-01496-5

Bahls, L.L. (2010) *Northwest Diatoms. Stauroneis in the Northern Rockies. 50 species of Stauroneis sensu stricto from western Montana, northern Idaho, northeastern Washington and southwestern Alberta, including 16 species described as new*. 174 pp.

Barral-Fraga, L., Morin, S., Rovira, M.D.M., Urrea, G., Magellan, K. & Guasch, H. (2016) Shortterm arsenic exposure reduces diatom cell size in biofilm communities. *Environmental Science and Pollution Research* 23: 4257–4270. https://doi.org/10.1007/s11356-015-4894-8

Bartozek, E.C.R., Zorzal-Almeida, S. & Bicudo, D.C. (2018) Surface sediment and phytoplankton diatoms across a trophic gradient in tropical reservoirs: new records for Brazil and São Paulo State. *Hoehnea* 45: 69–92. https://doi.org/10.1590/2236-8906-51/2017

Benito, X. & Fritz, S.C. (2020) Diatom Diversity and Biogeography Across Tropical South America. *In*: Rull, V. & Carnaval, A.C. (Eds.) *Neotropical Diversification: Patterns and Processes*. Cham: Springer International Publishing, pp. 121–143. https://doi.org/10.1007/978-3-030-31167-4_7

Bertolli, L.M., Tremarin, P.I. & Ludwig, T.A.V. (2010) Diatomáceas perifíticas em *Polygonum hydropiperoides* Michaux, reservatório do Passaúna, Região Metropolitana de Curitiba, Paraná, Brasil. *Acta Botanica Brasilica* 24: 1065–1081.

Bicudo, C.E. de M. & Menezes, M. (2017) *Gêneros de algas de águas continentais do Brasil (chave para identificação e descrições)*. 3rd ed. RiMa, São Carlos, 552 pp.

Bicudo, D.C., Tremarin, P.I., Almeida, P.D., Zorzal-Almeida, S., Wengrat, S., Faustino, S.B., Costa, L.F., Bartozek, E.C.R., Rocha, A.C.R., Bicudo, C.E.M. & Morales, E.A. (2016) Ecology and distribution of *Aulacoseira* species (Bacillariophyta) in tropical reservoirs from Brazil. *Diatom Research* 31: 199–215. https://doi.org/10.1080/0269249X.2016.1227376

Bruder, K. & Medlin, L.K. (2007) Molecular assessment of phylogenetic relationships in selected species/genera in the naviculoid diatoms (Bacillariophyta). I. The genus *Placoneis*. *Nova Hedwigia* 85: 331–352. https://doi.org/10.1127/0029-5035/2007/0085-0331

Buczkó, K., Wojtal, A.Z. & Jahn, R. (2009) *Kobayasiella* species of the Carpathian region: morphology, taxonomy and description of *K. tintinnus* spec. nov. *Diatom Research* 24: 1–21. https://doi.org/10.1080/0269249X.2009.9705780

Bukhtiyarova, L.N. & Pomazkina, G.B. (2013) *Bacillariophyta of Lake Baikal. Volume 1. Genera Baikalia, Slavia, Navigeia, Placogeia, Grachevia, Goldfishia, Nadiya, Cymbelgeia*. Lviv Lega-Pres, 184 pp.

Camburn, K.E. & Charles, D.F. (2000) *Diatoms of Low-Alkalinity Lakes in the Northeastern United States*. Academy of Natural Sciences of Philadelphia, Philadelphia. 152 pp.

Canani, L.G. de C., Menezes, M. & Torgan, L.C. (2011) Diatomáceas epilíticas de águas oligotróficas e ácidas do Sudeste do Brasil. *Acta Botanica Brasilica* 25: 130–140.

Cantonati, M., Angeli, N., Virtanen, L., Wojtal, A.Z., Gabrieli, J., Falasco, E., Lavoie, I., Morin, S., Marchetto, A., Fortin, C. & Smirnova, S. (2014) *Achnanthidium minutissimum* (Bacillariophyta) valve deformities as indicators of metal enrichment in diverse widely-distributed freshwater habitats. *Science of The Total Environment* 475: 201–215. https://doi.org/10.1016/j.scitotenv.2013.10.018

Casa, V., Mataloni, G. & Vijver, B. Van De (2018) Six new *Frustulia* species (Bacillariophyta) in Tierra del Fuego peatbogs, Patagonia, Argentina. *Fottea* 18: 55–71. https://doi.org/10.5507/fot.2017.016

Cattaneo, A., Couillard, Y., Wunsam, S. & Courcelles, M. (2004) Diatom taxonomic and morphological changes as indicators of metal pollution and recovery in Lac Dufault (Québec, Canada). *Journal of Paleolimnology* 32: 163–175.

Cavalier-Smith, T. (2015) Division Heterokontophyta/Ochrophyta. *In*: Frey, W. (Ed.) *Syllabus of Plant Families. A. Engler's Syllabus der Pflanzenfamilien Part 2/1: Photoautotrophic eukaryotic Algae*. Borntraeger, Stuttgart, pp. 61–139.

Cholnoky, B.J. (1963) Ein Beitrag zur Kenntnis der Diatomeenflora von Holländisch-Neuguinea. *Nova Hedwigia* 5(1–4): 157–198.

Cocquyt, C., Kusber, W.H. & Jahn, R. (2018) *Epithemia hirudiniformis* and Related Taxa within the Subgenus *Rhopalodiella* subg. nov. in Comparison to *Epithemia* subg. *Rhopalodia stat nov.* (Bacillariophyceae) from East Africa. *Cryptogamie, Algologie* 39: 35–62. https://doi.org/10.7872/crya/v39.iss1.2018.35

Companhia Ambiental do Estado de São Paulo (CETESB) & Agência Nacional das Águas (ANA).

(2011) *Guia Nacional De Coleta E Preservação De Amostras: água, sedimento, comunidades aquáticas e efluentes líquidos*. Companhia Ambiental do Estado de São Paulo e Agência Nacional das Águas, Brasília, 326 pp.

Corbi, J.J., Costa, C.G., Gorni, G.R., Colombo, V. & Rios, L. (2018) Environmental diagnosis of metals in streams near sugarcane cultivation areas: current and historical analysis in the central region of the State of São Paulo. *Anais da Academia Brasileira de Ciencias* 90: 2711–2719. https://doi.org/10.1590/0001-3765201820170808

Costa, L.F., Wetzel, C.E., Lange-Bertalot, H., Ector, L. & Bicudo, D.C. (2017a) *Taxonomy and ecology of Eunotia species (Bacillariophyta) in southearstern Brazilian reservoirs*. J. Cramer, Stuttgart, 302 pp.

Costa, L.F., Wengrat, S. & Bicudo, D.C. (2017b) Diatoms from distinct habitats of a highly heterogeneous reservoir, Billings Complex, southeastern Brazil. *Hoehnea* 44: 559–579. https://doi.org/10.1590/2236-8906-12/2017

Cox, E.J. (2003) *Placoneis* Mereschkowsky (Bacillariophyta) revisited: resolution of several typification and nomenclatural problems, including the generitype. *Botanical Journal of the Linnean Society* 141: 53–83. https://doi.org/10.1046/j.1095-8339.2003.00115.x

Dickman, M.D. (1998) Benthic marine diatom deformities associated with contaminated sediments in Hong Kong. *Environment International* 24: 749–759.

Downey, K.M., Julius, M.L., Theriot, E.C. & Alverson, A.J. (2021) Phylogenetic analysis places *Spicaticribra* within *Cyclotella*. *Diatom Research*: 1–7. https://doi.org/10.1080/0269249X.2021.1926332

Falasco, E., Bona, F., Badino, G., Hoffmann, L. & Ector, L. (2009a) Diatom teratological forms and environmental alterations: A review. *Hydrobiologia* 623: 1–35. https://doi.org/10.1007/s10750-008-9687-3

Falasco, E., Bona, F., Ginepro, M., Hlúbiková, D., Hoffmann, L. & Ector, L. (2009b) Morphological abnormalities of diatom silica walls in relation to heavy metal contamination and artificial growth conditions. *Water SA* 35: 595–606. https://doi.org/10.4314/wsa.v35i5.49185

Falasco, E., Ector, L., Wetzel, C.E., Badino, G. & Bona, F. (2021) Looking back, looking forward: a review of the new literature on diatom teratological forms (2010–2020). *Hydrobiologia* 848: 1675–1753. https://doi.org/10.1007/s10750-021-04540-x

Faria, D.M. De, Tremarin, P.I. & Ludwig, T.A.V. (2010) Diatomáceas perifíticas da represa Itaqui, São José dos Pinhais, Paraná: Fragilariales, Eunotiales, Achnanthales e *Gomphonema* Ehrenberg. *Biota Neotropica* 10: 415–427. https://doi.org/10.1590/S1676-06032010000300035

Faustino, S.B., Fontana, L., Bartozek, E.C.R., Bicudo, C.E. de M. & Bicudo, D. de C. (2016) Composition and distribution of diatom assemblages from core and surface sediments of a water supply reservoir in Southeastern Brazil. *Biota Neotropica* 16: 1–23. https://doi.org/http://dx.doi.org/10.1590/1676-0611-BN-2015-0129

Fernández, M.R., Martín, G., Corzo, J., de la Linde, A., García, E., López, M. & Sousa, M. (2018) Design and Testing of a New Diatom-Based Index for Heavy Metal Pollution. *Archives of Environmental Contamination and Toxicology* 74: 170–192. https://doi.org/10.1007/s00244-017-0409-6

Ferreira, K.S. de M. & Bicudo, C.E. de M. (2017) Criptógamos do Parque Estadual das Fontes do Ipiranga, São Paulo, SP. Algae, 42: Bacillariophyceae (Surirellales). *Hoehnea* 44: 10–28. https://doi.org/http://dx.doi.org/10.1590/2236-8906-34/2016

Finlay, B.J., Monaghan, E.B. & Maberly, S.C. (2002) Hypothesis: The rate and scale of dispersal of freshwater diatom species is a function of their global abundance. *Protist* 153: 261–273. https://doi.org/10.1078/1434-4610-00103

Fundação para o Desenvolvimento Científico e Tecnológico (FUNDETEC) (1995) *Bacia Hidrográfica do Rio Cascavel – Proposta para recuperação ambiental*. Prefeitura Municipal de Cascavel, Cascavel, 164 pp.

Furey, P.C., Lowe, R.L. & Johansen, J.R. (2009) Teratology in *Eunotia* taxa in the great smoky mountains national park and description of *Eunotia macroglossa sp. nov*. *Diatom Research* 24: 273–290. https://doi.org/10.1080/0269249X.2009.9705802

Furey, P.C., Lowe, R.L. & Johansen, J.R. (2011) *Eunotia Ehrenberg (Bacillariophyta) of the Great Smoky Mountains National Park, USA*. Bibliotheca Diatomologica, 56th ed., 134 pp.

Garnett, S.T. & Christidis, L. (2018) Science-based taxonomy still needs better governance : Response to Thomson et al. *PLOS Biology* 16: e2005249. https://doi.org/10.1371/journal.pbio.2005249 March

Gautam, S., Kumar, L., Vinayak, V. & Arya, A. (2017) Morphological and physiological alterations in the diatom *Gomphonema pseudoaugur* due to heavy metal stress. *Ecological Indicators* 72: 67–76. https://doi.org/10.1016/j.ecolind.2016.08.002

Gómez, N., Sierra, M. V., Cortelezzi, A. & Rodrigues Capítulo, A. (2008) Effects of discharges from the textile industry on the biotic integrity of benthic assemblages. *Ecotoxicology and Environmental Safety* 69: 472–479. https://doi.org/10.1016/j.ecoenv.2007.03.007

Guiry, M.D. & Guiry, G.M. (2021) *AlgaeBase*. World-wide electronic publication. National University of Ireland, Galway. Available from: http://www.algaebase.org (accessed: July 9 2021).

Heinrich, C.G., Leal, V.L., Düpont, M.S.A. & Lobo, E.A. (2014) Epilithic diatoms in headwater areas of the hydrographical sub-basin of the Andreas Stream, RS, Brazil, and their relation with eutrophication processes. *Acta Limnologica Brasiliensia* 26: 347–355. https://doi.org/10.1590/S2179-975X2014000400003

Hendey, N.I. (1964) *An introductory account of the smaller algae of British coastal waters: Part V. Bacillariophyceae (Diatoms)*. Her Majesty's Stationery Office, London, 317 pp.

Hofmann, G. (1994) *Aufwuchs diatoms in Seen und ihre Eignung als Indikatoren der Trophie*. Cramer, Berlin-Sttutgart, 241 pp.

Hofmann, G., Werum, M. & Lange-Bertalot, H. (2011) *Diatomeen im Süßwasser-Benthos von Mitteleuropa. Bestimmungsflora Kieselalgen für die ökologische Praxis. Über 700 der häufigsten Arten und ihre Ökologie*. Koeltz Scientific Books, Königstein, 908 pp.

Hofmann, G., Werum, M. & Lange-Bertalot, H. (2013) Bestimmungsflora Kieselalgen für die ökologische Praxis. Über 700 der häufigsten Arten und ihre Ökologie. *In*: Lange-Bertalot, H. (Ed.) *Diatomeen im Süßwasser-Benthos von Mitteleuropa*. pp. 1–908.

Hohn, M.H. & Hellerman, J. (1963) The taxonomy and structure of diatom populations from three eastern North American rivers using three sampling methods. *Transactions of the American Microscopical Society* 82: 250–329.

Houk, V. & Klee, R. (2004) The stelligeroid taxa of the genus *Cyclotella* (Kützing) Brébisson (Bacillariophyceae) and their transfer into the new genus *Discostella gen. nov. Diatom Research* 19: 203–228. https://doi.org/10.1080/0269249X.2004.9705871

Houk, V., Klee, R. & Tanaka, H. (2010) *Atlas of freshwater centric diatoms with a brief key and descriptions. Stephanodiscaceae - Cyclotella, Tertiarius, Discostella*. Fottea, Czech Republic, 498 pp.

Hustedt, F. (1935) Die fossile Diatomeenflora in den Ablagerungen des Tobasses auf Sumatra. “Tropische Binnengewasser, Band VI.” *Archiv für Hydrobiologie* 14: 143–192.

Hustedt, F. (1943) Die Diatomeenflora einiger Hochgebirgsseen der Landschaft Davos in den Schweizer Alpen. *Internationale revue der gesamten hydrobiologie und hydrographie* 43: 124–197.

Hustedt, F. (1945) Diatomeen aus Seen und Quellgebieten der Balkan-Halbinsel. *Archiv für Hydrobiologie* 40: 867–973.

Jahn, R., Abarca, N., Gemeinholzer, B., Mora, D., Skibbe, O., Kulikovskiy, M., Gusev, E., Kusber, W.-H. & Zimmermann, J. (2017) *Planothidium lanceolatum* and *Planothidium frequentissimum* reinvestigated with molecular methods and morphology: four new species and the taxonomic importance of the sinus and cavum. *Diatom Research* 32: 75–107. https://doi.org/10.1080/0269249X.2017.1312548

Johansen, J., Kociolek, P. & Lowe, R. (2008) *Spicaticribra kingstonii*, *gen. nov.* et *sp. nov.* (Thalassiosirales, Bacillariophyta) from Great Smoky Mountains National Park, U.S.A. *Diatom Research* 23: 367–375. https://doi.org/10.1080/0269249X.2008.9705763

De Jonge, M., Van de Vijver, B., Blust, R. & Bervoets, L. (2008) Responses of aquatic organisms to metal pollution in a lowland river in Flanders: A comparison of diatoms and macroinvertebrates. *Science of the Total Environment* 407: 615–629. https://doi.org/10.1016/j.scitotenv.2008.07.020

Jüttner, I., Chudaev, D. & Kusber, W.H. (2020) Re-examination of the type materials of *Navicula exilis* and *Navicula cryptocephala* (Naviculaceae, Bacillariophyceae). *Phytotaxa* 472: 123–134. https://doi.org/10.11646/phytotaxa.472.2.3

Jüttner, I., Ector, L., Reichardt, E., Van de Vijver, B., Jarlman, A., Krokowski, J. & Cox, E.J. (2013) *Gomphonema varioreduncum sp. nov.*, a new species from northern and western Europe and a re-examination of *Gomphonema exilissimum*. *Diatom Research* 28: 303–316. https://doi.org/10.1080/0269249X.2013.797924

Jyrkänkallio-Mikkola, J., Siljander, M., Heikinheimo, V., Pellikka, P. & Soininen, J. (2018) Tropical stream diatom communities – The importance of headwater streams for regional diversity. *Ecological Indicators* 95: 183–193. https://doi.org/10.1016/j.ecolind.2018.07.030

Kapetanović, T., Jahn, R., Redžić, S. & Carić, M. (2011) Diatoms in a poor fen of Bijambare protected landscape, Bosnia & Herzegovina. *Nova Hedwigia* 93: 125–151. https://doi.org/10.1127/0029-5035/2011/0093-0125

Kapustin, D. & Kulikovskiy, M. (2018) Transfer of *Stenopterobia* and *Surirella* taxa (Bacillariophyceae) described from the insular Southeast Asia to the genus *Iconella*. *Nova Hedwigia, Beihefte* 147: 237–245.

Kennedy, B. & Allott, N. (2017) A review of the genus *Brachysira* in Ireland with the description of *Brachysira praegeri* and *Brachysira conamarae*, new raphid diatoms (Bacillariophyceae) from high status waterbodies. *Phytotaxa* 326: 1–27. https://doi.org/10.11646/phytotaxa.326.1.1

Khan, R., Saxena, A., Shukla, S., Sekar, S., Senapathi, V. & Wu, J. (2021) Environmental contamination by heavy metals and associated human health risk assessment: a case study of surface water in Gomti River Basin, India. *Environmental Science and Pollution Research* 28: 56105–56116. https://doi.org/10.1007/s11356-021-14592-0

Kobayasi, H. & Nagumo, T. (1988) Examination of the type materials of *Navicula subtilissima* Cleve (Bacillariophyceae). *The Botanical Magazine Tokyo* 101: 239–253. https://doi.org/10.1007/BF02488602

Kociolek, J.P. & Spaulding, S.A. (2000) Freshwater diatoms biogeography. *Nova Hedwigia* 71: 223–241.

Krammer, K. (1992) *Pinnularia*. Eine Monographie der europäischen Taxa. *Bibliotheca Diatomologica* 26: 1–353.

Krammer, K. (1997a) Die cymbelloidean Diatomeen: eine Monographie der weltweit bekannten taxa. I Allgemeines und Encyonema part. *Bibliotheca Diatomologica* 36: 1–382.

Krammer, K. (1997b) Die cymbelloidean Diatomeen: eine Monographie der weltweit bekannten taxa. II Encyonema part., Encyonopsis and Cymbellopsis. *Bibliotheca Diatomologica* 37: 1–469.

Krammer, K. (2000) The genus *Pinnularia*. *In*: Lange-Bertalot, H. (Ed.) *Diatoms of Europe. Diatoms of the European inland waters and comparable habitats.* A.R.G. Gantner Verlag K.G., Ruggell, pp. 1–703.

Krammer, K. (2003) *Cymbopleura*, *Delicata*, *Navicymbula*, *Gomphocymbellopsis*, *Afrocymbella*. *In*: Lange-Bertalot, H. (Ed.) *Diatoms of Europe. Diatoms of the European inland waters and comparable habitats.* A.R.G. Gantner Verlag KG, Ruggell, pp. 1–584.

Krammer, K. & Lange-Bertalot, H. (1986) Bacillariophyceae: Naviculaceae. *In*: Ettl, H., Gerloff, J., Heynig, H. & Mollenhauer, D. (Eds.) *Süßwasserflora von Mitteleuropa*. Gustav Fischer Verlag, Stuttgard-New York, pp. 1–876.

Krammer, K. & Lange-Bertalot, H. (1988) Bacillariophyceae: Bacillariaceae, Epithemiaceae, Surirellaceae. *In*: Ettl, H., Gerloff, J., Heynig, H. & Mollenhauer, D. (Eds.) *Süßwasserflora von Mitteleuropa*. Gustav Fischer, Sttutgart, pp. 1–596.

Krammer, K. & Lange-Bertalot, H. (1991a) Bacillariophyceae: Centrales, Fragilariaceae, Eunotiaceae. *In*: Ettl, H., Gerloff, J., Heynig, H. & Mollenhauer, D. (Eds.) *Süßwasserflora von Mitteleuropa*. Gustav Fischer, Sttutgart, pp. 1–576.

Krammer, K. & Lange-Bertalot, H. (1991b) Bacillariophyceae: Achnanthaceae, Kritische Ergänzungen zu *Navicula* (Lineolatae) und *Gomphonema*. *In*: H. Ettl, J. Gerloff, H. Heyning, & D. Mollenhauer (eds.) *Süsswasserflora von Mitteleuropa*. Gustav Fischer, Stuttgart & Jena, pp. 1–437.

Krammer & Lange-Bertalot, H. (1985) Naviculaceae Neue und wenig bekannte Taxa, neue Kombinationen und Synonyme sowie Bemerkungen zu einigen Gattungen. *Bibliotheca Diatomologica* 9: 1–230.

Krasske, G. (1932) Beiträge zur Kenntnis der Diatomeenflora der Alpen. *Hedwigia* 72: 92–135.

Kulikovskiy, M., Lange-Bertalot, H., Witkowski, A., Dorofeyuk, N.I. & Genkal, S.I. (2010) Diatom assemblages from *Sphagnum* bogs of the world. Nur bog in northern Mongolia. *Bibliotheca Diatomologica* 18: 1–326.

Kulikovskiy, M., Maltsev, Y., Glushchenko, A., Kuznetsova, I., Kapustin, D., Gusev, E., Lange-Bertalot, H., Genkal, S. & Kociolek, J.P. (2020) *Gogorevia*, a new monoraphid diatom genus for *Achnanthes exigua* and allied taxa (Achnanthidiaceae) described on the basis of an integrated molecular and morphological approach. *Journal of Phycology* 56: 1601–1613. https://doi.org/10.1111/jpy.13064

Lange-Bertalot, H. (1993) 85 neue Taxa und über 100 weitere neu definierte Taxa ergänzend zur Süsswasserflora von Mitteleuropa, Vol. 2/1-4. *Bibliotheca Diatomologica* 27: 1–164.

Lange-Bertalot, H. (1999) Neue Kombinationen von taxa aus *Achnanthes* Bory (sensu lato). *Iconographia Diatomologica* 6: 276–289.

Lange-Bertalot, H. (2001) *Navicula* sensu stricto. 10 genera separated from *Navicula* sensu lato *Frustulia*. *Diatoms of Europe* 2: 1–526.

Lange-Bertalot, H., Bak, M., Witkowski, A. & Tagliaventi, N. (2011) *Eunotia* and some related genera. *Diatoms of Europe* 6: 1–747.

Lange-Bertalot, H. & Metzeltin, D. (1996) Indicators of oligotrophy. 800 taxa representative of three ecologically distinct lake types. Carbonate buffered-oligodys-trophic-weakly buffered soft water. *Iconographia Diatomologica* 2: 1–390.

Lange-Bertalot, H. & Moser, G. (1994) *Brachysira*, Monographie der Gattung. *Bibliotheca Diatomologica* 29: 1–212.

Lange-Bertalot, H. & Ulrich, S. (2014) Contributions to the taxonomy of needle-shaped *Fragilaria* and *Ulnaria* species. *Lauterbornia* 78: 1–73.

Lavoie, I., Hamilton, P.B., Morin, S., Kim Tiam, S., Kahlert, M., Gonçalves, S., Falasco, E., Fortin, C., Gontero, B., Heudre, D., Kojadinovic-Sirinelli, M., Manoylov, K., Pandey, L.K. & Taylor, J.C. (2017) Diatom teratologies as biomarkers of contamination: Are all deformities ecologically meaningful? *Ecological Indicators* 82: 539–550. https://doi.org/10.1016/j.ecolind.2017.06.048

Lavoie, I., Morin, S., Laderriere, V. & Fortin, C. (2018) Freshwater diatoms as indicators of combined long-term mining and urban stressors in junction creek (Ontario, Canada). *Environments* 5: 1–17. https://doi.org/10.3390/environments5020030

Lavoie, I., Lavoie, M. & Fortin, C. (2012) A mine of information: Benthic algal communities as biomonitors of metal contamination from abandoned tailings. *Science of the Total Environment* 425: 231–241. https://doi.org/10.1016/j.scitotenv.2012.02.057

Leguay, S., Lavoie, I., Levy, J.L. & Fortin, C. (2016) Using biofilms for monitoring metal contamination in lotic ecosystems: The protective effects of hardness and pH on metal bioaccumulation. *Environmental Toxicology and Chemistry* 35: 1489–1501. https://doi.org/10.1002/etc.3292

Lepskaya, E.V., Jewson, D.H. & Usoltseva, M. (2010) *Aulacoseira subarctica* in Kurilskoye Lake, Kamchatka: a deep, oligotrophic lake and important Pacific salmon nursery. *Diatom Research* 25: 323–335. https://doi.org/10.1080/0269249X.2010.9705853

Levkov, Z. (2009) *Amphora* sensu lato. *Diatoms of Europe* 5: 1–916.

Levkov, Z., Metzeltin, D. & Pavlov, A. (2013) *Luticola* and *Luticopsis*. *Diatoms of Europe* 7: 1–697.

Levkov, Z., Mitic-Kopanja, D. & Reichardt, E. (2016a) The diatom genus *Gomphonema* from the Republic of Macedonia. *Diatoms of Europe* 8: 1–552.

Levkov, Z., Tofilovska, S., Jovanovska, E., Cvetkoska, A. & Metzeltin, D. (2016b) Revision of the *Stauroneis smithii* Grunow (Bacillariophyceae) species complex from Macedonia. *Botanica Serbica* 40: 167–178. https://doi.org/10.5281/zenodo.162215

Levkov, Z., Tofilovska, S. & Mitic-Kopanja, D. (2016c) Species of the diatom genus *Craticula* Grunow (Bacillariophyceae) from Macedonia. *Contributions, Section of Natural, Mathematical and Biotechnical Sciences* 37: 129–165. https://doi.org/10.20903/CSNMBS

Liu, Y., Wang, Q. & Fu, C. (2011) Taxonomy and distribution of diatoms in the genus *Eunotia* from the Da'erbin Lake and Surrounding Bogs in the Great Xing'an Mountains, China. *Nova Hedwigia* 92: 205–232. https://doi.org/10.1127/0029-5035/2011/0092-0205

Lobo, E.A., Callegaro, V.L.M., Hermany, G., Bes, D., Wetzel, C.E. & Oliveira, M.A. (2004) Use of epilithic diatoms as bioindicators from lotic systems in southern Brazil, with special emphasis on eutrophication. *Acta Limnologica Brasiliensia* 16: 25–40.

Lobo, E.A., Heinrich, C.G., Schuch, M., Düpont, A., Costa, A.B. da, Wetzel, C.E. & Ector, L. (2016) *Índice trófico de qualidade da água: guia ilustrado para sistemas lóticos subtropicais e temperados brasileiros*. EDUNISC, Santa Cruz do Sul, 53 pp. Available from: https://repositorio.unisc.br/jspui/handle/11624/1767 (accessed: January 4 2021).

Lobo, E.A., Schuch, M., Heinrich, C.G., Costa, A.B. da, Düpont, A., Wetzel, C.E. & Ector, L. (2015) Development of the Trophic Water Quality Index (TWQI) for subtropical temperate Brazilian lotic systems. *Environmental Monitoring and Assessment* 187: 1–13. https://doi.org/10.1007/s10661-015-4586-3

Lowe, R.L., Kociolek, P., Johansen, J.R., Van De Vijver, B., Lange-Bertalot, H. & Kopalová, K. (2014) *Humidophila gen. nov.*, a new genus for a group of diatoms (Bacillariophyta) formerly within the genus *Diadesmis*: species from Hawai'i, including one new species. *Diatom Research* 29: 351–360. https://doi.org/10.1080/0269249X.2014.889039

Luchini, L. & Verona, C.A. (1972) *Catálogo de las diatomeas Argentinas. I. Diatomeas de aguas continentales (incluido el Sector Antártico).* Comisión de Investigaciones Científicas de la Provincia de Buenos Aires. Monografías, 2, La Plata.

Ludwig, T.A.V. & Flôres, T.L. (1997) Diatomoflórula dos rios da região a ser inundada para a construção da Usina Hidrelétrica de Segredo, Paraná: Fragilariophyceae (*Fragilaria* e *Synedra*). *Hoehnea* 24: 55–65.

Luís, A.T., Durães, N., de Almeida, S.F.P. & da Silva, E.F. (2016) Integrating geochemical (surface waters, stream sediments) and biological (diatoms) approaches to assess AMD environmental impact in a pyritic mining area: Aljustrel (Alentejo, Portugal). *Journal of Environmental Sciences (China)* 42: 215–226. https://doi.org/10.1016/j.jes.2015.07.008

Luís, A.T., Teixeira, P., Almeida, S.F.P., Matos, J.X. & Da Silva, E.F. (2011) Environmental impact of mining activities in the Lousal area (Portugal): Chemical and diatom characterization of metal-contaminated stream sediments and surface water of Corona stream. *Science of the Total Environment* 409: 4312–4325. https://doi.org/10.1016/j.scitotenv.2011.06.052

Luís, A.T., Teixeira, P., Almeida, S.F.P., Ector, L., Matos, J.X. & Silva, A.F. da (2009) Impact of Acid Mine Drainage (AMD) on Water Quality, Stream Sediments and Periphytic Diatom Communities in the Surrounding Streams of Aljustrel Mining Area (Portugal). *Water, Air, and Soil Pollution* 200: 147–167. https://doi.org/10.1007/s11270-008-9900-z

Maasri, A., Jähnig, S.C., Adamescu, M.C., Adrian, R., Baigun, C., Baird, D. & … Worischka, S. (2021) A Global Agenda for Advancing Freshwater Biodiversity Research. *EcoEvoRxiv*: 1–12. [preprint]. https://doi.org/10.32942/osf.io/4pg7f

Mann, D.G., Mcdonald, S.M., Bayer, M.M., Droop, S.J.M., Chepurnov, V.A., Loke, R.E., Ciobanu, A. & Hans du buf, J.M. (2004) The *Sellaphora pupula* species complex (Bacillariophyceae): morphometric analysis, ultrastructure and mating data provide evidence for five new species. *Phycologia* 43: 459–482.

Mann, D.G., Thomas, S.J. & Evans, K.M. (2008) Revision of the diatom genus *Sellaphora*: A first account of the larger species in the British Isles. *Fottea* 8: 15–78. https://doi.org/10.5507/fot.2008.002

Mann, D.G. & Vanormelingen, P. (2013) An inordinate fondness? The number, distributions, and origins of diatom species. *Journal of Eukaryotic Microbiology* 60: 414–420. https://doi.org/10.1111/jeu.12047

Marquardt, G.C. & Bicudo, C.E.M. (2014) Criptógamos do Parque Estadual das Fontes do Ipiranga, São Paulo, SP. Algas 36: Bacillariophyceae (Cymbellales). *Hoehnea* 41: 209–246.

Marquardt, G.C., Costa, L.F., Bicudo, D.C., Bicudo, C.E. de M., Blanco, S., Wetzel, C.E. & Ector, L. (2017) Type analysis of *Achnanthidium minutissimum* and *A. catenatum* and description of *A. tropicocatenatum sp. nov.* (Bacillariophyta), a common species in Brazilian reservoirs. *Plant Ecology and Evolution* 150: 313–330. https://doi.org/10.5091/plecevo.2017.1325

Marra, R.C., Tremarin, P.I., Algarte, V.M. & Ludwig, T.V. (2016) Epiphytic diatoms (Diatomeae) from Piraquara II urban reservoir, Paraná state. *Biota Neotropica* 16: 1–20. https://doi.org/10.1590/1676-0611-BN-2016-0200

Martins, W.A., Martins, L.L., De Maria, I.C., de Moraes, J.F.L. & Pedro Júnior, M.J. (2021) Reduction of sediment yield by riparian vegetation recovery at distinct levels of soil erosion in a tropical watershed. *Ciencia e Agrotecnologia* 45: e028220. https://doi.org/10.1590/1413-7054202145028220

Mayama, S., Idei, M., Osada, K. & Tamotsu, N. (2002) Nomenclatural changes for 20 diatom taxa occurring in Japan. *Diatom* 18: 89–91. https://doi.org/10.11464/diatom1985.18.0_89

McFarland, B.H., Hill, B.H. & Willingham, W.T. (1997) Abnormal *Fragilaria* spp. (Bacillariophyceae) in streams impacted by mine drainage. *Journal of Freshwater Ecology* 12: 141–149. https://doi.org/10.1080/02705060.1997.9663517

McGowan, S., Gunn, H. V., Whiteford, E.J., John Anderson, N., Jones, V.J. & Law, A.C. (2018) Functional attributes of epilithic diatoms for palaeoenvironmental interpretations in South-West Greenland lakes. *Journal of Paleolimnology* 60: 273–298. https://doi.org/10.1007/s10933-017-9968-9

Medeiros, G., Amaral, M.W.W., Ferreira, P.C., Ludwig, T.V. & Bueno, N.C. (2018) *Gomphonema* Ehrenberg (Bacillariophyceae, Gomphonemataceae) of the São Francisco Falso River, Paraná, Brazil. *Biota Neotropica* 18: e20170495. http://dx.doi.org/10.1590/1676-0611-BN-2017-0495

Medeiros, G., Padial, A.A., Wedig Amaral, M.W., Ludwig, T.A.V. & Bueno, N.C. (2020) Environmental variables likely influence the periphytic diatom community in a subtropical lotic environment. *Limnologica* 80: 125718. https://doi.org/10.1016/j.limno.2019.125718

Metzeltin, D. & Lange-Bertalot, H. (1998) Tropical Diatoms of South America I: About 700 predominantly rarely known or new taxa representative of the neotropical flora. *Iconographia Diatomologica* 5: 1–695.

Metzeltin, D. & Lange-Bertalot, H. (2002) Diatoms from the ″Island Continent″ Madagascar. *Iconographia Diatomologica* 11: 1–286.

Metzeltin, D. & Lange-Bertalot, H. (2007) Tropical diatoms of South America II. Special remarks on biogeographic disjunction. *Iconographia Diatomologica* 18: 1–877.

Metzeltin, D., Lange-Bertalot, H. & García-Rodríguez, F. (2005) Diatoms of Uruguay. Compared with other taxa from South America and elsewhere. *Iconographia Diatomologica* 15: 1–736.

Meyer, J.L., Strayer, D.L., Wallace, J.B., Eggert, S.L., Helfman, G.S. & Leonard, N.E. (2007) The contribution of headwater streams to biodiversity in river networks. *Journal of the American Water Resources Association* 43: 86–103. https://doi.org/10.1111/j.1752-1688.2007.00008.x

Millan, F., Izere, C., Breton, V., Voldoire, O., Biron, D.G., Wetzel, C.E., Miallier, D., Allain, E., Ector, L. & Beauger, A. (2019) The effect of natural radioactivity on diatom communities in mineral springs. *Botany Letters* 167: 95–113. https://doi.org/10.1080/23818107.2019.1691051

Moir, K.E., Ridal, J.J. & Cumming, B.F. (2022) Spatiotemporal and teratological analyses of diatom assemblages from sediments contaminated with industrial effluents in the St. Lawrence River near Cornwall (Ontario, Canada). *Hydrobiologia* 849: 1417–1436. https://doi.org/10.1007/s10750-021-04792-7

Mora, D., Carmona, J. & Cantoral-Uriza, E.A. (2015) Diatomeas epilíticas de la cuenca alta del río Laja, Guanajuato, México. *Revista Mexicana de Biodiversidad* 86: 1024–1040. https://doi.org/10.7550/rmb.41027

Morais, K.S. De, Bartozek, E.R., Zorzal-Almeida, S., Bicudo, D.C. & Bicudo, C.E. de M. (2018) Taxonomy and ecology of order Surirellales (Bacillariophyceae) in tropical reservoirs in Southeastern of Brazil. *Acta Limnologica Brasiliensia* 30: e204. https://doi.org/10.1590/S2179-975X9817

Morales, E. a. & Vis, M.L. (2007) Epilithic diatoms (Bacillariophyceae) from cloud forest and alpine streams in Bolivia, South America. *Proceedings of the Academy of Natural Sciences of Philadelphia* 156: 123–155. https://doi.org/10.1635/0097-3157(2007)156[123:EDBFCF]2.0.CO;2

Morales, E.A., Ector, L., Fernández, E., Novais, M.H., Hlúbiková, D., Hamilton, P.B., Blanco, S., Vis, M.L. & Kociolek, P.J. (2011) The genus *Achnanthidium* Kütz. (Achnanthales, Bacillariophyceae) in Bolivian streams: a report of taxa found in recent investigations. *Algological Studies* 136/137: 89–130. https://doi.org/10.1127/1864-1318/2011/0136-0089

Moreira-Filho, H. & Valente-Moreira, I.M. (1981) Avaliação taxonômica e ecológica das diatomáceas (Bacillariophyceae) epífitas em algas pluricelulares obtidas nos litorais dos Estados do Paraná, Santa Catarina e São Paulo. *Boletim do Museu Botânica Municipal* 47: 1–17.

Moresco, C., Tremarin, P.I., Ludwig, T.A.V. & Rodrigues, L. (2011) Diatomáceas perifíticas abundantes em três córregos com diferentes ações antrópicas em Maringá, PR, Brasil. *Revista Brasileira de Botânica* 34: 359–373.

Morin, S., Cordonier, A., Lavoie, I., Arini, A., Blanco, S., Duong, T.T., Tornés, E., Bonet, B., Corcoll, N., Faggiano, L., Laviale, M., Pérès, F., Becares, E., Coste, M., Feurtet-Mazel, A., Fortin, C., Guasch, H. & Sabater, S. (2012) Consistency in Diatom Response to Metal-Contaminated Environments. *In*: Guasch, H., Ginebreda, A. & Geiszinger, A. (Eds.) *Emerging and priority pollutants in rivers*. Springer-Verlag, Berlin Heidelberg, pp. 117–146.

Morin, S., Corcoll, N., Bonet, B., Tlili, A. & Guasch, H. (2014) Diatom responses to zinc contamination along a Mediterranean river. *Plant Ecology and Evolution* 147: 325–332. https://doi.org/10.5091/plecevo.2014.986

Morin, S., Duong, T.T., Dabrin, A., Coynel, A., Herlory, O., Baudrimont, M., Delmas, F., Durrieu, G., Schäfer, J., Winterton, P., Blanc, G. & Coste, M. (2008) Long-term survey of heavy-metal pollution, biofilm contamination and diatom community structure in the Riou Mort watershed, South-West France. *Environmental Pollution* 151: 532–542. https://doi.org/10.1016/j.envpol.2007.04.023

Morin, S. & Coste, M. (2006) Metal-induced shifts in the morphology of diatoms from the Riou Mort and Riou Viou streams (South West France). *Use of algae for monitoring rivers VI*: 91–106.

Morin, S., Vivas-Nogues, M., Thi, T.D., Boudou, A., Coste, M. & Delmas, F. (2007) Dynamics of benthic diatom colonization in a cadmium/zinc-polluted river (Riou-Mort, France). *Fundamental and Applied Limnology* 168: 179–187. https://doi.org/10.1127/1863-9135/2007/0168-0179

Moro, R.S. & Fürstenberger, C.B. (1997) *Catálogo dos principais parâmetros ecológicos de diatomáceas não-marinhas*. Editora da Universidade Estadual de Ponta Grossa, Ponta Grossa, 282 pp.

Nardelli, M.S., Bueno, N.C., Ludwig, T.A. V. & Guimarães, A.T.B. (2016) Structure and dynamics of the planktonic diatom community in the Iguassu River, Paraná State, Brazil. *Brazilian*

Journal of Biology 76: 374–386. https://doi.org/10.1590/1519-6984.16114

Ohtsuka, T. (2018) LM and SEM observation of *Kurtkrammeria spicula* (Hust.) comb. nov. *Diatom*: 49–50. https://doi.org/10.11464/diatom.34.49

Olenici, A., Baciu, C., Blanco, S. & Morin, S. (2020) Naturally and Environmentally Driven Variations in Diatom Morphology: Implications for Diatom-Based Assessment of Water Quality. *In*: Cristóbal, G., Blanco, S. & Bueno, G. (Eds.) *Modern Trends in Diatom Identification*. Springer International Publishing, Cham, pp. 39–50.

Olenici, A., Blanco, S., Borrego-Ramos, M., Jimenez-Gomez, F., Guerrero, F., Momeu, L. & Baciu, C. (2019) A new diatom teratology driven by metal pollution in a temperate river (Roșia Montană, Romania). *Annali di Botanica* 9: 113–118. https://doi.org/10.13133/2239-3129/14624

Olenici, A., Blanco, S., Borrego-Ramos, M., Momeu, L. & Baciu, C. (2017) Exploring the effects of acid mine drainage on diatom teratology using geometric morphometry. *Ecotoxicology* 26: 1018–1030. https://doi.org/10.1007/s10646-017-1830-3

Olodo, I.Y., Cocquyt, C., Abou, Y. & Kokou, K. (2020) Seasonal variations and distribution of diatom flora of Lake Ahémé (Benin, West Africa). *Botany Letters* 167: 160–173. https://doi.org/10.1080/23818107.2019.1657495

Pandey, L.K. & Bergey, E.A. (2016) Exploring the status of motility, lipid bodies, deformities and size reduction in periphytic diatom community from chronically metal (Cu, Zn) polluted waterbodies as a biomonitoring tool. *Science of the Total Environment* 550: 372–381. https://doi.org/10.1016/j.scitotenv.2015.11.151

Pandey, L.K., Bergey, E.A., Lyu, J., Park, J., Choi, S., Lee, H., Depuydt, S., Oh, Y.T., Lee, S.M. & Han, T. (2017) The use of diatoms in ecotoxicology and bioassessment: Insights, advances and challenges. *Water Research* 118: 39–58. https://doi.org/10.1016/j.watres.2017.01.062

Pandey, L.K., Kumar, D., Yadav, A., Rai, J. & Gaur, J.P. (2014) Morphological abnormalities in periphytic diatoms as a tool for biomonitoring of heavy metal pollution in a river. *Ecological Indicators* 36: 272–279. https://doi.org/10.1016/j.ecolind.2013.08.002

Pandey, L.K., Lavoie, I., Morin, S., Depuydt, S., Lyu, J., Lee, H., Jung, J., Yeom, D.-H., Han, T. & Park, J. (2019) Towards a multi-bioassay-based index for toxicity assessment of fluvial waters. *Environmental Monitoring and Assessment* 191: 112. https://doi.org/10.1007/s10661-019-7234-5

Pandey, L.K., Lavoie, I., Morin, S., Park, J., Lyu, J., Choi, S., Lee, H. & Han, T. (2018) River water quality assessment based on a multi-descriptor approach including chemistry, diatom assemblage structure, and non-taxonomical diatom metrics. *Ecological Indicators* 84: 140–151. https://doi.org/10.1016/j.ecolind.2017.07.043

Pandey, L.K., Sharma, Y.C., Park, J., Choi, S., Lee, H., Lyu, J. & Han, T. (2018) Evaluating features of periphytic diatom communities as biomonitoring tools in fresh, brackish and marine waters. *Aquatic Toxicology* 194: 67–77. https://doi.org/10.1016/j.aquatox.2017.11.003

Park, J., Bergey, E.A., Han, T. & Pandey, L.K. (2020) Diatoms as indicators of environmental health on Korean islands. *Aquatic Toxicology* 227: 105594. https://doi.org/10.1016/j.aquatox.2020.105594

Patrick, R. & Reimer, C.W. (1966) *The Diatoms of the United States: exclusive of Alaska and Hawaii*. Academy of Natural Sciences of Philadelphia, Philadelphia, 688 pp.

Potapova, M. & Charles, D.F. (2007) Diatom metrics for monitoring eutrophication in rivers of the United States. *Ecological Indicators* 7: 48–70. https://doi.org/10.1016/j.ecolind.2005.10.001

Potapova, M. & Hamilton, P.B. (2007) Morphological and ecological variation within the *Achnanthidium minutissimum* (Bacillariophyceae) species complex. *Journal of Phycology* 43: 561–575. https://doi.org/10.1111/j.1529-8817.2007.00332.x

Reichardt, E. (1995) Die Diatomeen (Bacillariophyceae) in Ehrenberg's Material von Cayenne, Guyana Gallica (1843). *Iconographia Diatomologica* 1: 1–23.

Reichardt, E. (1997) Taxonomische Revision des Artenkomplexes um *Gomphonema pumilum* (Bacillariophyceae). *Nova Hedwigia* 65: 99–129.

Reichardt, E. (1999) Zur Revision der Gattung *Gomphonema*. *Iconographia Diatomologica* 8: 1–203.
Reichardt, E. (2005) Die Identität von *Gomphonema entolejum* Østrup (Bacillariophyceae) sowie Revision ähnlicher Arten mit weiter Axialarea. *Nova Hedwigia* 81: 115–144. https://doi.org/10.1127/0029-5035/2005/0081-0115
Reichardt, E. (2015) *Gomphonema gracile* Ehrenberg sensu stricto et sensu auct. (Bacillariophyceae): A taxonomic revision. *Nova Hedwigia* 101: 367–393. https://doi.org/10.1127/nova_hedwigia/2015/0275
Remor, M.B., Sampaio, S.C., de Rijk, S., Vilas Boas, M.A., Gotardo, J.T., Pinto, E.T. & Schardong, F.A. (2018) Sediment geochemistry of the urban Lake Paulo Gorski. *International Journal of Sediment Research* 33: 406–414. https://doi.org/10.1016/j.ijsrc.2018.04.009
Richards, J., Tibby, J., Barr, C. & Goonan, P. (2020) Effect of substrate type on diatom-based water quality assessments in the Mount Lofty Ranges, South Australia. *Hydrobiologia* 847: 3077–3090. https://doi.org/10.1007/s10750-020-04316-9
Rieuwerts, J.S. (2007) The mobility and bioavailability of trace metals in tropical soils: A review. *Chemical Speciation and Bioavailability* 19: 75–85. https://doi.org/10.3184/095422907X211918
Rimet, F. (2012) Recent views on river pollution and diatoms. *Hydrobiologia* 683: 1–24. https://doi.org/10.1007/s10750-011-0949-0
Rondón, J.C. & Abuhatab Aragón, Y.A. (2018) Factors driving diversity and succession of diatom assemblages in a Neotropical rainforest stream. *Annales de Limnologie* 54: 1–9. https://doi.org/10.1051/limn/2018021
Round, F.E. & Bukhtiyarova, L. (1996) Four new genera based on *Achnanthes* (*Achnanthidium*) together with a re-definition of *Achnanthidium*. *Diatom Research* 11: 345–361.
Round, F.E., Crawford, R.M. & Mann, D.G. (1990) *The Diatoms. Biology and morfology of the genera*. Cambridge University Press, Cambridge, 747 pp.
Rumrich, U., Lange-Bertalot, H. & Rumrich, M. (2000) Diatoms of the Andes. From Venezuela to Patagonia/Tierra del Fuego and two additional contributions. *Iconographia Diatomologica* 9: 1–673.
Ruwer, D.T., Ludwig, T.A. V & Rodrigues, L. (2019) Two new diatom species (Bacillariophyceae) from Brazilian floodplain: *Actinella hermes-moreirae sp. nov.* and *Gomphonema mutunensis sp. nov. Phytotaxa* 395: 71–80. https://doi.org/10.11646/phytotaxa.395.2.3
Santos, E.M. dos, Tremarin, P.I. & Ludwig, T.A.V. (2011) Diatomáceas perifíticas em *Potamogeton polygonus* Cham. & Schltdl.: citações pioneiras para o estado do Paraná. *Biota Neotropica* 11: 303–315.
dos Santos, H.G. *et al*. (2018) *Sistema brasileiro de classificação de solos*. 5th ed. Embrapa, Brasília, 355 pp.
Schoefs, B., Van de Vijver, B., Wetzel, C.E. & Ector, L. (2020) From diatom species identification to ecological and biotechnological applications. *Botany Letters* 167: 2–5. https://doi.org/10.1080/23818107.2020.1719883
Schoeman, F.R. & Archibald, R.E.M. (1986) Observations on *Amphora* species (Bacillariophyceae) in the British Museum (Natural History). V. Some species from the subgenus *Amphora*. *South African Journal of Botany* 52: 425–437.
Sgro, G. V, Poole, J.B. & Johansen, J.R. (2007) Diatom species composition and ecology of the animas river watershed, Colorado, USA. *Western North American Naturalist* 67: 510–519.
Sienkiewicz, E. & Gasiorowski, M. (2016) The evolution of a mining lake - From acidity to natural neutralization. *Science of the Total Environment* 557–558: 343–354. https://doi.org/10.1016/j.scitotenv.2016.03.088
Silva-Lehmkuhl, A.M. da, Tremarin, P.I., Vercellino, I.S. & Ludwig, T.A.V. (2019) Periphytic diatoms from an oligotrophic lentic system, Piraquara I reservoir, Paraná state, Brazil. *Biota Neotropica* 19: e20180568. https://doi.org/10.1590/1676-0611-bn-2018-0568
Silva, A.M. Da, Ludwig, T.A.V., Tremarin, P.I. & Vercellino, I.S. (2010) Diatomáceas perifíticas

em um sistema eutrófico brasileiro (Reservatório do Iraí, estado do Paraná). *Acta Botanica Brasilica* 24: 997–1016. https://doi.org/10.1590/S0102-33062010000400015

da Silva, E.F., Almeida, S.F.P., Nunes, M.L., Luís, A.T., Borg, F., Hedlund, M., de Sá, C.M., Patinha, C. & Teixeira, P. (2009) Heavy metal pollution downstream the abandoned Coval da Mó mine (Portugal) and associated effects on epilithic diatom communities. *Science of the Total Environment* 407: 5620–5636. https://doi.org/10.1016/j.scitotenv.2009.06.047

da Silva, W.J., Ruwer, D., Nogueira, I. & Dunck, B. (2016) The genus *Pinnularia* (Bacillariophyta, Pinnulariaceae) from Lago dos Tigres, Britânia, Goiás, Brazil. *Biota Neotropica* 16: 1–26. https://doi.org/10.1590/1676-0611-BN-2015-0028

Simić, S., Petrović, A., Đorđević, N., Vasiljević, B., Radojković, N., Mitrović, A. & Janković, M. (2018) Indicative ecological status assessment of the Despotovica river. *Kragujevac Journal of Science*: 227–242. https://doi.org/10.5937/KgJSci1840227S

Simonsen, R. (1974) The diatom plankton of the Indian Ocean Expedition of RV Meteor 1964-1965. Meteor Forschungsergebnisse Reihe D. *Biologie* 19: 1–107.

Siver, P.A. & Hamilton, P.B. (2011) The freshwater flora of waterbodies on the Atlantic Coastal Plain. *Iconographia Diatomologica* 22: 1–916.

Siver, P.A. & Kling, H. (1997) Morphological observations of *Aulacoseira* using scanning electron microscopy. *Canadian Journal of Botany* 75: 1807–1835. https://doi.org/10.1139/b97-894

Soleimani, M., Rutten, L., Maddala, S.P., Wu, H., Eren, E.D., Mezari, B., Schreur-Piet, I., Friedrich, H. & van Benthem, R.A.T.M. (2020) Modifying the thickness, pore size, and composition of diatom frustule in *Pinnularia sp.* with Al3+ ions. *Scientific Reports* 10: 1–13. https://doi.org/10.1038/s41598-020-76318-5

Stenger-Kovács, C., Buczkó, K., Hajnal, É. & Padisák, J. (2007) Epiphytic, littoral diatoms as bioindicators of shallow lake trophic status: Trophic Diatom Index for Lakes (TDIL) developed in Hungary. *Hydrobiologia* 589: 141–154. https://doi.org/10.1007/s10750-007-0729-z

Su, Y., Lundholm, N. & Ellegaard, M. (2018) Effects of abiotic factors on the nanostructure of diatom frustules—ranges and variability. *Applied Microbiology and Biotechnology* 102: 5889–5899. https://doi.org/10.1007/s00253-018-9087-1

Sunda, W.G., Price, N.M. & Morel, F.M.M. (2005) Trace metal ion buffers and their use in culture studies. *In*: Andersen, R.A. (Ed.) *Algal Culturing Techniques*. Elsevier, Amsterdam, pp. 35–63.

Szabó, K., Kiss, K.T., Taba, G. & Ács, É. (2005) Epiphytic diatoms of the Tisza River, Kisköre Reservoir and some oxbows of the Tisza River after the cyanide and heavy metal pollution in 2000. *Acta Botanica Croatica* 64: 1–46.

Tapia, P.M. (2008) Diatoms as bioindicators of pollution in the Mantaro River, Central Andes, Peru. *International Journal of Environment and Health* 2: 82–91. https://doi.org/10.1504/IJENVH.2008.018674

Tavares, B. & Valente-Moreira, I.M. (2000) Diatomoflórula do lago de Cascavel, município de Cascavel, estado do Paraná, Brasil. *Hoehnea* 27: 1–24.

Taylor, J.C., Harding, W.R. & Archibald, C.G.M. (2007) *An Illustrated Guide to Some Common Diatom Species from South Africa*. Water Research Comission, South Africa. 190 pp.

Townsend, S.A. & Gell, P.A. (2005) The role of substrate type on benthic diatom assemblages in the Daly and Roper Rivers of the Australian wet/dry tropics. *Hydrobiologia* 548: 101–115. https://doi.org/10.1007/s10750-005-0828-7

Tremarin, P.I., Ludwig, T.A.V. & Torgan, L.C. (2012) Ultrastructure of *Aulacoseira brasiliensis sp. nov.* (Coscinodiscophyceae) and comparison with related species. *Fottea* 12: 171–188. https://doi.org/10.5507/fot.2012.013

Tremarin, P.I., Ludwig, T.V. & Torgan, L.C. (2013) Morphological variation and distribution of the freshwater diatom *Aulacoseira ambigua* (Grunow) Simonsen in Brazilian continental environments. *Iheringia - Série Botânica* 68: 139–157.

Tremarin, P.I., Moreira-filho, H. & Ludwig, T.A.V. (2010) Pinnulariaceae (Bacillariophyceae) do rio Guaraguaçu, bacia hidrográfica litorânea paranaense, Brasil. *Acta Botanica Brasilica* 24: 335–353. https://doi.org/10.1590/S0102-33062010000200005

Tremarin, P.I., Straube, A. & Ludwig, T.A. V. (2015) *Nupela* (Bacillariophyceae) in littoral rivers from south Brazil, and description of six new species of the genus. *Fottea* 15: 77–93. https://doi.org/10.5507/fot.2015.007

Tremarin, P.I., Wetzel, C.E., Ludwig, T.A.V. & Ector, L. (2011) *Encyonema exuberans sp. nov.* (Bacillariophyceae) from southern brazilian lotic systems. *Nova Hedwigia* 92: 107–120. https://doi.org/10.1127/0029-5035/2011/0092-0107

Trobajo, R., Rovira, L., Ector, L., Wetzel, C.E., Kelly, M. & Mann, D.G. (2013) Morphology and identity of some ecologically important small *Nitzschia* species. *Diatom Research* 28: 37–59. https://doi.org/10.1080/0269249X.2012.734531

Tuji, A. (2007) Type Examination of *Fragilaria gracilis*. *Bulletin of the National Museum of Nature and Science, Series B* 33: 9–12.

Tuji, A. & Houki, A. (2004) Taxonomy, ultrastructure, and biogeography of the *Aulacoseira subarctica* species comples. *Bulletin of the National Museum of Nature and Science, Series B* 30: 35–54.

Tuji, A. & Williams, D.M. (2007) Type examination of japanese diatoms described by Friedrich Meister (1913) from Lake Suwa. *Bulletin of the National Museum of Nature and Science, Series B* 33: 69–79.

Tuji, A. & Williams, D.M. (2008) Examination of types in the *Fragilaria pectinalis-capitellata* species complex. *In*: Likhoshway, Y. (Ed.) *Proceedings of the Nineteenth International Diatom Symposium 2006, Listvyanka, Russia*. Biopress Limited, Bristol, pp. 125–139.

U S Environmental Protection Agency (USEPA) (1996) Acid digestion of sediments, sludges, and soils. *Method 3050B*: 12. Available from: https://www.epa.gov/esam/epa-method-3050b-acid-digestion-sediments-sludges-and-soils (accessed: 19 February 2018).

Udovič, M.G., Cvetkoska, A., Žutinić, P., Bosak, S., Stanković, I., Špoljarić, I., Mršić, G., Kralj Borojević, K., Ćukurin, A. & Plenković-Moraj, A. (2017) Defining centric diatoms of most relevant phytoplankton functional groups in deep karst lakes. *Hydrobiologia* 788: 169–191. https://doi.org/10.1007/s10750-016-2996-z

Van Dam, H., Mertens, A. & Sinkeldam, J. (1994) A coded checklist and ecological indicator values of freshwater diatoms from the Netherlands. *Netherlands Journal of Aquatic Ecology* 28: 117–133. https://doi.org/10.1007/BF02334251

Vörösmarty, C.J., McIntyre, P.B., Gessner, M.O., Dudgeon, D., Prusevich, A., Green, P., Glidden, S., Bunn, S.E., Sullivan, C.A., Liermann, C.R. & Davies, P.M. (2010) Global threats to human water security and river biodiversity. *Nature* 467: 555–561. https://doi.org/10.1038/nature09440

Vouilloud, A.A., Sala, S.E., Avellaneda, M.N. & Duque, S.R. (2010) Diatoms from the Colombian and Peruvian Amazon: the Genera *Encyonema*, *Encyonopsis* and *Gomphonema* (Cymbellales: Bacillariophyceae). *Revista de biologia tropical* 58: 45–62.

Vyverman, W. (1991) Diatoms from Papua New Guinea. *Bibliotheca Diatomologica* 22: 1–223.

Vyverman, W., Verleyen, E., Sabbe, K., Vanhoutte, K., Sterken, M., Hodgson, D.A., Mann, D.G., Juggins, S., Van de Vijver, B., Jones, V., Flower, R., Roberts, D., Chepurnov, V.A., Kilroy, C., Vanormelingen, P. & Wever, A. de (2007) Historical processes constrain patterns in global diatom diversity. *Ecology* 88: 1924–1931.

Weiler, A., Núñez, K., Airaldi, K., Caballero, A., Bauer, F., Santos, M. dos, Bueno, D., Carosini, A., Cardozo, R. & Pérez, P. (2016) Las Aguas Del Lago Ypacarai – Análisis a Través De Bioindicadores. *Investigaciones y Estudios de la UNA* 9: 59–81.

Wengrat, S., Marquardt, G.C., Bicudo, D.C., Bicudo, C.E. d. M., Wetzel, C.E. & Ector, L. (2015) Type analysis of *Cymbella schubartii* and two new *Encyonopsis* species (Bacillariophyceae) from southeastern Brazil. *Phytotaxa* 221: 247–264. https://doi.org/10.11646/phytotaxa.221.3.3

Werum, M. & Lange-Bertalot, H. (2004) Diatoms in Springs from Central Europe and elsewhere under the influence of hydrogeology and anthropogenic impacts. *Iconographia Diatomologica*

13: 1–417.
Wetzel, C.E. (2011) *Biodiversidade e distribuição de diatomáceas (Ochrophyta, Bacillariophyceae) na bacia hidrográfica do Rio Negro, Amazonas, Brasil*. Instituto de Botânica da Secretaria do Meio Ambiente, 1876 pp.
Wetzel, C.E. & Ector, L. (2014a) Taxonomy, distribution and autecology of *Planothidium bagualensis sp. nov.* (Bacillariophyta) a common monoraphid species from southern Brazilian rivers. *Phytotaxa* 156: 201–210. https://doi.org/10.11646/phytotaxa.156.4.2
Wetzel, C.E. & Ector, L. (2014b) *Planothidium lagerheimii comb. nov.* (Bacillariophyta, Achnanthales) a forgotten diatom from South America. *Phytotaxa* 188: 261–267. https://doi.org/10.11646/phytotaxa.188.5.3
Wetzel, C.E. & Ector, L. (2015) Taxonomy and Ecology of *Fragilaria microvaucheriae sp. nov.* and Comparison with the Type Materials of *F. uliginosa* and *F. vaucheriae*. *Cryptogamie, Algologie* 36: 271–289. https://doi.org/10.7872/crya/v36.iss3.2015.271
Wetzel, C.E., Ector, L., Van De Vijver, B., Compère, P. & Mann, D.G. (2015) Morphology, typification and critical analysis of some ecologically important small naviculoid species (Bacillariophyta). *Fottea* 15: 203–234. https://doi.org/10.5507/fot.2015.020
Wetzel, C.E., Lobo, E.A., Oliveira, M.A., Bes, D. & Hermany, G. (2002) Diatomáceas epilíticas relacionadas a fatores ambientais em diferentes trechos dos rios Pardo e Pardinho, Bacia Hidrográfica do Rio Pardo, RS, Brasil: resultados preliminares. *Caderno de Pesquisa Série Biologia* 14: 17–38.
Wetzel, C.E., Morales, E.A., Hinz, F., Bicudo, D.C. & Ector, L. (2013) *Fragilariforma javanica comb. nov.*: Analysis of type material of a widely reported species with a tropical distribution. *Diatom Research* 28: 373–379. https://doi.org/10.1080/0269249X.2013.809668
Wiegleb, G., (1980) Some applications of principal components analysis in vegetation: ecological research of aquatic communities. *In*: Maarel, E. Van Der (Org.) *Classification and ordination*. Springer, Dordrecht, pp. 67–73. https://doi.org/10.1007/978-94-009-9197-2.
Wojtal, A.Z., Ector, L., Vijver, B. Van De, Morales, E.A., Blanco, S., Piatek, J. & Smieja, A. (2011) The *Achnanthidium minutissimum* complex (Bacillariophyceae) in southern Poland. *Algological Studies* 136/137: 211–238. https://doi.org/10.1127/1864-1318/2011/0136-0211
Wunsam, S., Schmidt, R. & Klee, R. (1995) *Cyclotella*-taxa (Bacillariophyceae) in lakes of the Alpine region and their relationship to environmental variables. *Aquatic Sciences* 57: 360–386. https://doi.org/10.1007/BF00878399
Yang, J.R. & Dickman, M. (1993) Diatoms as indicators of lake trophic status in central Ontario, Canada. *Diatom Research* 8: 179–193. https://doi.org/http://dx.doi.org/10.1080/0269249X.1993.9705249
Yang, J.-R. & H. C. Duthie, 1993. Morphology and ultrastructure of teratological forms of the diatoms *Stephanodiscus niagarae* and *S. parvus* (Bacillariophyceae) from Hamilton Harbour (Lake Ontario, Canada). *Hydrobiologia* 269/270: 57–66.

APPENDIX A – TABLE 1. Predominant land use, and physical characteristics of sampling sites.

Sampling stations	Land use	Physical characteristics
S1	Urban	Conservation area, with the presence of *Hydrochoerus hydrochaeris* Linnaeus populations. Stream with visible silting up process
S2	Urban	Close to a highway, containing ciliary vegetation
S3	Urban	Close to a highway, lacking ciliary vegetation and visible silting up process
S4	Urban	Close to a garbage collection property, with sparse ciliary vegetation. Presence of a bridge over the stream for pedestrian traffic
S5	Rural	Close to temporary croplands and a highway, containing ciliary vegetation. Presence of a bridge over the stream for pedestrian traffic
S6	Rural	Conservation area within a rural property, with goat farming, *Pinus* sp. plantation, and temporary croplands
S7	Urban	Close to a deactivated abattoir, containing ciliary vegetation. Riverbanks in erosive process and stream with visible silting up process
S8	Rural	Close to temporary croplands and to a basalt mining company using mineral deposits. Presence of a bridge over the stream for vehicle traffic

APPENDIX B - TABLE 1. Location of sampling sites (S), and sample register number at Universidade Estadual do Oeste do Paraná Herbarium (UNOPA).

Sampling sites	Geographic coordinates		UNOPA											
	Latitude	Longitude	autumn/ 2016	spring/ 2016	winter/ 2017	spring/ 2017	summer/ 2018	autumn/ 2018	winter/ 2018	spring/ 2018	summer/ 2019	autumn/ 2019	winter/ 2019	spring/ 2019
S1	24°57'32.93"S	53°26'33.32"W	1036 1066 1038 1068 1040 1070 1042 1072 1044 1074	4342 4372 4344 4374 4346 4376 4348 4378 4350 4380	4867 4869 4871	5042 5044 5046	5350 5352 5354	5568 5570 5572	5651 5653 5655	5825 5827 5829	5889 5891 5893	6212 6214 6216	6277 6279 6281	6341 6343 6345
S2	24°58'6.80"S	53°25'21.70"W	not sampled	not sampled	4873 4875 4877	5048 5050 5052	5356 5358 5360	5574 5576 5578	5657 5659 5661	5831 5833 5835	5895 5897 5899	6218 6220 6222	6283 6285 6287	6347 6349 6351
S3	24°58'35.81"S	53°26'6.85"W	1046 1223 1048 1225 1050 1227 1052 1229 1054 1231	4352 4382 4354 4384 4356 4386 4358 4388 4360 4390	4885 4887 4889	5060 5062 5064	5368 5370 5372	5586 5588 5590	5669 5671 5673	5843 5845 5847	5907 5909 5911	6224 6226 6228	6289 6291 6293	6353 6355 6357
S4	24°58'17.29"S	53°24'24.75"W	not sampled	not sampled	4879 4881 4883	5054 5056 5058	5362 5364 5366	5580 5582 5584	5663 5665 5667	5837 5839 5841	5901 5903 5905	6230 6232 6234	6295 6297 6299	6359 6361 6363
S5	24°59'5.99"S	53°25'23.83"W	not sampled	not sampled	4891 4893 4895	5066 5068 5070	5374 5376 5378	5592 5594 5596	5675 5677 5679	5849 5851 5853	5913 5915 5917	6236 6238 6240	6301 6303 6305	6365 6367 6369
S6	24°59'18.90"S	53°25'32.20"W	not sampled	not sampled	4897 4899 4901	5072 5074 5076	5380 5382 5384	5598 5600 5602	5681 5683 5685	5855 5857 5859	5919 5921 5923	6242 6244 6246	6307 6309 6311	6371 6373 6375
S7	24°59'48.82"S	53°26'42.08"W	not sampled	not sampled	4909 4911 4913	5078 5080 5082	5386 5388 5390	5604 5606 5608	5687 5689 5691	5861 5863 5865	5925 5927 5929	6248 6250 6252	6313 6315 6317	6377 6379 6381
S8	25° 0'13.36"S	53°26'19.12"W	1056 1233 1058 1235 1060 1237 1062 1239 1064 1241	4362 4392 4364 4394 4366 4396 4368 4398 4370 4400	4903 4905 4907	5084 5086 5088	5392 5394 5396	5610 5612 5614	5693 5695 5697	5867 5869 5871	5931 5933 5935	6254 6256 6258	6319 6321 6323	6383 6385 6387

APPENDIX C - TABLE 1. Limnological variables (mean ± standard deviation) analyzed from water samples collected in the eight sampling sites from Cascavel River microbasin (Cond: electrical conductivity; CLa: chlorophyll *a*; TC: total coliforms; BOD: biochemical oxygen demand; COD: chemical oxygen demand; *E. coli*: *Escherichia coli*; N-NH$_3$: ammoniacal nitrogen; NO$_3$: nitrate; DO: dissolved oxygen; PO_4^-: orthophosphate; TP: total phosphorus; TS: total solids; temp: temperature; turb: turbidity; Prec: precipitation).

Variables (mean ± standard deviation)		**Cond**	**DO**	**BOD**	**COD**	**N-NH3**	**NO3**	**PO4-**	**TP**	**TS**	**pH**	**Temp**	**Turb**	**Flow**	**Depth**	**Prec**	**CLa**	***E. coli***	**TC**
		mS cm-1	mg L-1	mg L-1	mg L-1	mg L-1	mg L-1	mg L-1	mg L-1	mg L-1		°C	NTU	m3 s−1	m	mm	mg L-1	NMP 100 mL-1	NMP 100 mL-1
S1	Autumn	0.06 ± 0.01	15.29 ± 4.81	2.94 ± 0.85	5.52 ± 5.81	0.27 ± 0.12	2.24 ± 0.12	0.04 ± 0.04	0.1 ± 0.12	55.33 ± 8.5	6.22 ± 0.33	18.01 ± 0.99	4.71 ± 0.31	0.11 ± 0.07	0.04 ± 0.02	5.01 ± 4.15	0.6 ± 0.91	9807.78 ± 7958.08	11572.22 ± 9715.93
	Winter	0.06 ± 0	23.12 ± 23.28	6.76 ± 6.25	12.11 ± 11.42	0.2 ± 0	6.7 ± 4.71	0.03 ± 0.03	0.02 ± 0.01	57 ± 13.53	6.53 ± 0.24	18.48 ± 0.54	3.47 ± 0.69	0.07 ± 0.02	0.04 ± 0.01	3.29 ± 1.45	1.03 ±1.05	2242 ± 762.03	5213.33 ± 6384 ± 63
	Spring	0.06 ± 0.01	12.28 ± 5.28	3.24 ± 2.13	6.29 ± 5.89	0.2 ± 0	9.8 ± 6.74	0.04 ± 0.02	0.16 ± 0.24	165.67 ± 182.73	5.79 ± 0.79	20.11 ± 1.41	10.99 ± 15.09	0.13 ± 0.13	0.05 ± 0.03	5.74 ± 3.67	0.56 ± 0.53	31276.67 ± 42614.57	38993.33 ± 53359.09
	Summer	0.03 ± 0.03	11.45 ± 2.95	2.5 ± 2.1	3.72 ± 4.62	0.2 ± 0	8.85 ± .5	0.04 ± 0.02	0.026 ± 0.021	31.67 ± 13.5	6.22 ± 0.81	21.42 ± 0.68	4.53 ± 0.86	0.12 ± 0.05	0.05 ± 0.01	6.51 ± 4.05	1.45 ± 2.44	1829.33 ± 1821.46	4151 ± 2452.62
S2	Autumn	0.04 ± 0.04	10.35 ± 2.29	2.38 ± 1.3	10.73 ± 14.66	0.37 ± 0.21	1.64 ± 0.62	0.14 ± 0.16	0.26 ± 0.14	63 ± 22.91	5.42 ± 0.28	18.12 ± 2.44	2.96 ± 1.64	0.65 ± 0.29	0.12 ± 0.05	5.01 ± 4.15	0.12 ± 0.17	36077.78 ± 55005.17	11572.22 ± 9715.93
	Winter	0.06 ± 0.01	13.31 ± 2.46	5.46 ± 4.51	9.74 ± 11	0.2 ± 0	3.99 ± 2.61	0.04 ± 0.01	0.05 ± 0.05	101.67 ± 62.29	6.3 ± 0.28	19.12 ± 1.39	1.93 ± 0.54	0.89 ± 0.58	0.15 ± 0.07	3.29 ± 1.45	0.58 ± 0.52	24809.33 ± 38103 ± 95	28170 ± 41454.65
	Spring	0.08 ± 0.01	10.6 ± 3.52	3.83 ± 2.65	7.4 ± 8.64	0.2 ± 0	8.97 ± 4.05	0.04 ± 0.02	0.36 ± 0.49	63 ± 5.57	5.64 ± 0.82	20.3 ± 1.17	4.5 ± 6.46	1.16 ± 0.93	0.16 ± 0.09	5.74 ± 3.67	0.38 ± 0.28	38018 ± 41445.63	75386.67 ± 4809.3
	Summer	0.08 ± 0.01	15.18 ± 6.87	3.15 ± 3.07	4.31 ± 3.1	0.2 ± 0	7.38 ± 5.1	0.05 ± 0	0.1 ± 0.06	43 ± 20.3	5.91 ± 0.23	21.13 ± 0.36	2.34 ± 1.14	1.02 ± 0.53	0.17 ± 0.08	6.51 ± 4.05	0.37 ± 0.29	43666.67 ± 37056.35	64289 ± 47700.82
S3	Autumn	0.05 ± 0.02	11.56 ± 4.59	3.7 ± 0.75	6.36 ± 7.95	0.27 ± 0.12	1.76 ± 0.72	0.04 ± 0.02	0.12 ± 0.1	51.33 ± 16.07	5.81 ± 0.23	18.22 ± 3.18	9.7 ± 2.37	4.65 ± 3.96	0.37 ± 0.23	5.01 ± 4.15	0.21 ± 0.28	3220 ± 3236.85	4546.67 ± 1955.13
	Winter	0.06 ± 0	12.23 ± 3.47	6.3 ± 3.4	10.9 ± 11.88	0.2 ± 0	4.46 ± 4.53	0.04 ± 0.02	0.03 ± 0.02	60.33 ± 22.23	6.46 ± 0.31	18.39 ± 1.74	8.15 ± 1.93	2.75 ± 2.16	0.29 ± 0.17	3.29 ± 1.45	0.3 ± 0.22	47640 ± 80509.7	94606.67 ± 159010.23
	Spring	0.06 ± 0	9.55 ± 5.39	3.86 ± 2.13	8.16 ± 8.46	0.2 ± 0	6.77 ± 1.54	0.04 ± 0.01	0.35 ± 0.5	48.67 ± 2.52	5.94 ± 0.12	22.93 ± 1.46	11.07 ± 10.01	4.83 ± 4.06	0.15 ± 0.27	5.74 ± 3.67	1.99 ± 3.37	22147.33 ± 26441.61	27756.67 ± 33821.17

Variables (mean ± standard deviation)		Cond	DO	BOD	COD	N-NH3	NO3	PO4-	TP	TS	pH	Temp	Turb	Flow	Depth	Prec	CLa	*E. coli*	TC
		mS cm-1	mg L-1	mg L-1	mg L-1	mg L-1	mg L-1	mg L-1	mg L-1	mg L-1		°C	NTU	m3 s−1	m	mm	mg L-1	NMP 100 mL-1	NMP 100 mL-1
	Summer	0.05 ± 0	13.15 ± 4.76	1.39 ± 0.9	4.07 ± 5.13	0.2 ± 0	5.72 ± 3.13	0.03 ± 0.03	0.03 ± 0.02	35.67 ± 17.56	5.99 ± 0.20	23.60 ± 0.39	19.12 ± 15.99	4 ± 2.17	0.39 ± 0.13	6.51 ± 4.05	1.61 ± 2.32	15240 ± 17234.99	18393.33 ± 19018.1
S4	Autumn	0.06 ± 0.01	14.01 ± 5.52	2.55 ± 0.79	7.78 ± 9.05	0.13 ± 0.17	2.48 ± 0.3	0.05 ± 0	0.1 ± 0.06	79 ± 22.61	5.96 ± 0.43	17.82 ± 2.56	6.73 ± 2.57	0.51 ± 0.13	0.12 ± 0.04	5.01 ± 4.15	0.08 ± 0.02	5840 ± 9498.46	8360 ± 13555.4
	Winter	0.06 ± 0	10.48 ± 2.4	4.98 ± 4.19	8.84 ± 9.96	0.2 ± 0	3.66 ± 1.24	0.04 ± 0.02	0.02 ± 0.01	76 ± 16.52	6.55 ± 0.18	18.65 ± 1.74	3.4 ± 0.52	0.49 ± 0.44	0.12 ± 0.11	3.29 ± 1.45	1.28 ± 1.67	2253.33 ± 2557.54	3203.33 ± 2352.45
	Spring	0.06 ± 0.02	10.28 ± 3.68	3.37 ± 3.2	7.11 ± 8.39	0.2 ± 0	10.6 ±6.06	0.04 ± 0.02	0.33 ± 0.53	65.33 ± 2.08	5.81 ± 0.4	20.33 ± 1.38	12.37 ± 18.88	0.48 ±0.28	0.1 ± 0.03	5.74 ± 3.67	0.4 ± 0.3	206830 ± 345713.98	207763.33 ±344924.64
	Summer	0.06 ± 0.01	15.96 ± 6.65	2.66 ± 2.47	3.73 ± 3.46	0.2 ± 0	57.67 ± 6.11	0.03 ± 0.03	0.03 ± 0.02	39 ± 8.89	6.08 ± 0.34	21.32 ± 0.43	3.1 ± 0.28	0.68 ± 0.52	0.13 ± 0.10	6.51 ± 4.05	0.1 ± 0.13	7202.33 ± 9685.05	7730 ± 9471.05
S5	Autumn	0.01 ± 0	9.34 ± 3.12	2.39 ± 1.78	15.74 ± 5.14	0.27 ± 0.12	1.06 ± 1.14	0.03 ± 0.0.3	0.11 ± 0.11	41.33 ± 13.5	6.60 ± 0.29	19.24 ± 1.75	17.66 ± 27.34	0.02 ± 0.02	0.02 ± 0.01	5.01 ± 4.15	0.06 ± 0.04	3333.33 ± 4499.3	6253;33 ± 9342.58
	Winter	0.01 ± 0.01	10.98 ± 1.13	3.96 ± 2.57	6.43 ± 6.03	0.2 ± 0	0.66 ± 0.55	0.03 ± 0.03	0.03 ± 0.04	38.67 ± 10.26	6.88 ± 0.42	20.16 ± 2.41	2.67 ± 0.43	0.05 ± 0.01	0.03 ± 0.01	3.29 ± 1.45	0.58 ± 0.47	67.33 ± 114.89	6067 ± 5139.09
	Spring	0.01 ± 0	12.03 ± 7.82	2.66 ± 2.26	7.30 ±6.17	0.2 ± 0	1.2 ± 0.92	0.04 ± 0.01	0.27 ± 0.45	27 ± 3.61	5.7 ± 1.27	20.97 ± 0.85	4.26 ± 4.47	0.29 ± 0.34	0.08 ± 0.06	5.74 ± 3.67	0.35 ± 0.28	15444.53 ± 22708.48	23566.67 ± 24964.84
	Summer	0.01 ± 0	14.43 ± 5.53	1.57 ± 0.34	3.51 ± 2.22	0.2 ± 0	1.8 ± 2.21	0.03 ± 0.03	0.03 ± 0.04	11.67 ± 5.13	6.44 ± 0.8	21.42 ± 0.71	4.05 ± 4.58	0.05 ± 0.06	0.03 ± 0.02	6.51 ± 4.05	1.63 ± 2.31	17131.33 ±27127.25	19346.67 ± 30494.72
S6	Autumn	0.03 ± 0.01	9.88 ± 1.91	3.1 ± 2.91	16.82 ± 19.32	0.23 ± 0.06	0.83 ± 0.2	0.04 ± 0.02	0.07 ± 0.05	49.33 ± 13.5	6.47 ± 0.38	17.83 ± 2.56	7.41 ± 2.63	1.25 ± 0.37	0.14 ± 0.02	5.01 ± 4.15	0.05 ± 0.04	1964.67 ± 3287.52	2504.78 ± 3481.12
	Winter	0.04 ± 0.01	11.72 ± 1	2.86 ± 1.63	6.02 ± 2.79	0.2 ± 0	2.04 ± 1.01	0.03 ± 0.03	0.03 0.04	33.33 ± 12.58	6.59 ± 0.31	19.20 ± 2.3	5.6 ± 1.25	1.19 ± 0.25	0.14 ± 0.02	3.29 ± 1.45	1.01 ± 1.46	2173.33 ± 3660.62	2800 ± 4504.44
	Spring	0.03 ± 0.01	11.31 ± 6.36	2.98 ± 2.79	8.8 ±1.92	0.2 ± 0	2.15 ± 1.24	0.04 ± 0.02	0.28 ± 0.46	35 ± 27.15	6.42 ± 0.17	21,01 ± 1.69	8.86 ± 11.01	1.25 ± 0.49	0.13 ±0.03	5.74 ± 3.67	0.04 ± 0.04	42476.67 ± 39741.54	47466.67 ± 41812.12

Variables (mean ± standard deviation)		Cond	DO	BOD	COD	N-NH3	NO3	PO4-	TP	TS	pH	Temp	Turb	Flow	Depth	Prec	CLa	*E. coli*	TC
		mS cm-1	mg L-1	mg L-1	mg L-1	mg L-1	mg L-1	mg L-1	mg L-1	mg L-1		°C	NTU	m3 s−1	m	mm	mg L-1	NMP 100 mL-1	NMP 100 mL-1
	Summer	0.04 ± 0.01	14.47 ± 5.32	1.98 ± 1.85	5.66 ±7.48	0.2 ± 0	2.59 ± 1.59	0.03 ± 0.03	0.03 ± 0.02	27 ± 12.29	6.86 ± 0.31	21.80 ± 0.84	7.26 ± 5.36	1.69 ± 1.08	0.17 ± 0.07	6.51 ± 4.05	0.39 ± 0.34	1235.67 ± 869.85	3076.67 ± 2726.29
S7	Autumn	0.05 ± 0.01	10.37 ± 3.09	3.2 ± 0.74	15.8 ± 19.32	0.27 ± 0.12	0.56 ± 0.16	0.04 ± 0.02	0.06 ± 0.04	53.67 ± 7.51	6.43 ± 0.49	19.41 ± 2.08	0.01 ± 0.01	0.16 ± 0.07	0.06 ± 0.03	5.01 ± 4.15	0.24 ± 0.33	2696.67 ± 3556.27	3353.33 ± 4203.87
	Winter	0.04 ± 0.01	13.49 ± 1.7	3.65 ± 2.38	5.61 ± 4.09	0.2 ± 0	2.48 ± 2.74	0.03 ± 0.03	0.01 ± 0.01	41.67 ± 21.55	6.72 ± 0.18	20.25 ± 1.19	0.11 ± 0.15	0.30 ± 0.22	0.1 ± 0.05	3.29 ± 1.45	0.38 ± 0.54	75 ± 65.2	3516 ± 5788.99
	Spring	0.05 ± 0.01	11.09 ± 5.97	2.78 ± 2.28	8.51 ± 4.63	0.2 ± 0	2.60 ± 1.64	0.04 ± 0.02	032 ± 0.48	49.67 ± 27.15	6.41 ± 0.44	21.31 ± 0.62	14.16 ± 24.03	0.11 ± 0.04	0.05 ± 0.02	5.74 ± 3.67	0.21 ± 0.29	171463.67 ± 290692.99	24026.67 ± 35244.21
	Summer	0.05 ± 0.01	14.99 ± 5.88	1.12 ± 0.68	1.25 ± 0.27	0.2 ± 0	2.43 ± 1.76	0.04 ± 0.03	0.03 ± 0.02	32.67 ± 12.01	6.78 ± 0.18	21.69 ± 0.32	0.84 ± 1.28	0.25 ± 0.12	0.09 ± 0.03	6.51 ± 4.05	0.81 ± 1.15	32768 ± 53833.74	46803.33 ± 76911.24
S8	Autumn	0.05 ± 0.01	6.45 ± 5.86	2.5 ± 0.88	7.96 ± 9.2	0.3 ± 0.17	1.72 ± 0.57	0.03 ± 0.03	0.09 ± 0.07	48.44 ± 17.44	6.52 ± 0.39	18.75 ± 1.61	4.35 ± 4.17	4.2 ± 1.38	0.3 ± 0.06	5.01 ± 4.15	0.04 ± 0.03	4377.78 ± 2436.88	4887.78 ± 2649.78
	Winter	0.05 ± 0	11.44 ± 3.42	3.44 ± 2.11	5.69 ± 4.54	0.2 ± 0	1.65 ± 0.48	0.03 ± 0.03	0.03 ± 0.02	57.67 ± 20.4	6.81 ± 0.28	18.38 ± 0.99	4.56 ± 0.91	3.58 ± 1.67	0.28 ± 0.07	3.29 ± 1.45	0.37 ± 0.6	1776.33 ± 1755.03	3063.33 ± 3629.56
	Spring	0.05 ± 0.01	14.35 ± 10.53	3.72 ± 2.5	9.09 ± 6.74	0.2 ± 0	5.35 ± 3.7	0.04 ± 0.01	0.31 ± 0.47	32.67 ± 25.01	6.47 ± 0.40	21.58 ± 1.29	11.26 ± 12.31	5.16 ± 1.67	0.34 ± 0.03	5.74 ± 3.67	0.43 ± 0.56	14318 ± 8167.5	16033.33 ± 7480.86
	Summer	0.05 ± 0.01	15.27 ± 7.14	1.3 ± 0.74	4.02 ± 4.77	0.2 ± 0	5.07 ± 0.8	0.03 ± 0.03	0.03 ± 0.02	30.33 ± 19.35	6.94 ± 0.22	22.78 ± 0.92	6.63 ± 4.94	6.09 ± 4.38	0.36 ± 0.14	6.51 ± 4.05	0.05 ± 0.04	6020 ± 4966	7416.67 ± 6362.85
	R^2	0.66	0.10	0.21	0.12	0.28	0.49	0.12	0.25	0.23	44,00	0.53	0.14	0.65	0.70	0.17	0.19	0.14	0.127
	F	16.46	0.90	2.24	1.14	3.32	8.00	1.20	2.57	2.56	6.67	9.38	1.38	15.61	19.57	1.47	1.14	1.38	1.235
	p	< **0.0001**	0.54	**0.02**	0.35	**0.001**	< **0.0001**	0.30	**0.004**	**0.01**	< **0.0001**	< **0.0001**	0.20	< **0.0001**	< **0.0001**	0.17	0.35	0.20	0.28

APPENDIX D - TABLE 1. Mean concentrations of metals in sediment samples collected from the eight sampling sites in the Cascavel River microbasin.

Metals – sediment		Aluminum mg L^{-1}	Barium mg L^{-1}	Cadmium mg L^{-1}	Chromium mg L^{-1}	Cobalt mg L^{-1}	Copper mg L^{-1}	Iron mg L^{-1}	Lead mg L^{-1}	Manganese mg L^{-1}	Nickel mg L^{-1}	Zinc mg L^{-1}
S1	Autumn	40,148.52	626.42	22.78	32.12	25.08	210.08	77,564.67	549.67	349.80	471.83	81.88
	Winter	36,411.17	606.53	24.62	23.11	25.93	196.72	82,294.08	549.67	329.01	400.51	78.36
	Spring	38,819.96	735.80	27.91	33.58	27.33	197.56	89,191.63	522.44	398.50	449.39	93.81
	Summer	41,011.46	879.97	43.30	31.83	23.67	222.88	86,451.67	522.44	393.75	543.65	99.55
S2	Autumn	41,346.70	715.91	14.57	36.34	21.98	184.29	86,999.66	544.22	276.04	435.92	73.98
	Winter	38,608.88	760.65	21.55	35.32	21.70	191.39	88,298.16	446.21	500.30	368.59	68.08
	Spring	37,131.33	1.049.01	36.94	46.66	22.26	196.25	88,321.99	465.27	647.00	457.87	93.08
	Summer	35,604.11	1.098.72	41.66	39.39	28.18	170.55	88,059.90	567.36	606.73	489.79	79.00
S3	Autumn	39,633.24	934.66	24.62	40.85	39.73	292.31	88,762.76	789.24	423.57	484.80	112.59
	Winter	40,862.46	919.74	26.27	37.07	24.24	195.31	86,737.58	601.39	397.55	511.23	78.89
	Spring	41,222.54	1,193.18	35.09	37.79	28.46	211.76	91,931.59	508.83	465.71	583.06	94.80
	Summer	34,399.71	1,441.76	72.23	44.92	27.05	231.94	86,523.15	583.70	523.82	917.23	127.17
S4	Autumn	36,634.67	969.46	24.01	45.50	23.39	172.51	78,684.48	474.80	266.77	409.49	84.88
	Winter	37,441.74	1,098.72	30.57	50.59	23.11	173.92	85,045.95	458.46	622.77	428.94	71.01
	Spring	41,309.46	1,556.11	65.87	57.56	29.87	225.59	98,233.49	621.81	745.83	729.69	124.82
	Summer	34,225.88	1,252.84	46.79	55.53	24.52	170.46	84,438.39	484.33	639.87	489.29	123.32
S5	Autumn	40,011.94	1,213.07	34.68	49.28	32.69	189.05	87,416.61	627.26	370.35	693.28	113.26
	Winter	42,203.44	1,133.52	27.70	47.68	31.28	206.14	89,608.58	639.51	373.56	465.87	97.71
	Spring	35,225.41	1,342.33	47.81	47.24	28.46	160.65	79,756.64	459.82	431.41	579.07	78.98
	Summer	40,074.02	1,580.97	51.92	55.09	35.23	228.86	89,644.32	678.98	490.80	638.92	119.34
S6	Autumn	36,572.59	1,103.69	22.98	51.60	19.44	149.34	75,432.27	499.30	234.22	420.96	68.52
	Winter	36,479.47	1,297.59	35.70	58.29	26.49	153.45	83,378.15	502.02	470.60	422.95	73.15
	Spring	37,180.99	1,392.05	43.30	65.85	28.74	186.90	87,309.39	491.13	642.37	460.36	112.75
	Summer	36,715.38	1,491.48	47.81	60.76	33.25	163.45	84,807.69	542.86	538.55	469.34	83.43
S7	Autumn	42,215.85	546.88	25.86	21.08	26.49	244.28	87,595.30	567.36	393.75	547.15	108.37
	Winter	42,085.48	447.44	26.88	22.68	23.67	231.38	87,237.92	610.92	291.12	548.14	99.43
	Spring	41,793.70	611.51	30.99	26.31	21.98	214.38	90,561.61	523.80	387.57	476.32	96.46
	Summer	42,066.86	700.99	40.42	26.60	24.24	268.85	93,694.69	593.23	468.94	596.52	103.05
S8	Autumn	41,464.66	377.84	14.98	23.55	21.98	192.51	85,724.98	574.17	289.70	384.05	76.38
	Winter	40,223.02	412.64	22.78	28.35	16.91	195.50	92,789.31	473.44	458.49	477.82	78.27
	Spring	38,689.59	820.31	36.11	48.41	28.46	231.94	94,576.24	519.72	809.38	429.44	100.19
	Summer	40,154.73	760.65	41.66	37.79	23.95	199.43	94,004.42	615.00	552.09	584.55	91.99